

Classification of cone photoreceptor spectral types

Ramkumar Sabesan, Ph.D.
University of Washington
rsabesan@uw.edu

Young-Helmholtz Trichromatic Theory of Color Vision



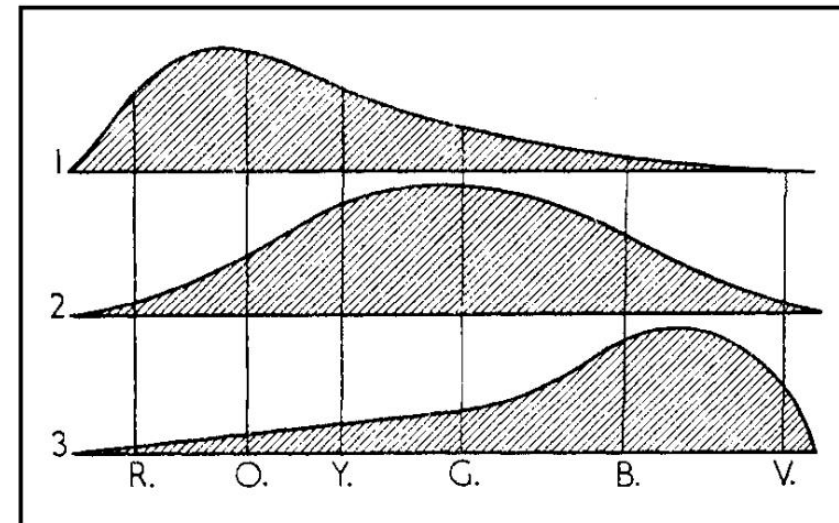
Thomas Young



Hermann von Helmholtz

“The eye is provided with three distinct sets of nervous fibers. Stimulation of the first excites the sensation of red, stimulation of the second the sensation of green, and stimulation of the third the sensation of violet”

Each is sensitive across the entire visible spectrum, with differences in their peak spectral response and distribution



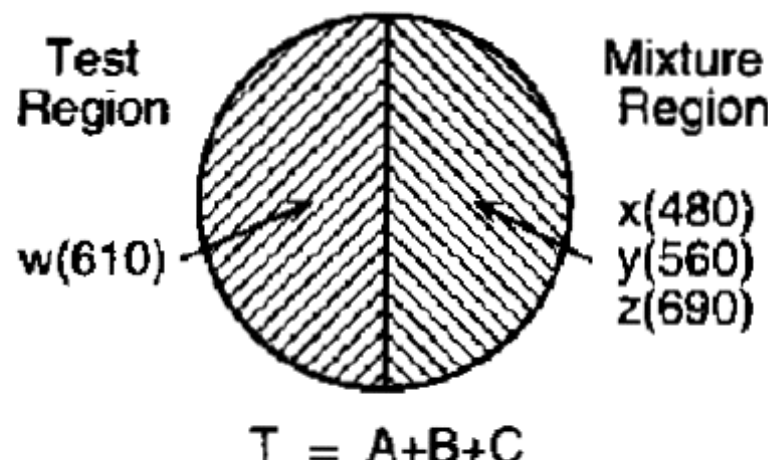
Color-matching experiments - Behavioral evidence for trichromacy

- Color-matching experiments

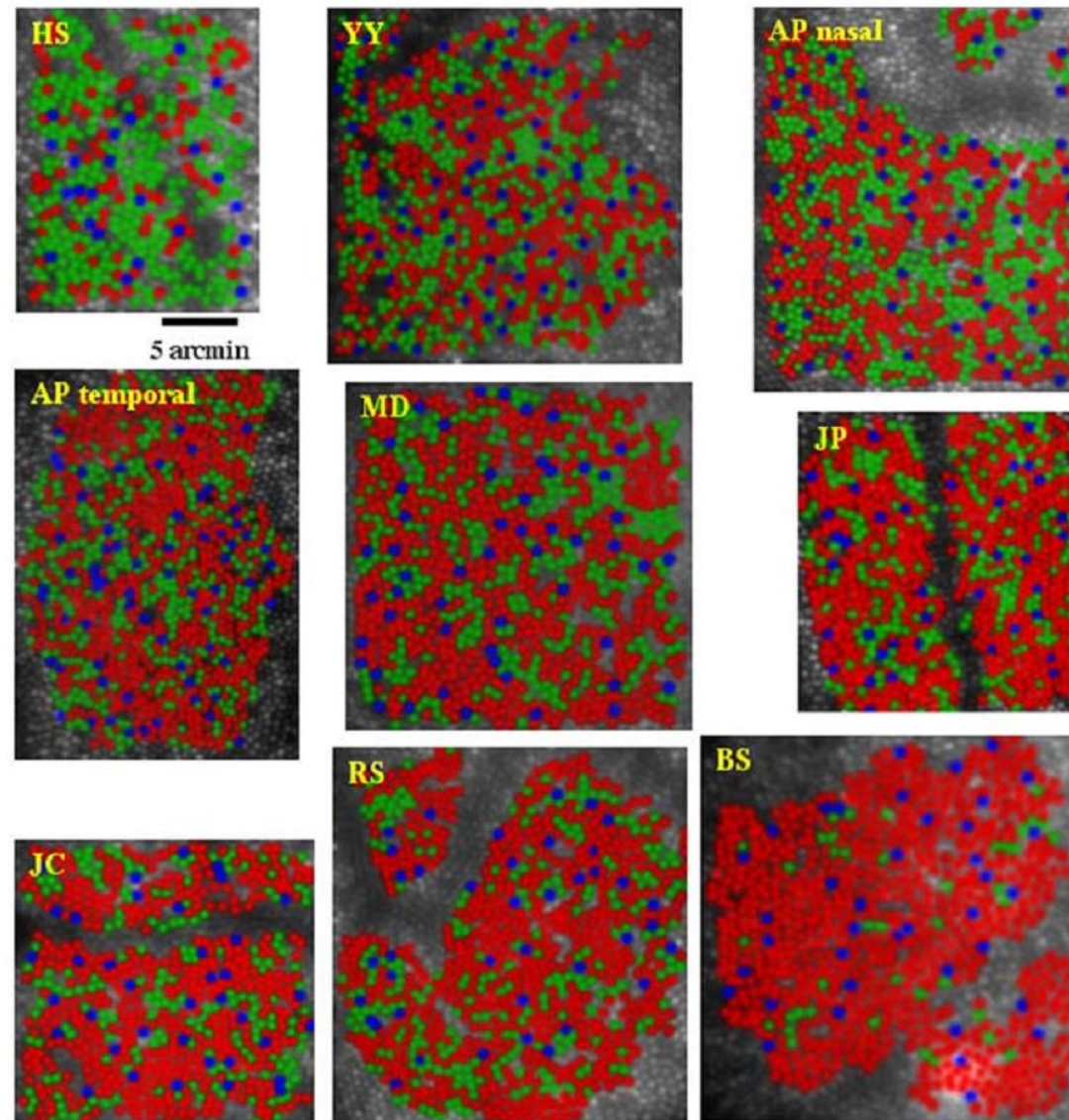
- Observers adjusted amounts of three lights to make a match with any other light.
- Need no more than three mixture lights to make the matches

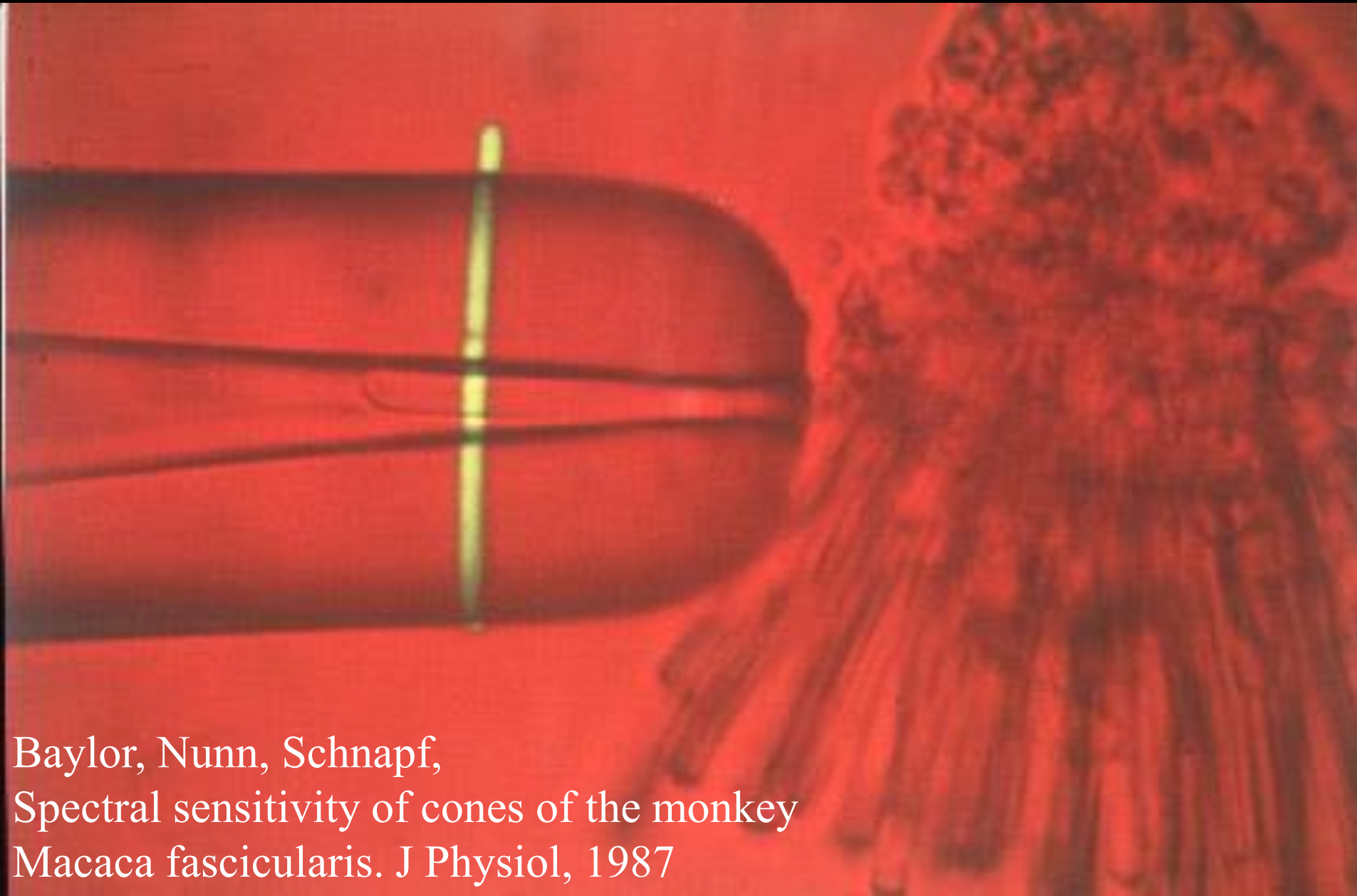
Three variables needed for match shows , normal color vision is trichromatic, a three-variable system

A. Standard Mixture Task

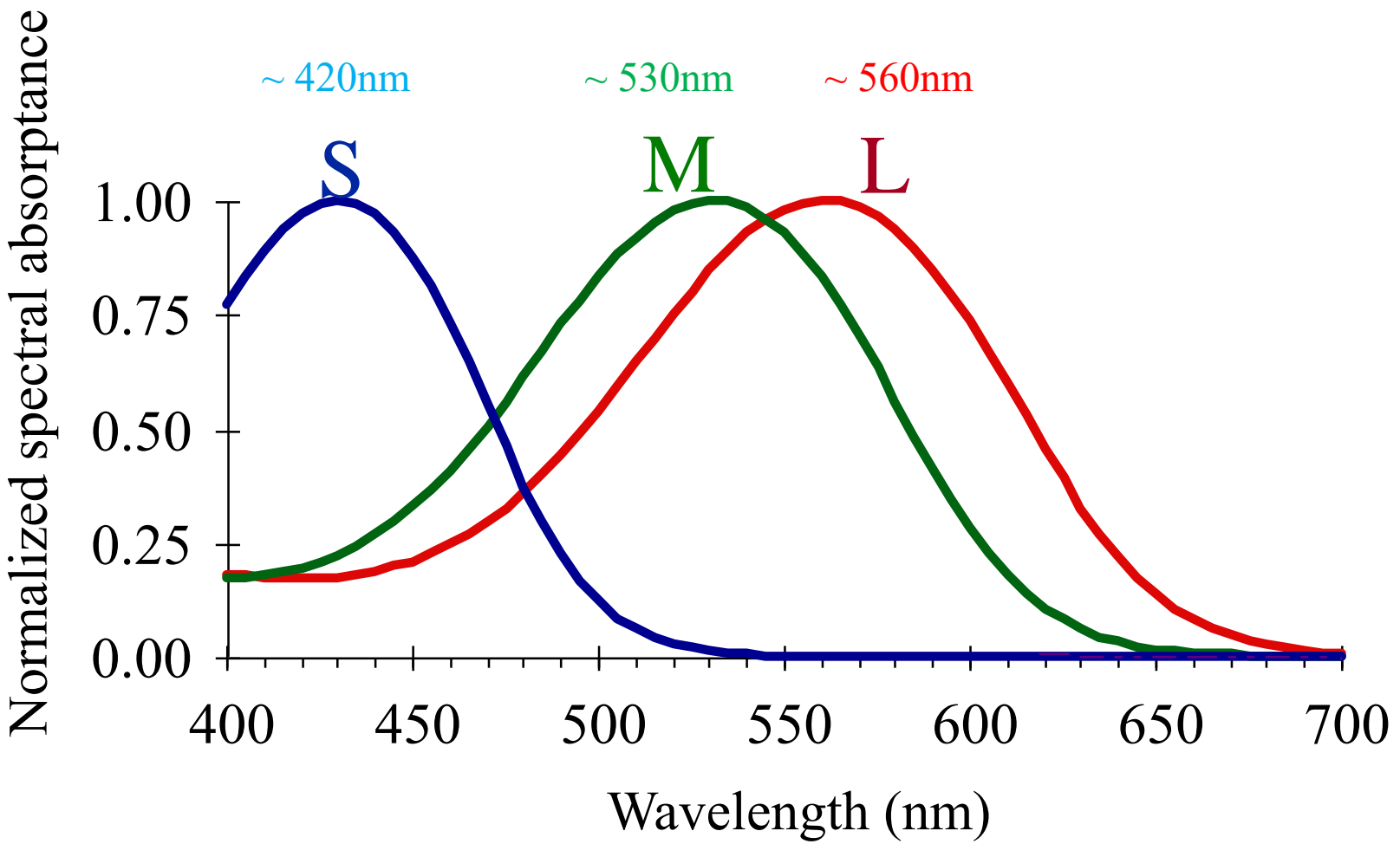


Wavelengths in the external world are sampled by the visual system by 3 classes of photoreceptors



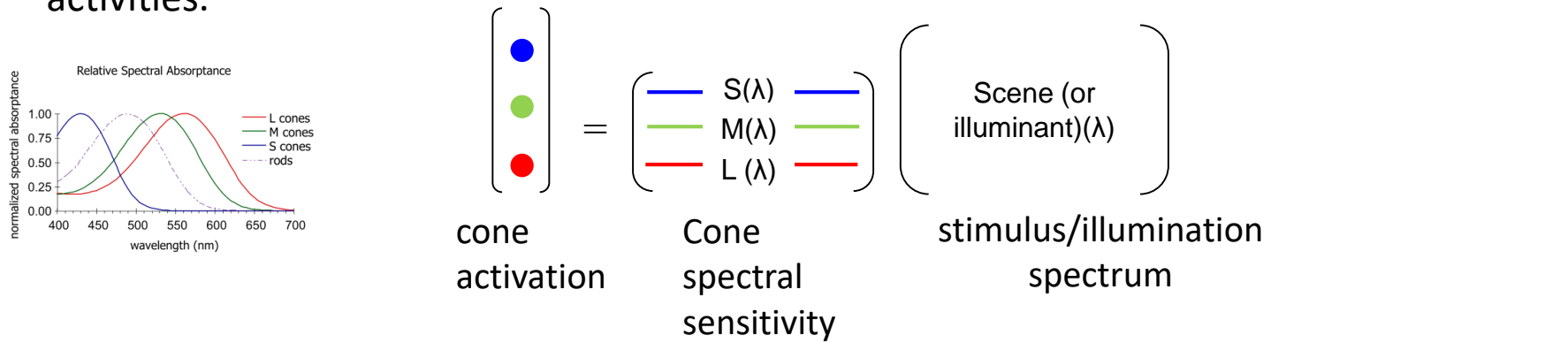


Baylor, Nunn, Schnapf,
Spectral sensitivity of cones of the monkey
Macaca fascicularis. J Physiol, 1987



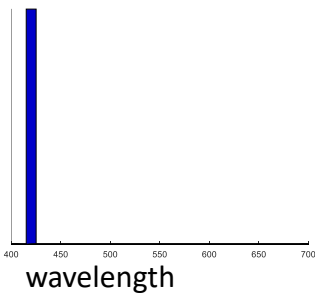
Trichromatic Theory

Color perception is based on the relative amount of activity in the three cone types.
Almost any color can be produced by combining relative amounts of L, M and S-cone activities.

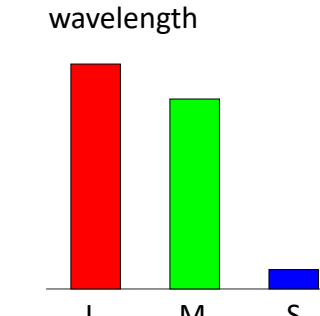
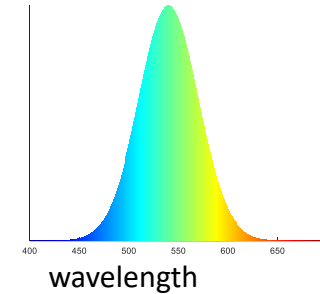
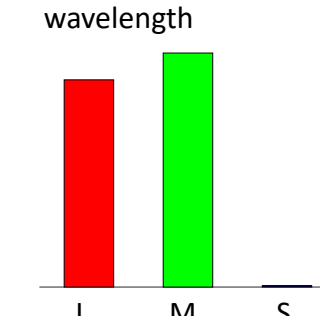
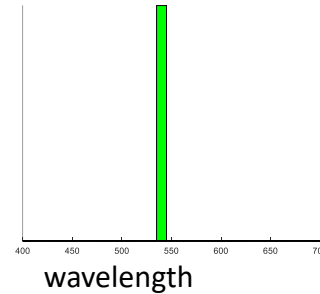
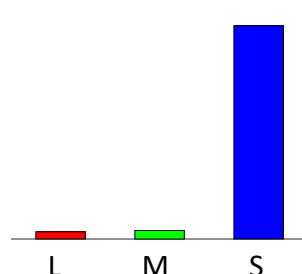


examples

Physical stimulus

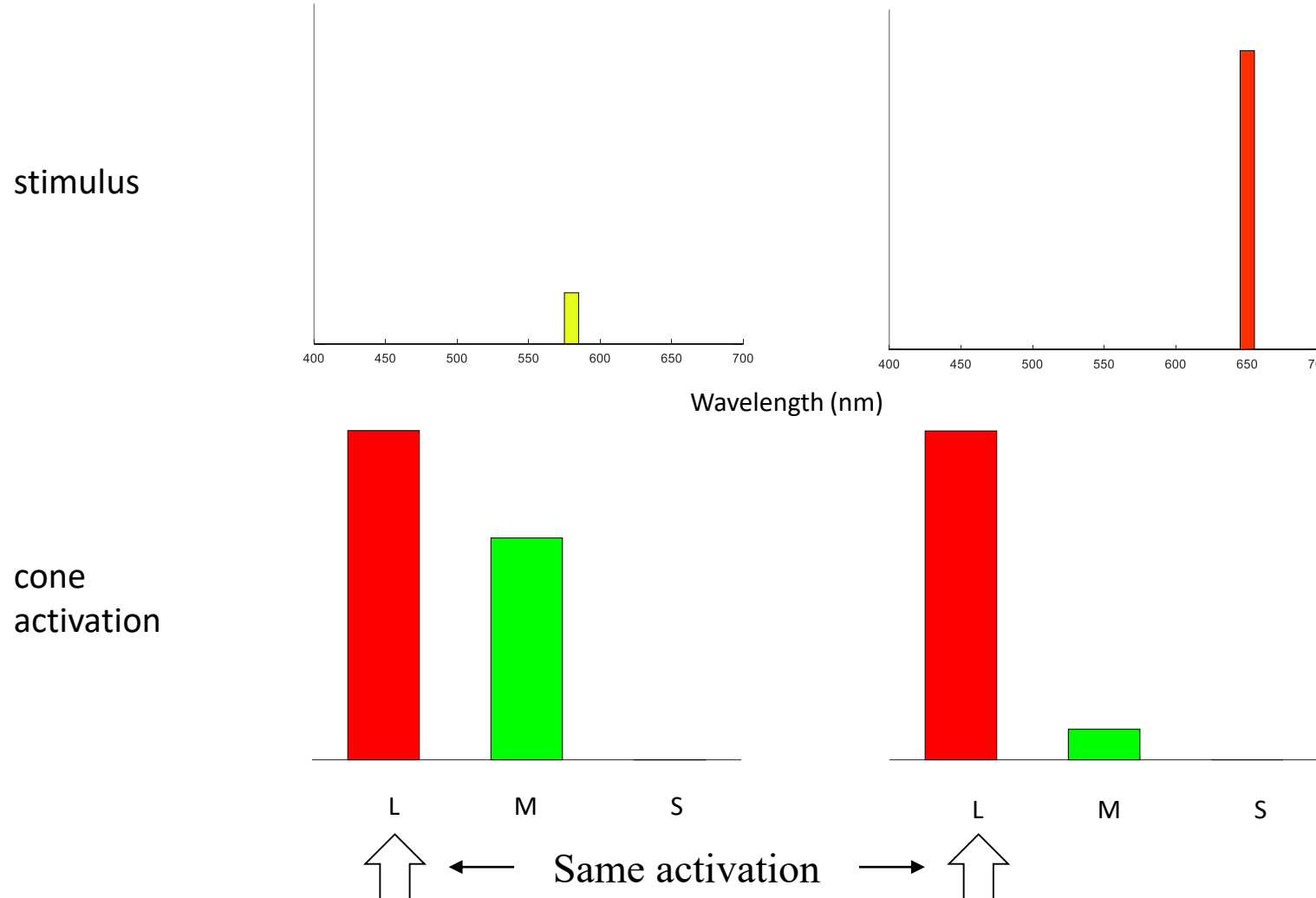
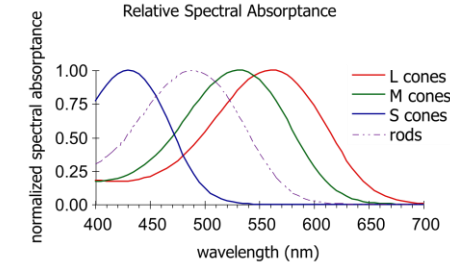


cone activation



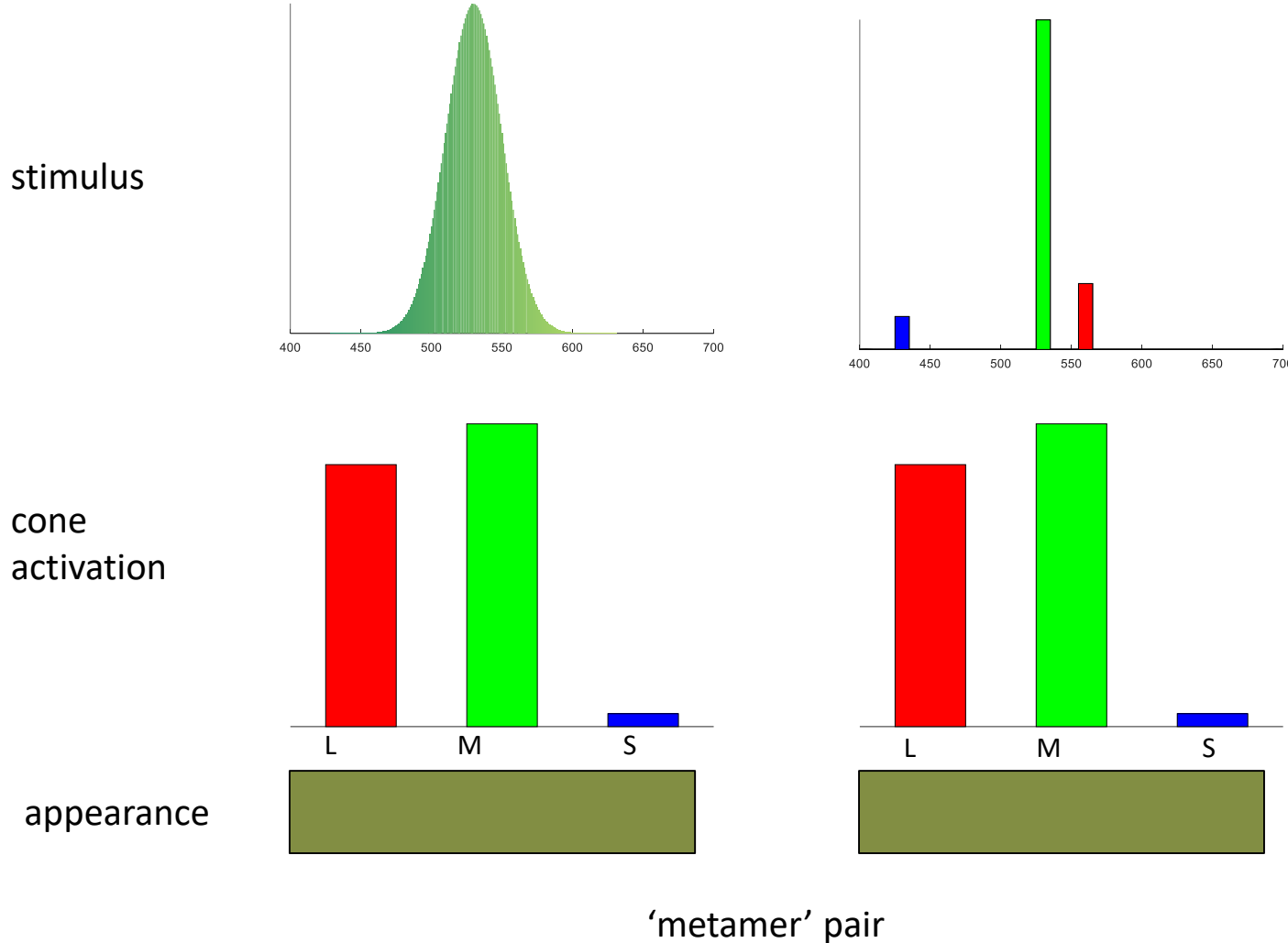
Principal of Univariance

Individual cone photoreceptors can be excited to same level of activation, regardless of the wavelength of light. Thus, individual cone photoreceptors are “colorblind”.



Metamers

Two different spectra that cause the same level of L, M and S cone activations will appear the same.



Molecular Genetics of Human Color Vision: The Genes Encoding Blue, Green, and Red Pigments

JEREMY NATHANS, DARCY THOMAS, DAVID S. HOGNESS

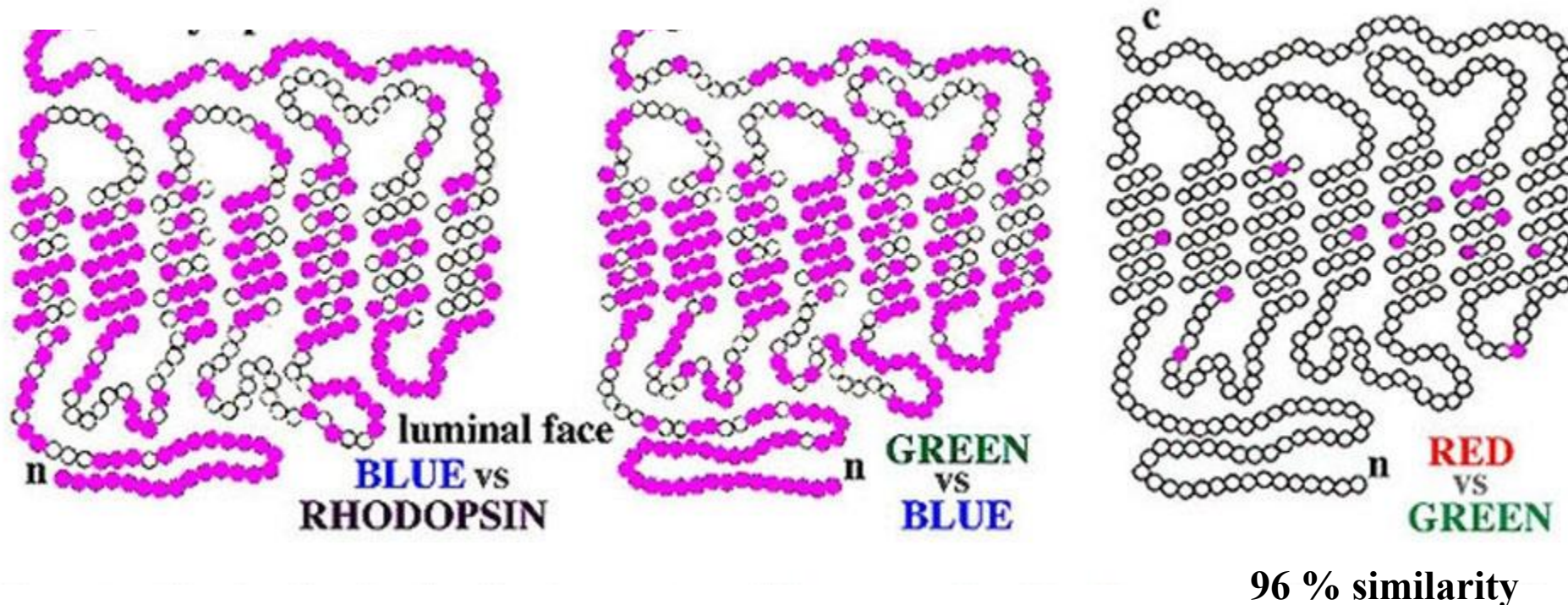
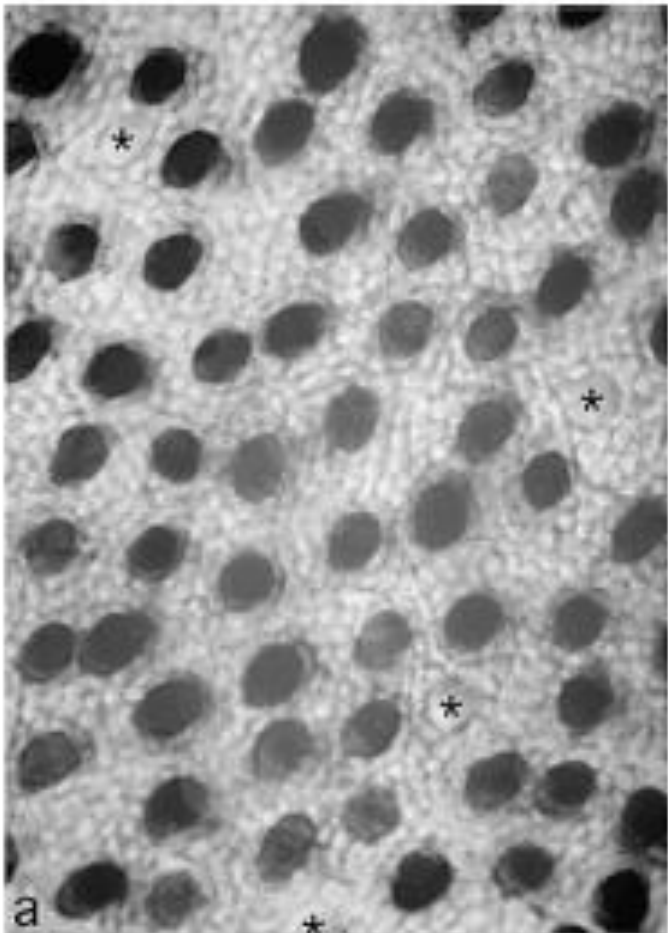


Fig. 14b. The closely related molecular structure of the cone opsins. The blue-cone opsin compared with rhodopsin. The blue-cone opsin compared with the green opsin and the minimal difference between the red- and green-cone opsins. The pink-filled circles represent amino acid substitutions between these molecules. The open circles indicate identical amino acids. Adapted from Nathans et al. (1986). Webvision

S-cones



Ahnelt & Kolb (2000)

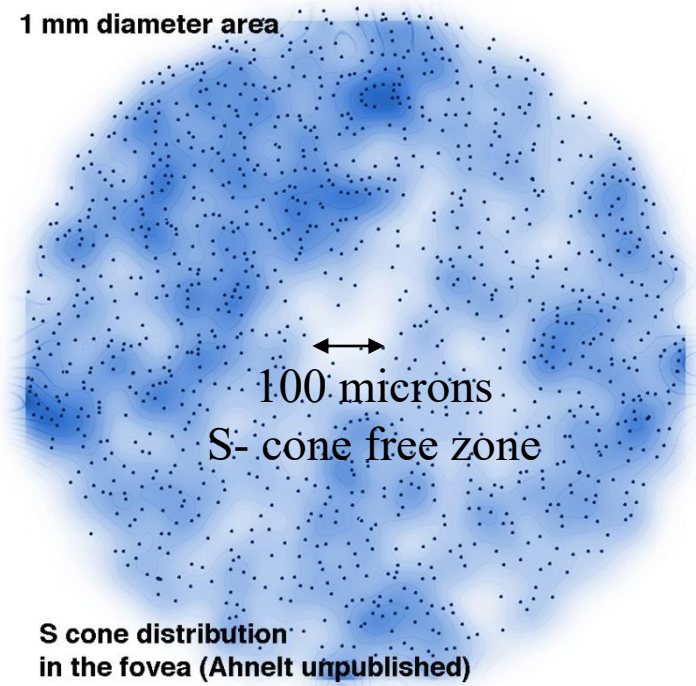
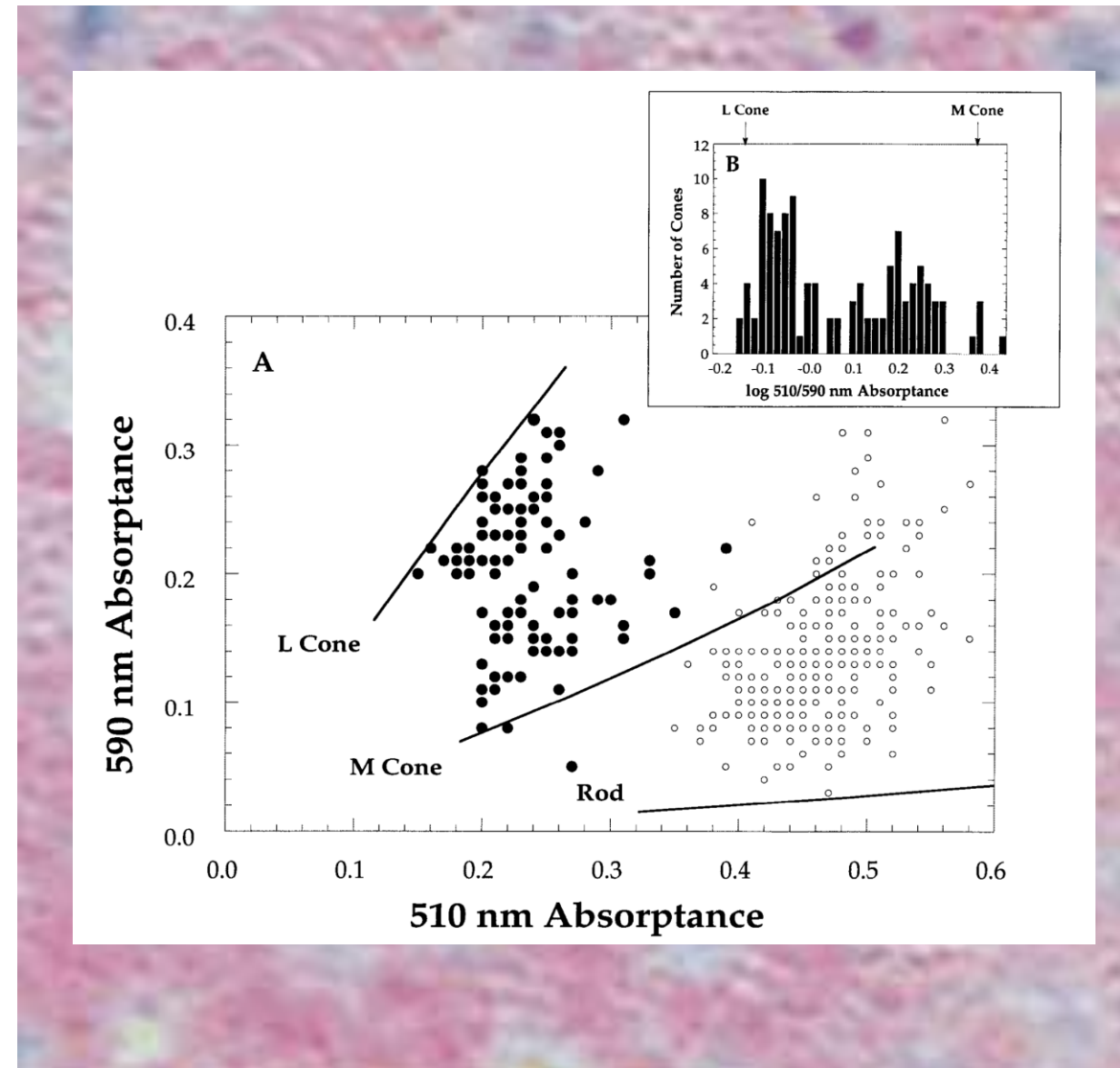
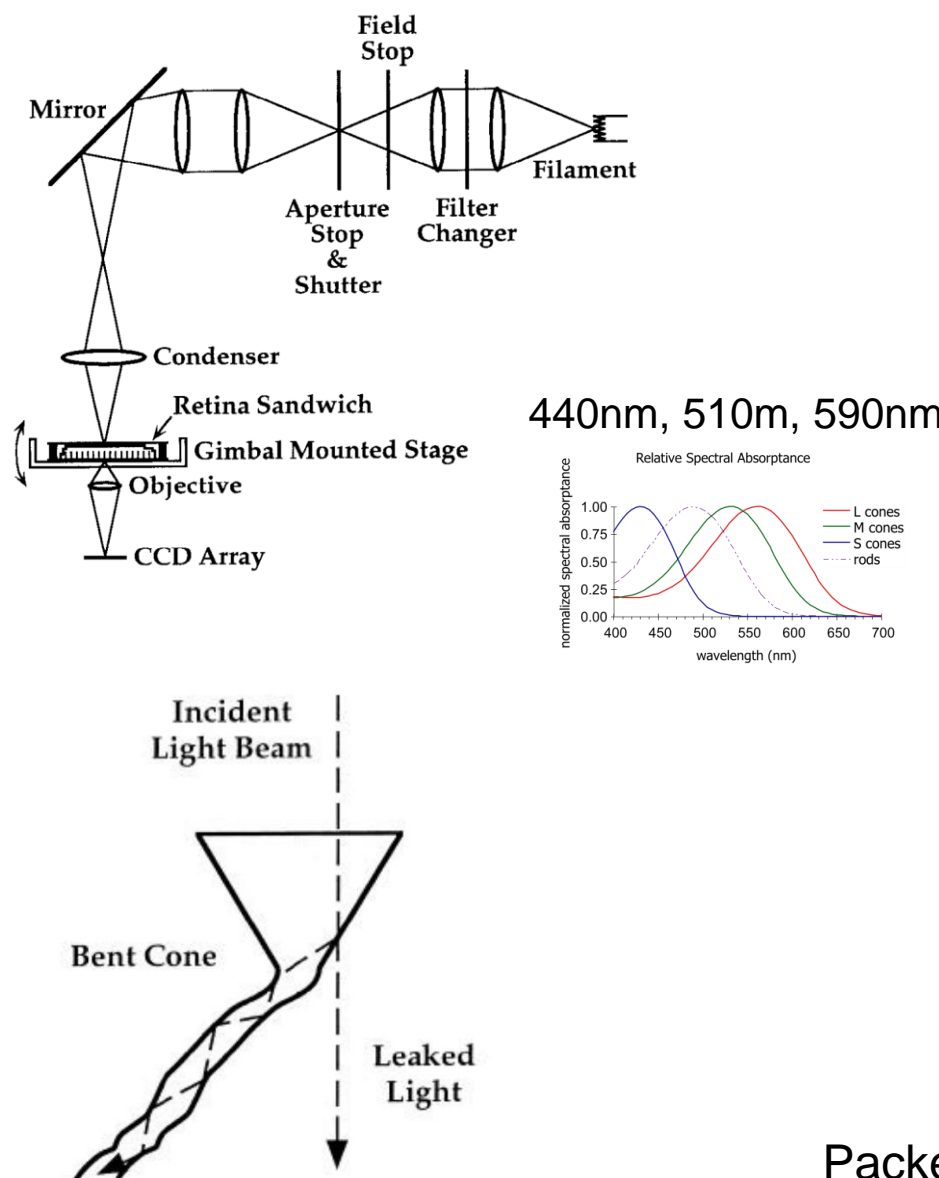


Figure 15. Every S-cone labelled with S-cone opsin in a human fovea. The more intense the blue shading indicates larger numbers of S-cones in the foveal slope where they reach 12% of the cone population.

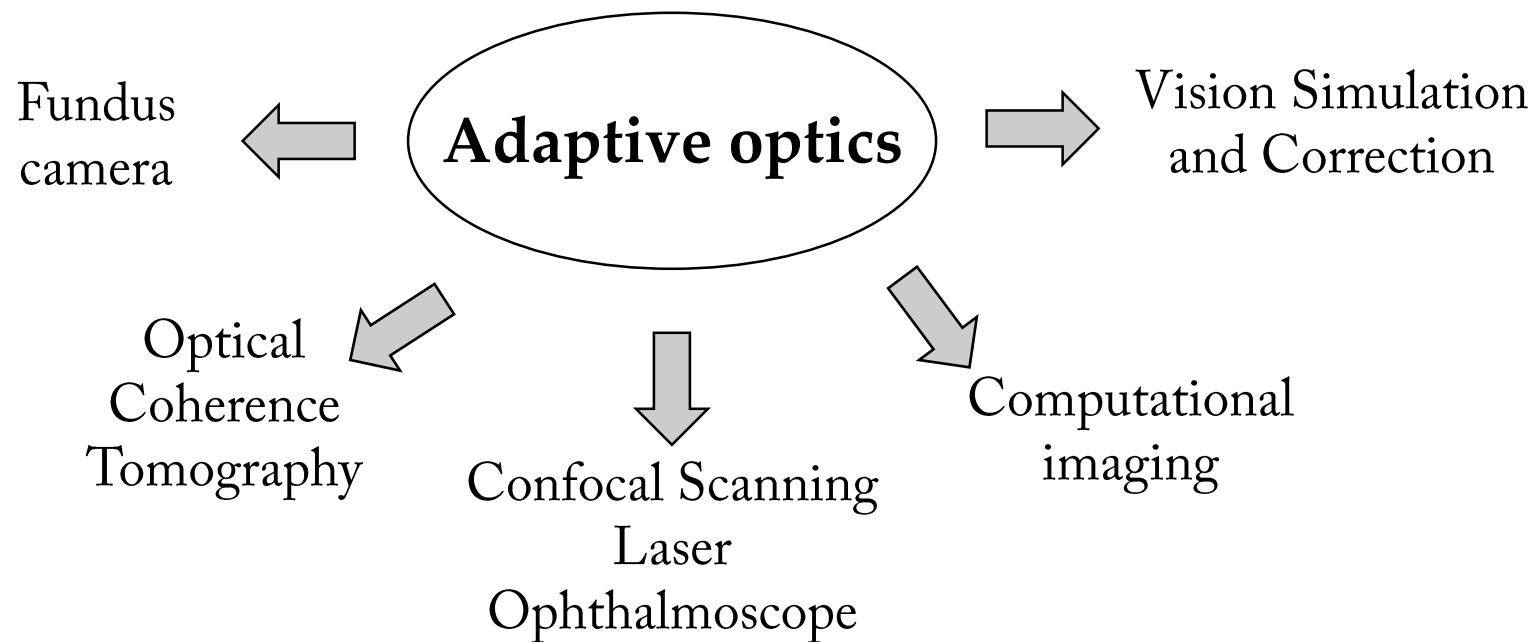
Webvision



Packer, O.S., Williams, D.R., Bensinger, D.G. (1996) Photopigment transmittance imaging of the primate photoreceptor mosaic. *J. Neurosci.*, 16, 2251-2260.

From *ex vivo* to *in vivo* imaging of the photoreceptor mosaic

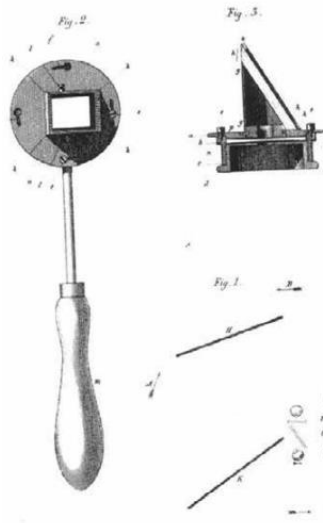
Adaptive Optics Ophthalmoscopy



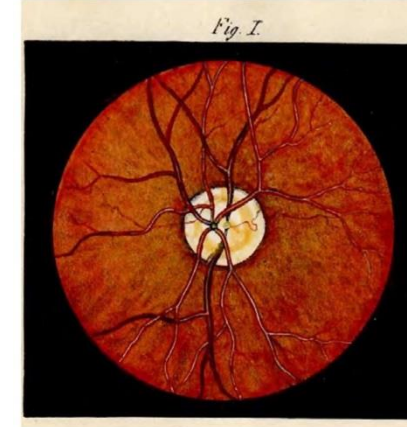
The native optical quality of the eye is poor, and not diffraction-limited



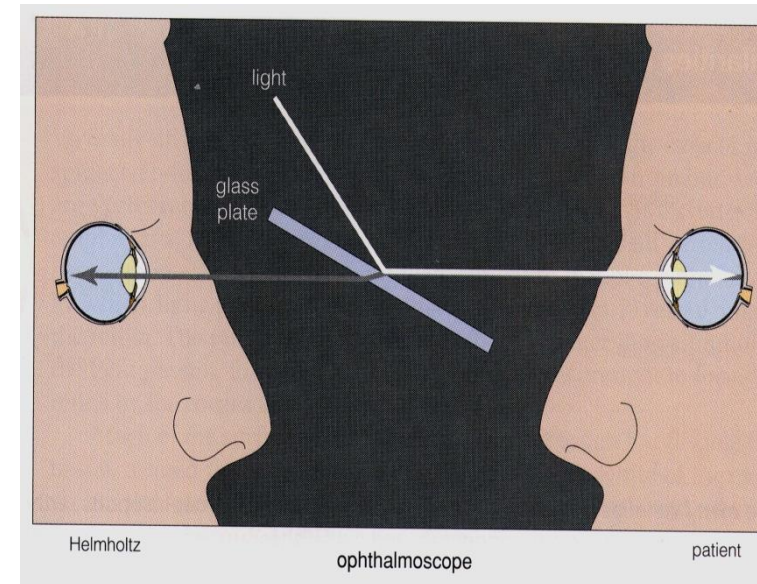
Hermann von Helmholtz



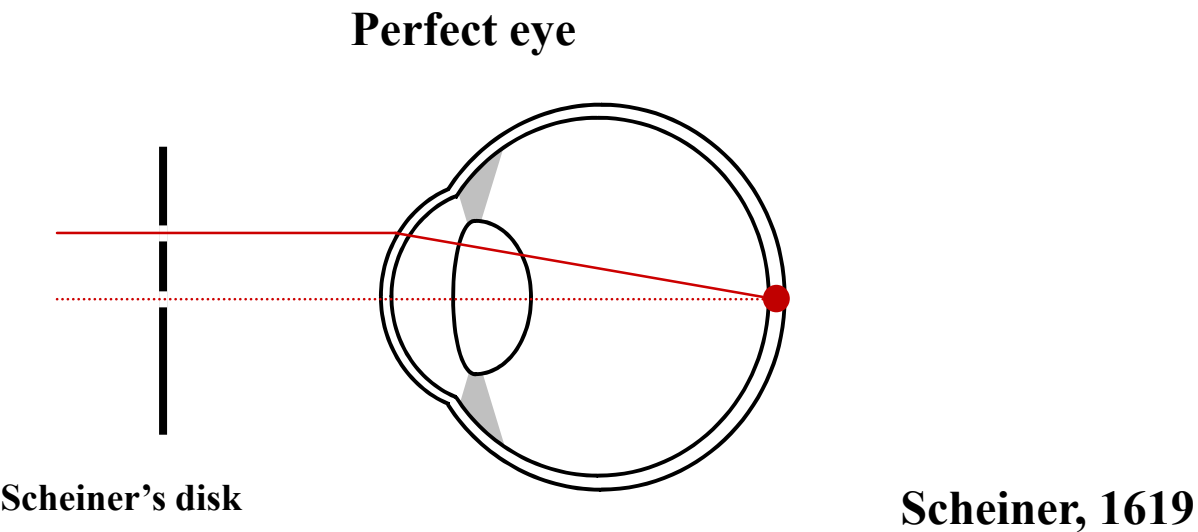
Ophthalmoscope



1st color fundus drawing
by Van Trigt, 1853

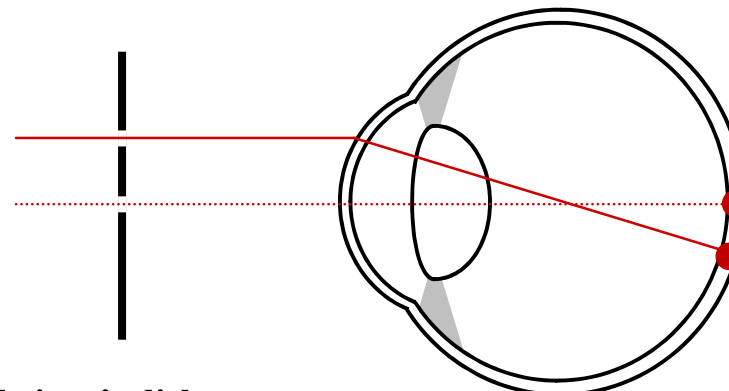


Measuring optical imperfections in the eye



Measuring optical imperfections in the eye

Myopic (Near-sighted) eye

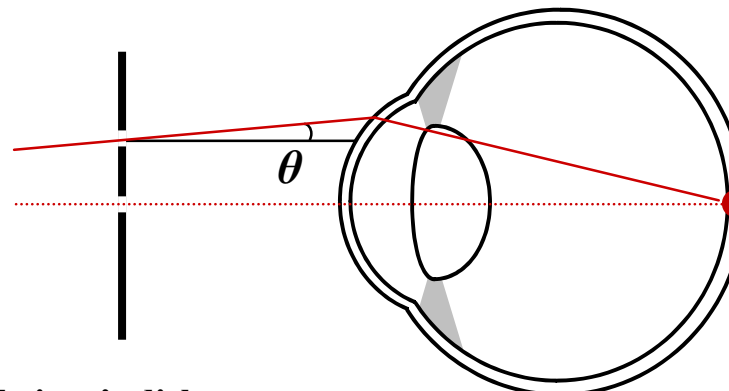


Scheiner's disk

Scheiner, 1619

Measuring optical imperfections in the eye

Myopic (Near-sighted) eye

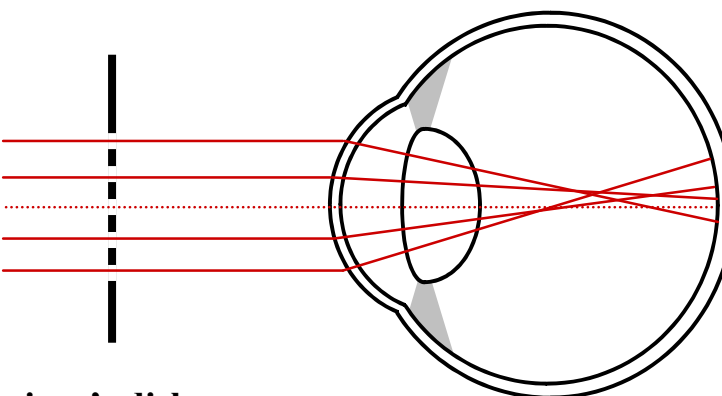


Scheiner's disk

Scheiner, 1619

Measuring optical imperfections in the eye

First measurement of higher order aberrations

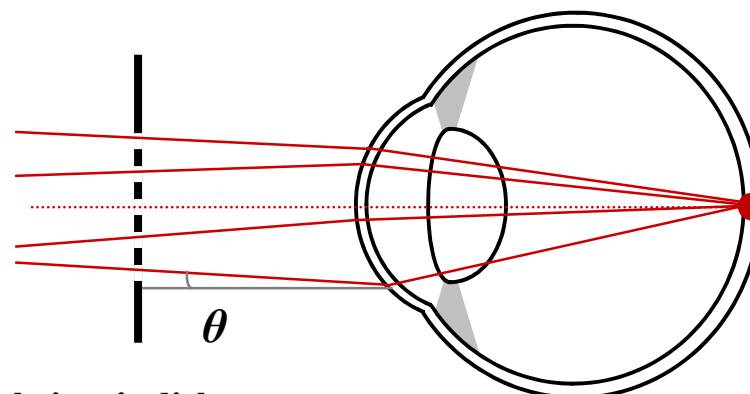


Scheiner's disk

Scheiner, 1619
Smirnov, 1961

Measuring optical imperfections in the eye

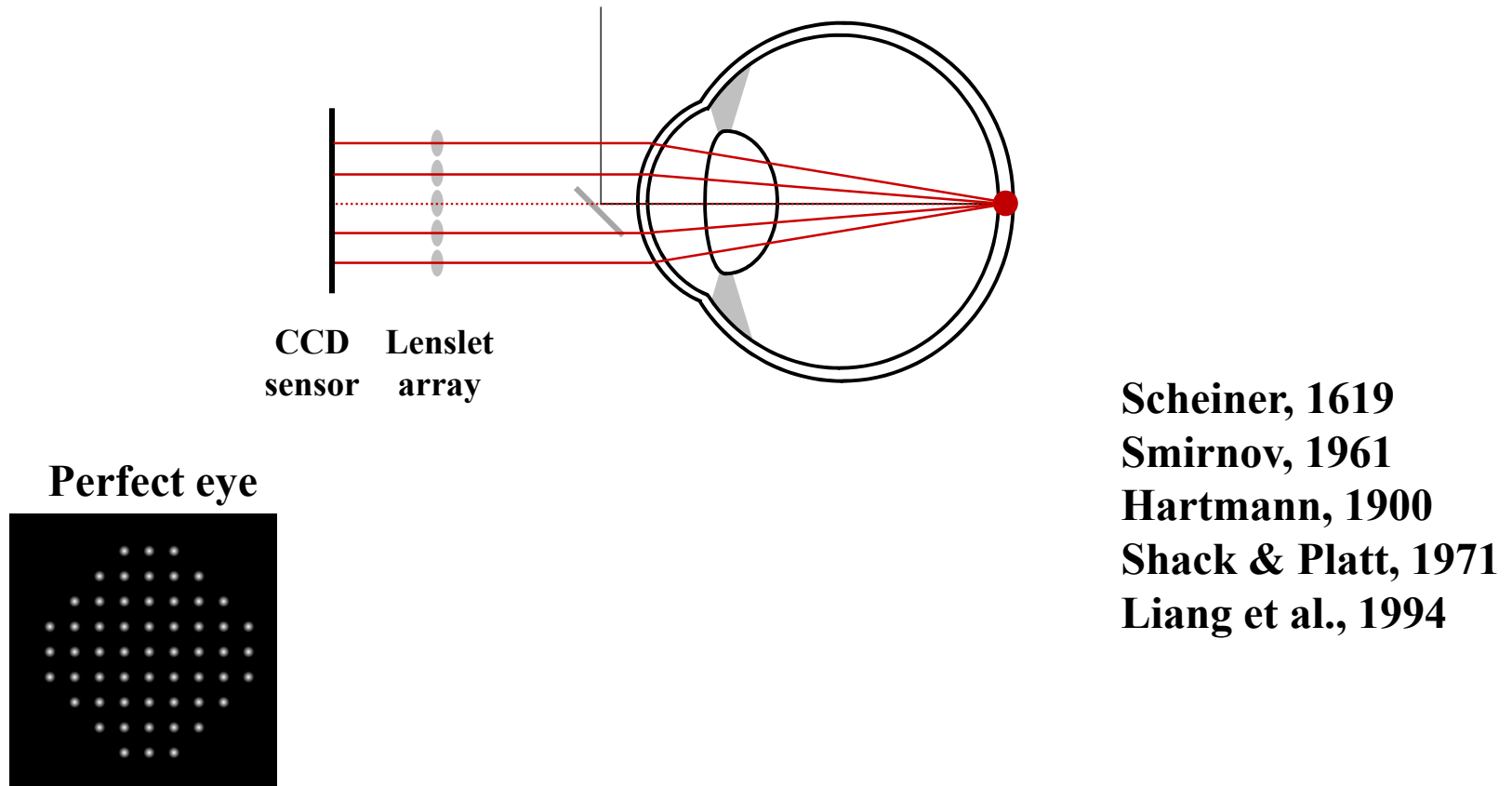
First measurement of higher order aberrations



Scheiner, 1619
Smirnov, 1961

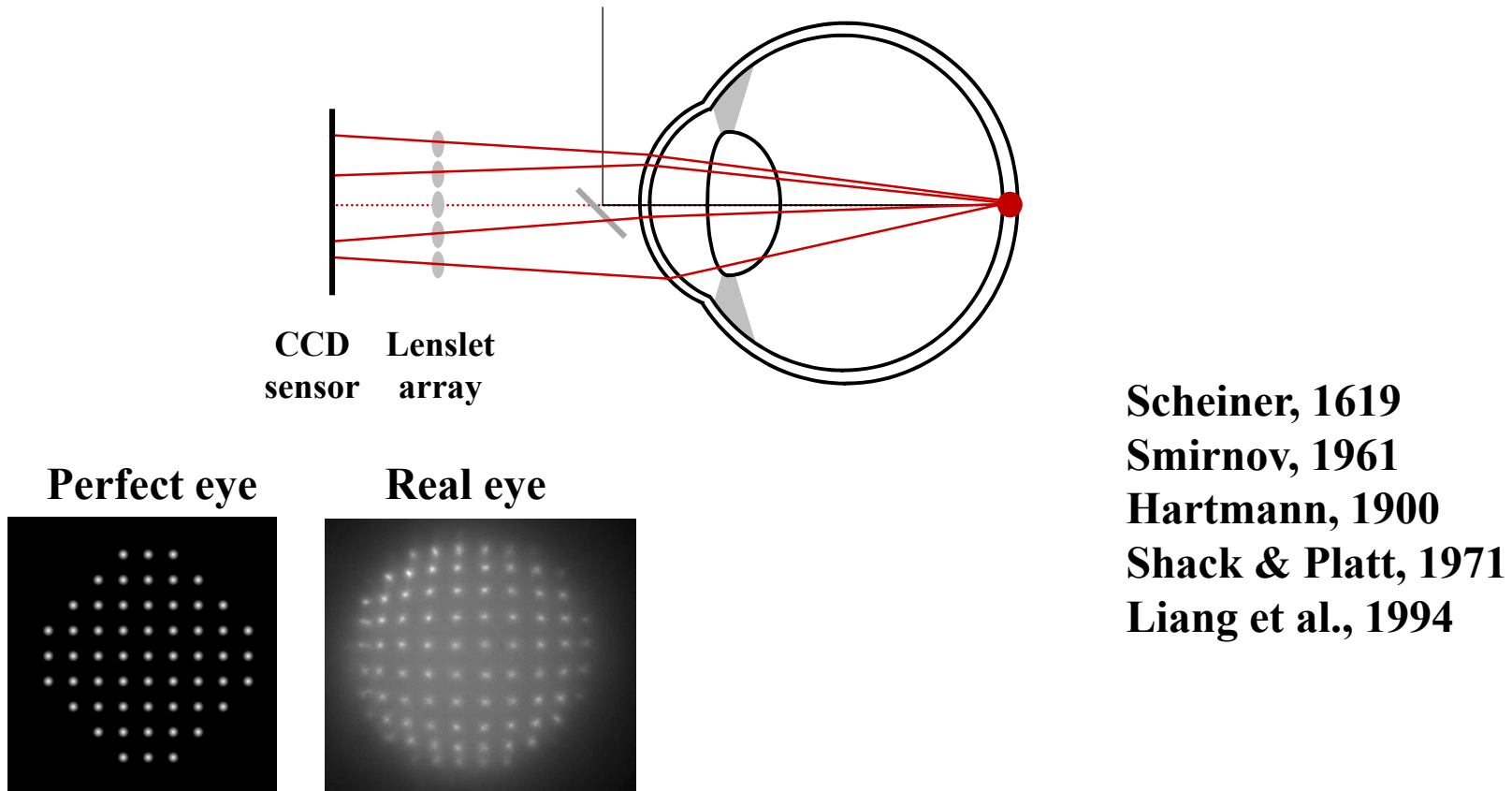
Measuring optical imperfections in the eye

Shack-Hartmann Wavefront Sensor

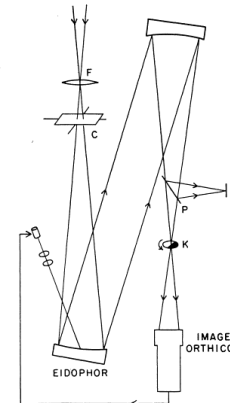


Measuring optical imperfections in the eye

Shack-Hartmann Wavefront Sensor



Adaptive Optics



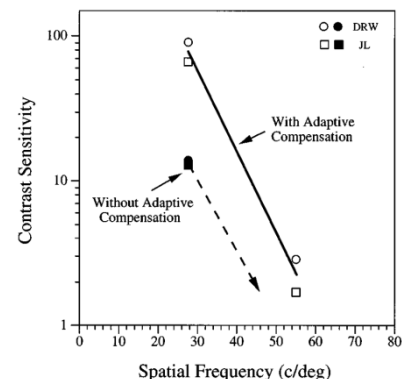
Babcock, H.W. The possibility of compensating astronomical seeing.(1953)

Supernormal vision and high-resolution retinal imaging through adaptive optics

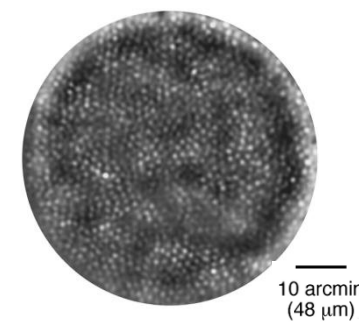
Junzhong Liang, David R. Williams, and Donald T. Miller*

Center for Visual Science, University of Rochester, Rochester, New York 14627

Vision correction



Retinal imaging

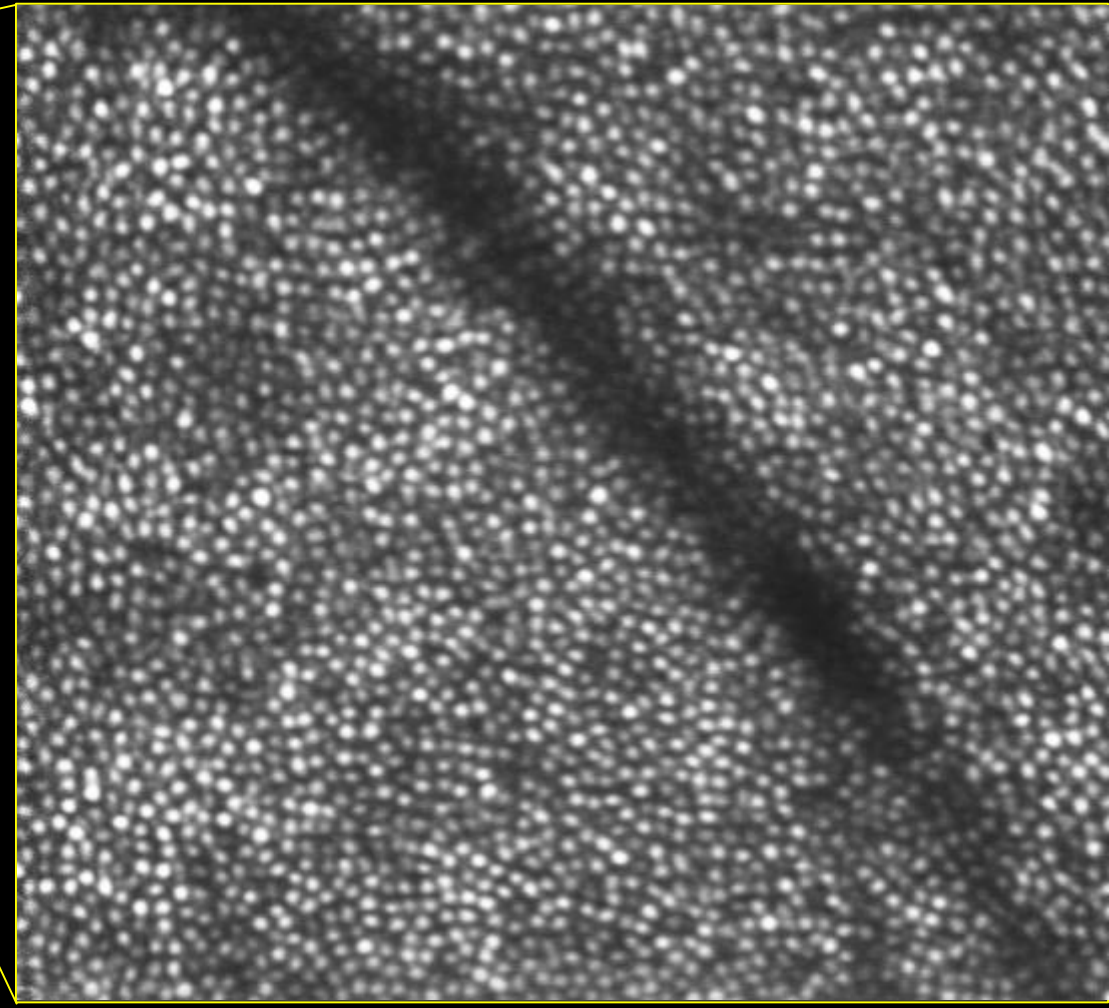
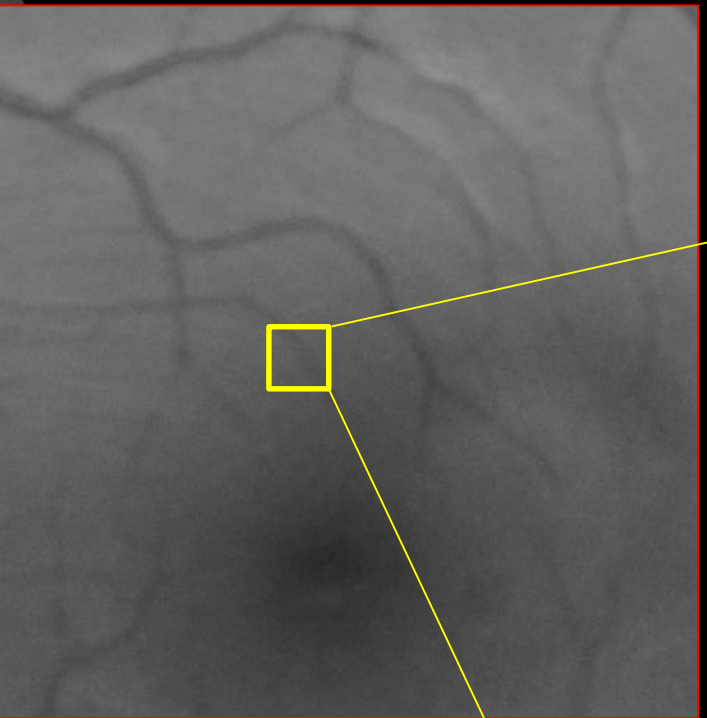
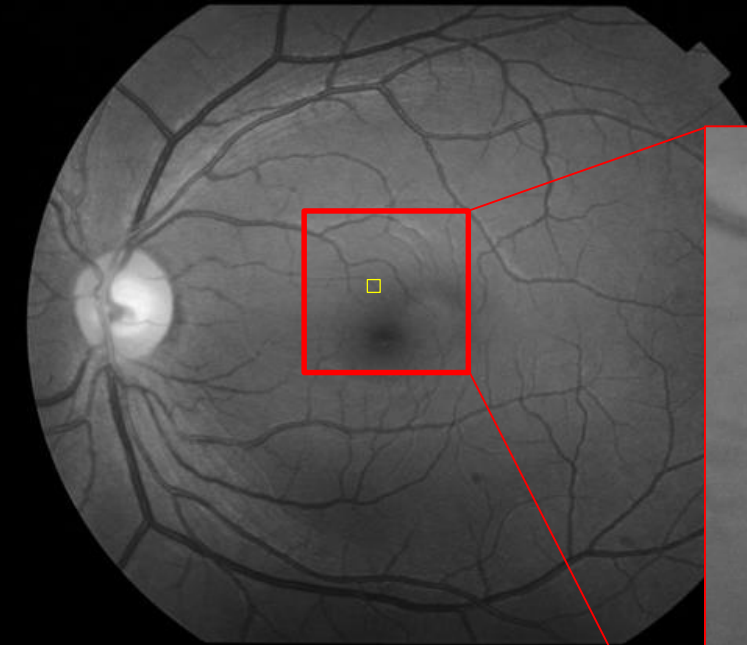


Adaptive Optics

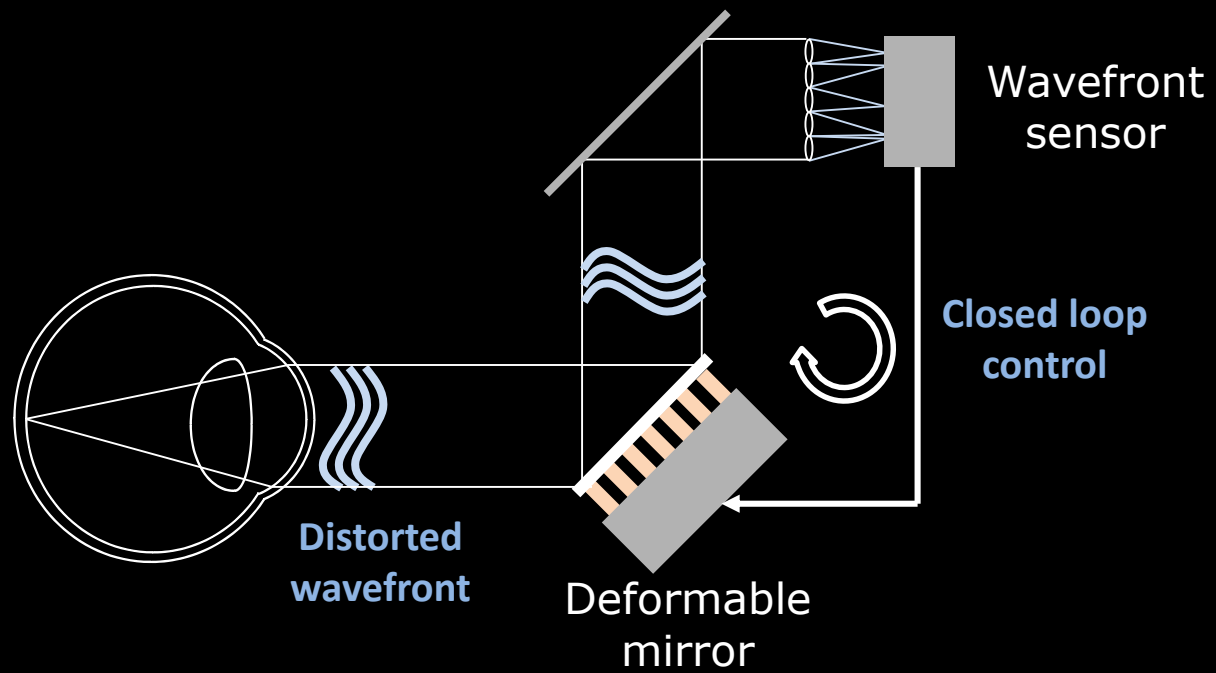
- key components -

- Illumination
 - Imaging
 - Wavefront sensing
 - Fluorescent excitation
 - ...
- Wavefront sensor
 - Microlens array and CCD/CMOS sensor
- Deformable mirror(DM)
 - Single DM : MEMS-based, Magnetic membrane, Segmented
 - Woofer-tweeter : two DMs, one each for large and small magnitude of aberration correction
- Detection
 - Photomultiplier tube (SLOs)
 - CCD/CMOS (Fundus camera)
 - Spectrometer (OCT)
 - Retina itself (vision correction or simulation)

Adaptive Optics



Adaptive Optics



Adaptive Optics

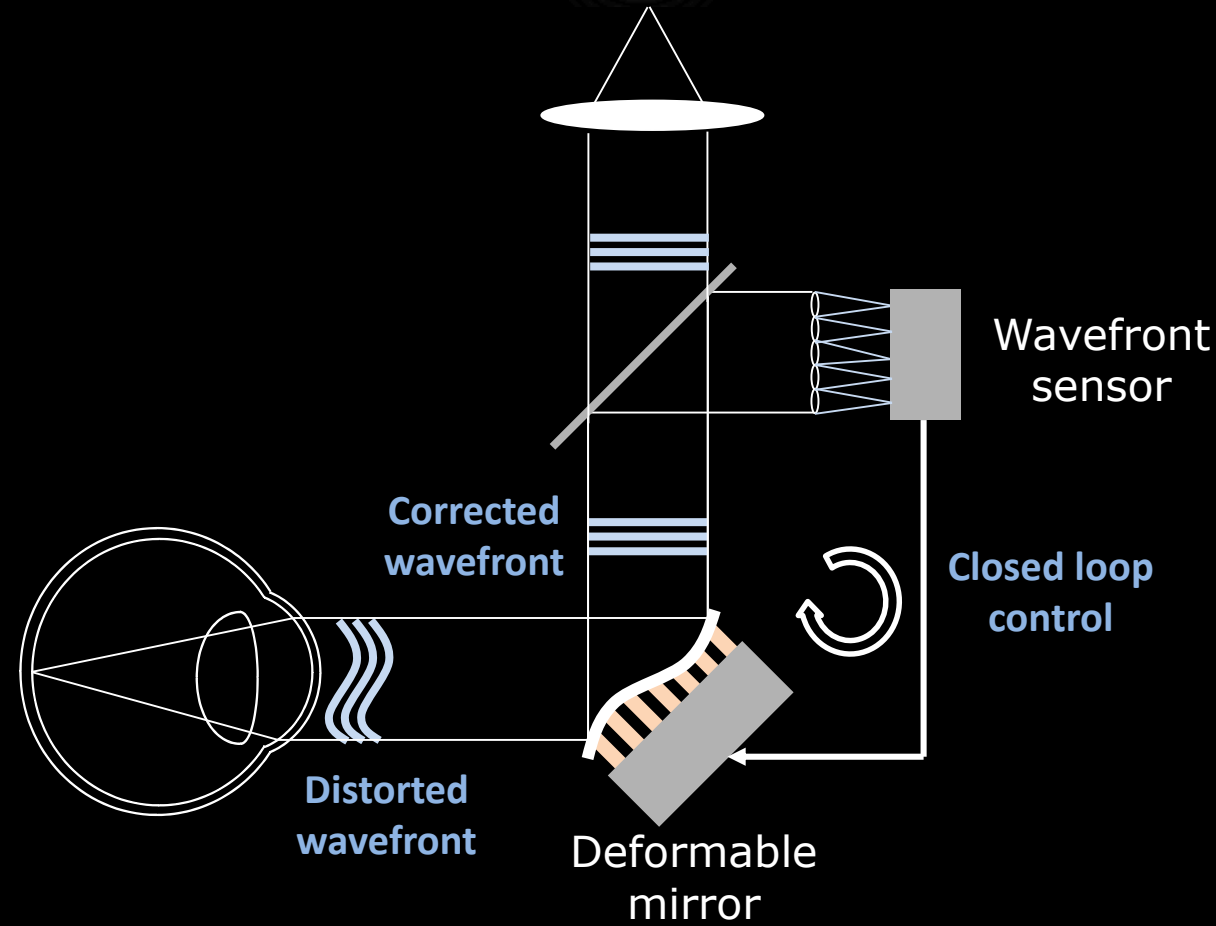
Visual function

Vision Correction &
Simulation

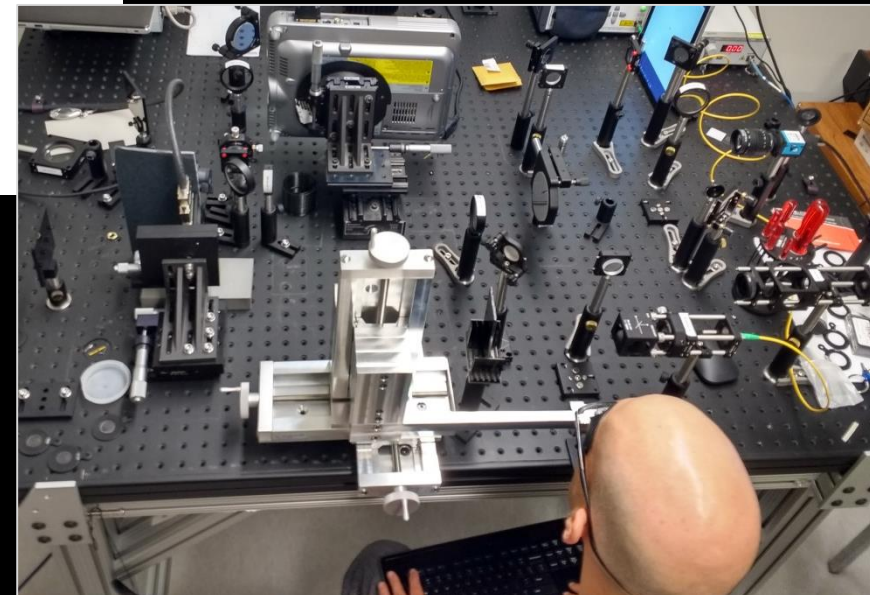
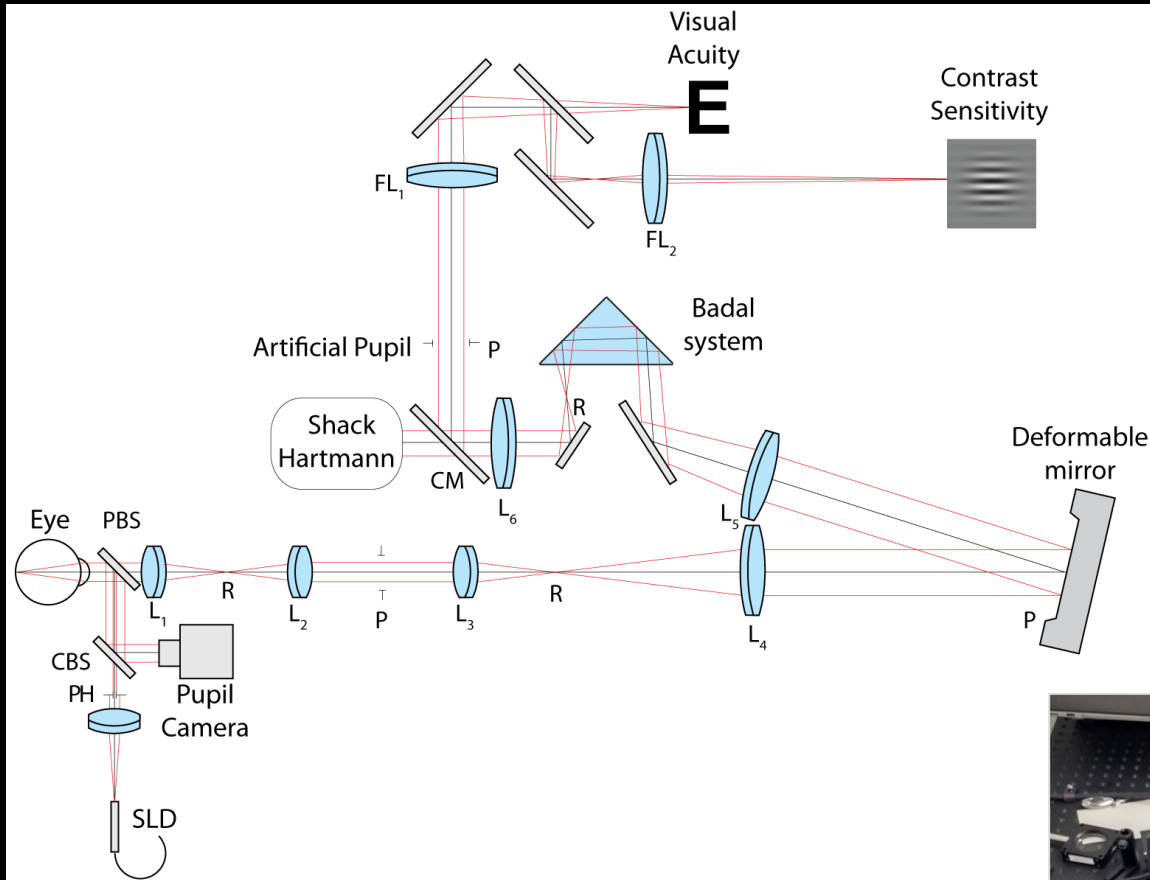


Retinal structure

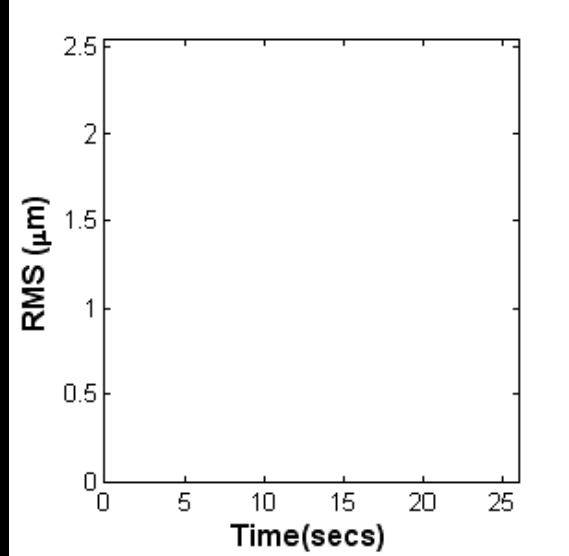
SLO, OCT,
fundus camera ...



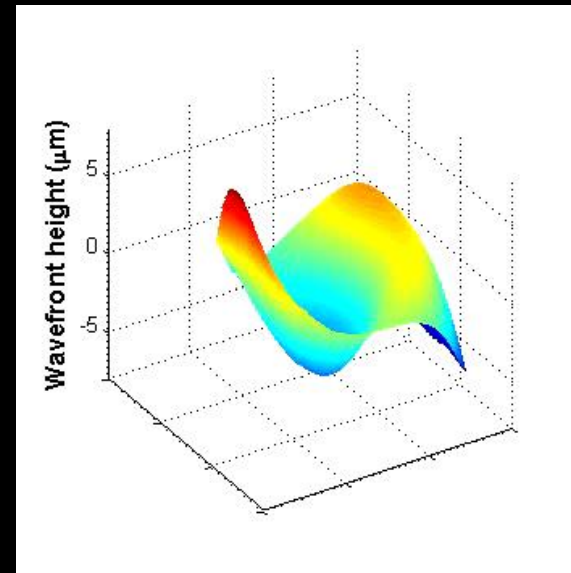
AO for Vision Simulation & Correction : No imaging



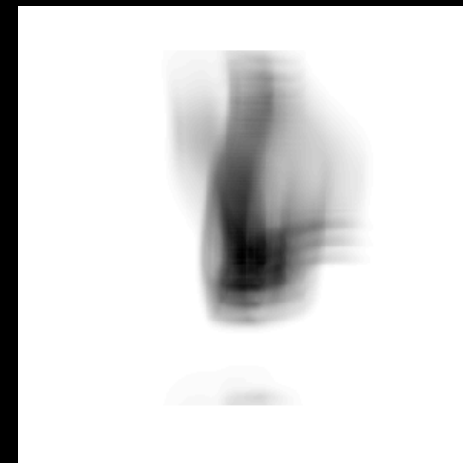
Time-course of aberration correction



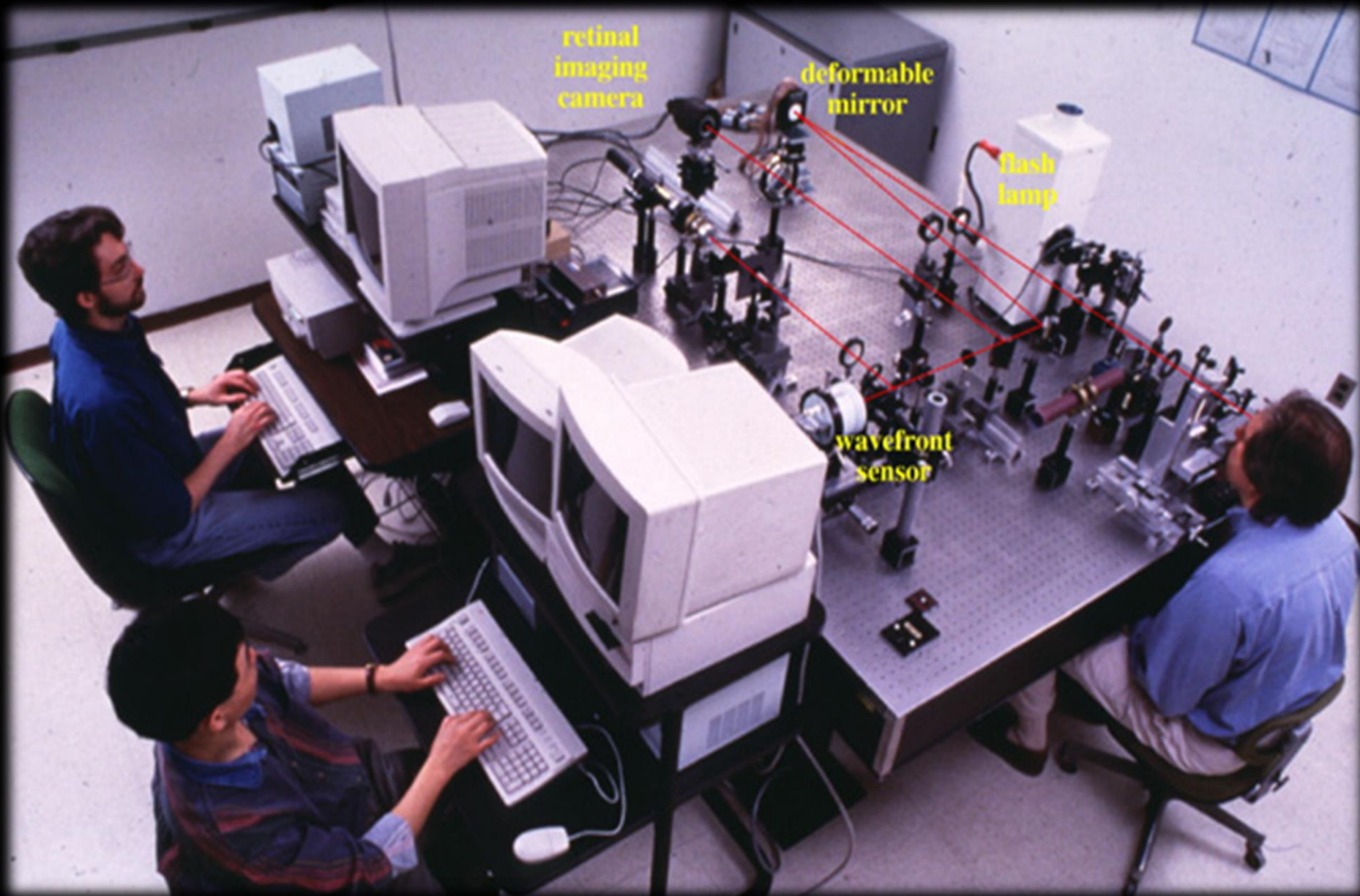
Wavefront



Retinal Image Quality

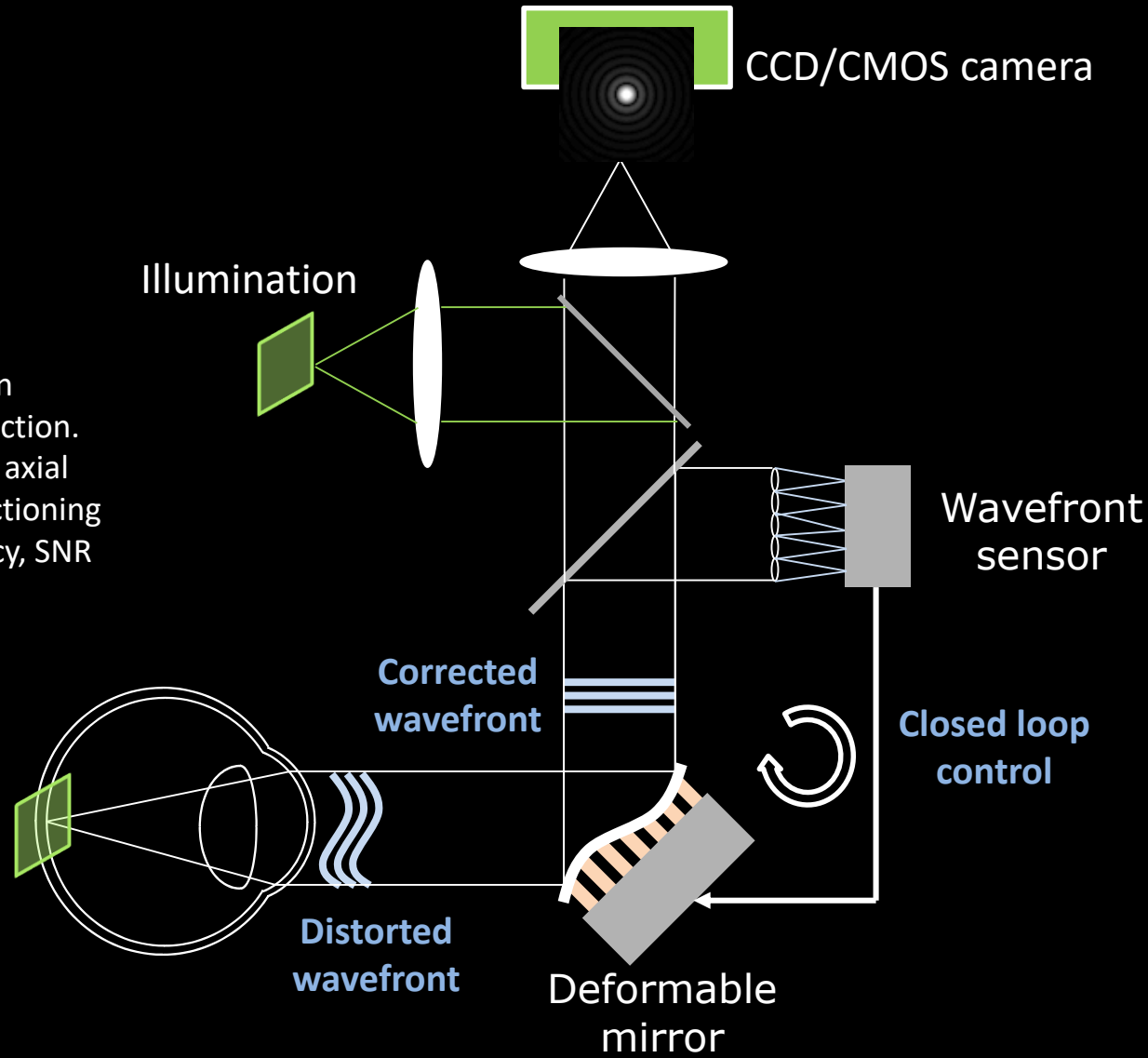


Adaptive Optics Ophthalmoscope, University of Rochester, 1996

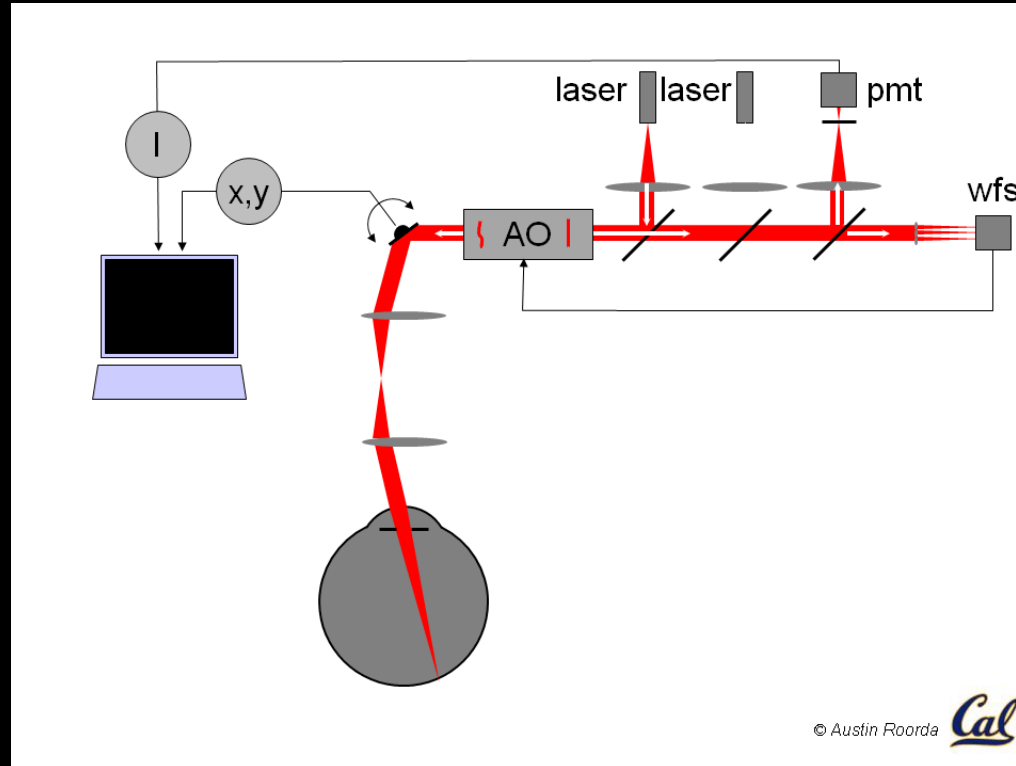


Adaptive Optics Fundus (flood-illuminated) camera

- Extended illumination
- Area camera for detection.
- No confocality : poor axial resolution, hence sectioning
- Limited light efficiency, SNR



Adaptive Optics Scanning Laser Ophthalmoscope



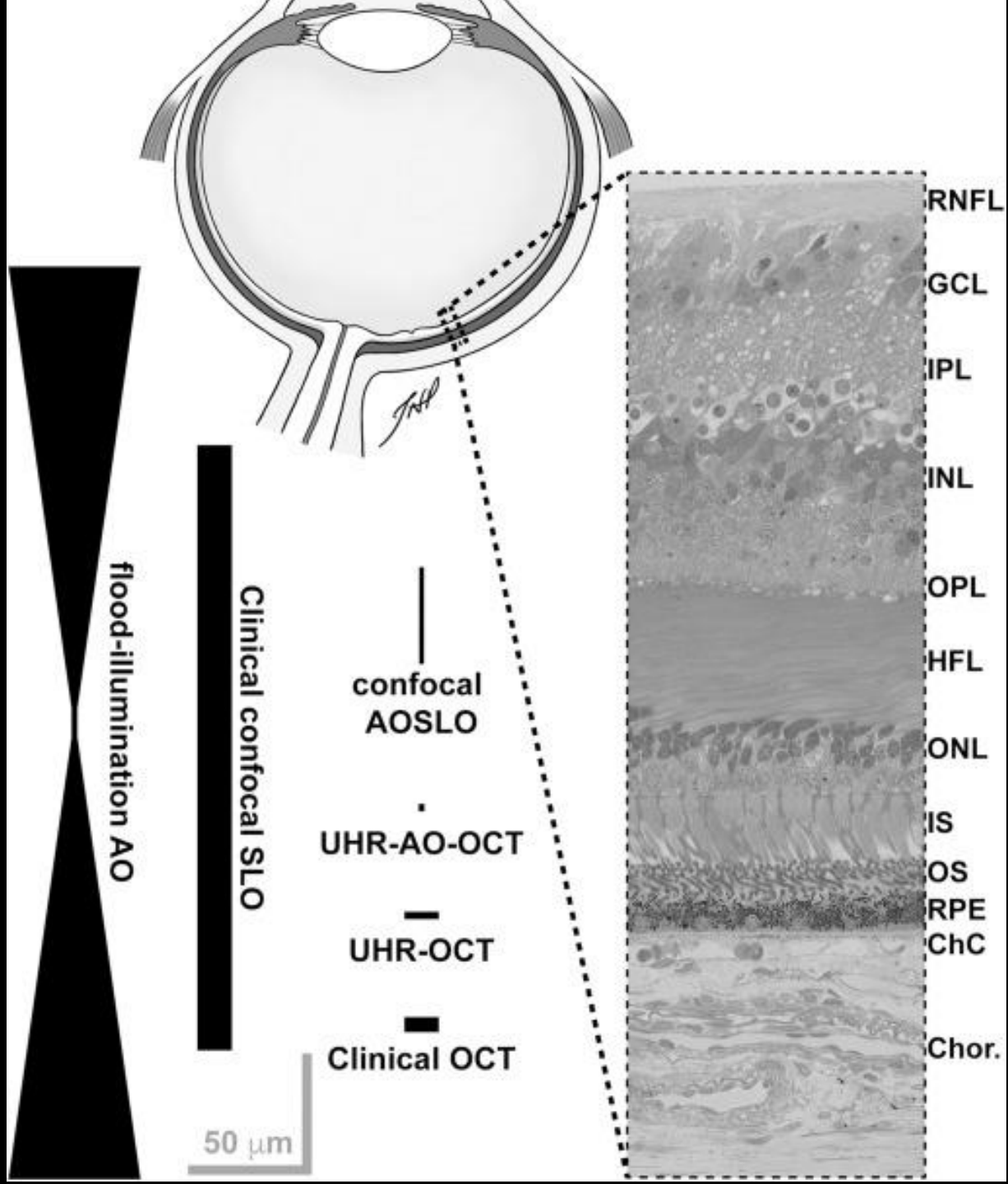
© Austin Roorda *Cal*

Fundus camera

- Extended illumination
- Area camera for detection.
- No confocality : poor axial resolution, hence sectioning
- Poor light efficiency, SNR

SLO

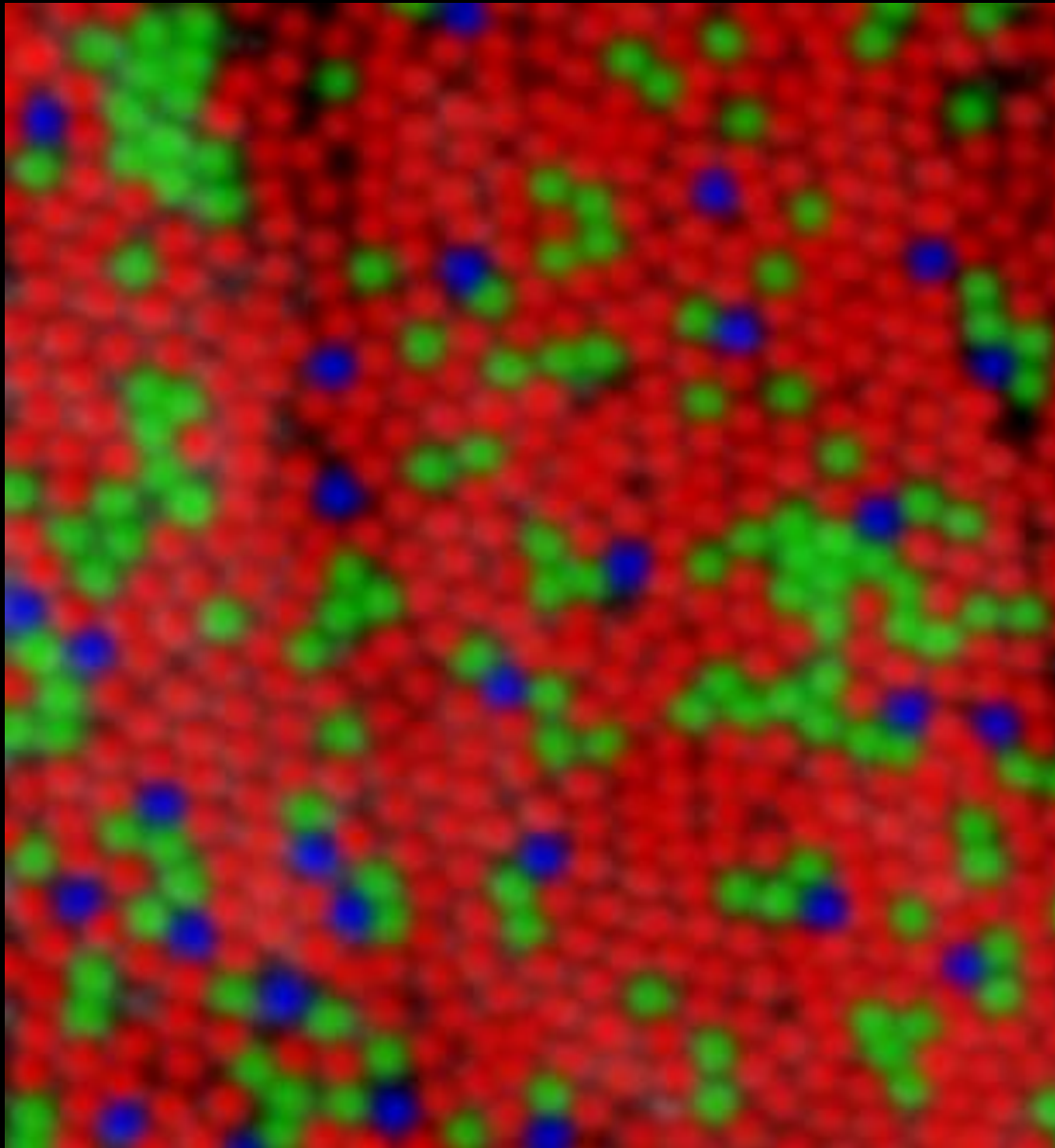
- Point illumination
- Photomultiplier or avalanche photodiode for detection
- Confocal : good axial resolution
- High SNR



First images of the human trichromatic cone mosaic



Austin Roorda



human cone mosaic ~ 300 microns from fovea

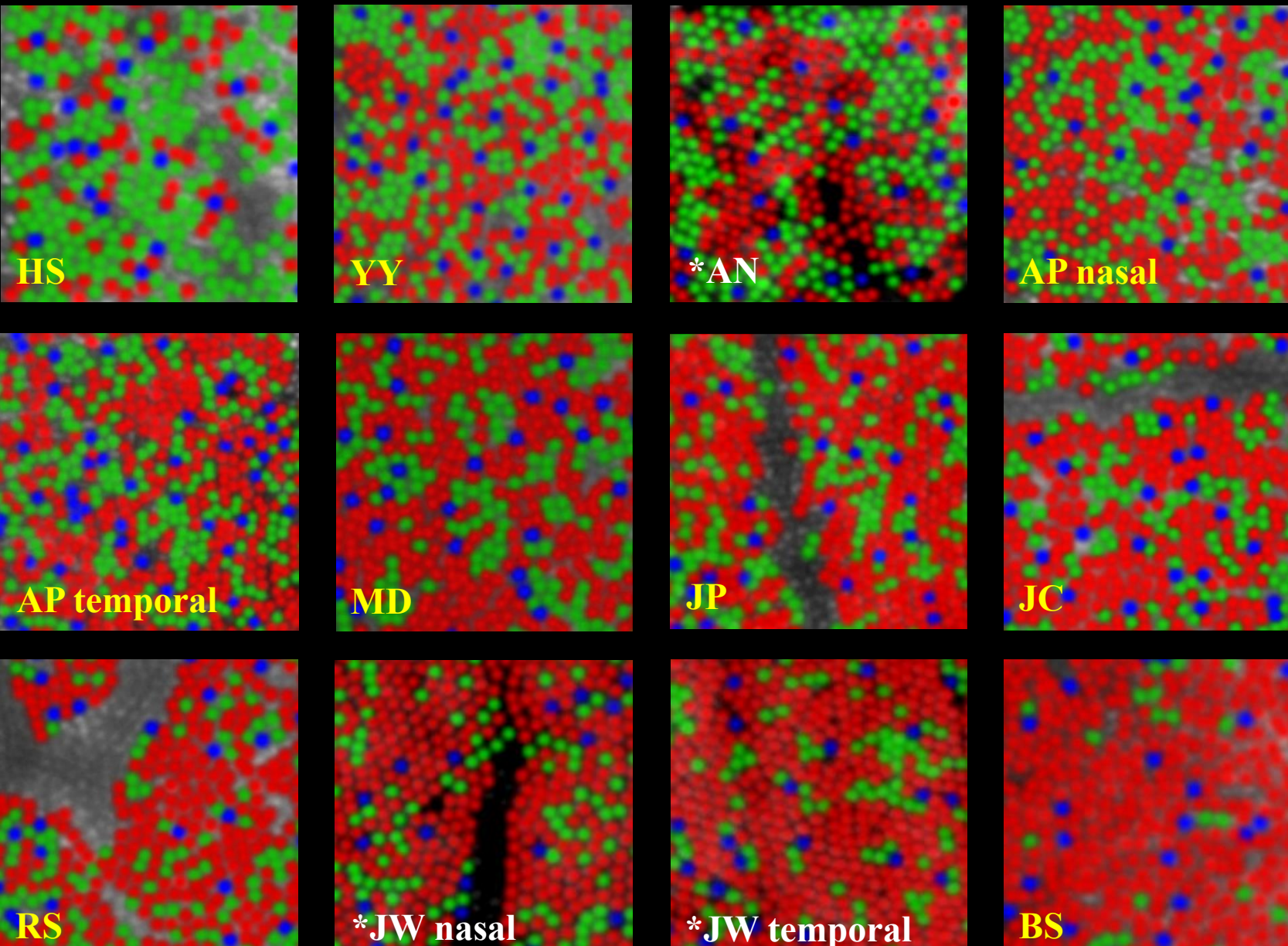
Roorda and Williams, Nature, 2001

Photoreceptors

● L-cone

● M-cone

● S-cone



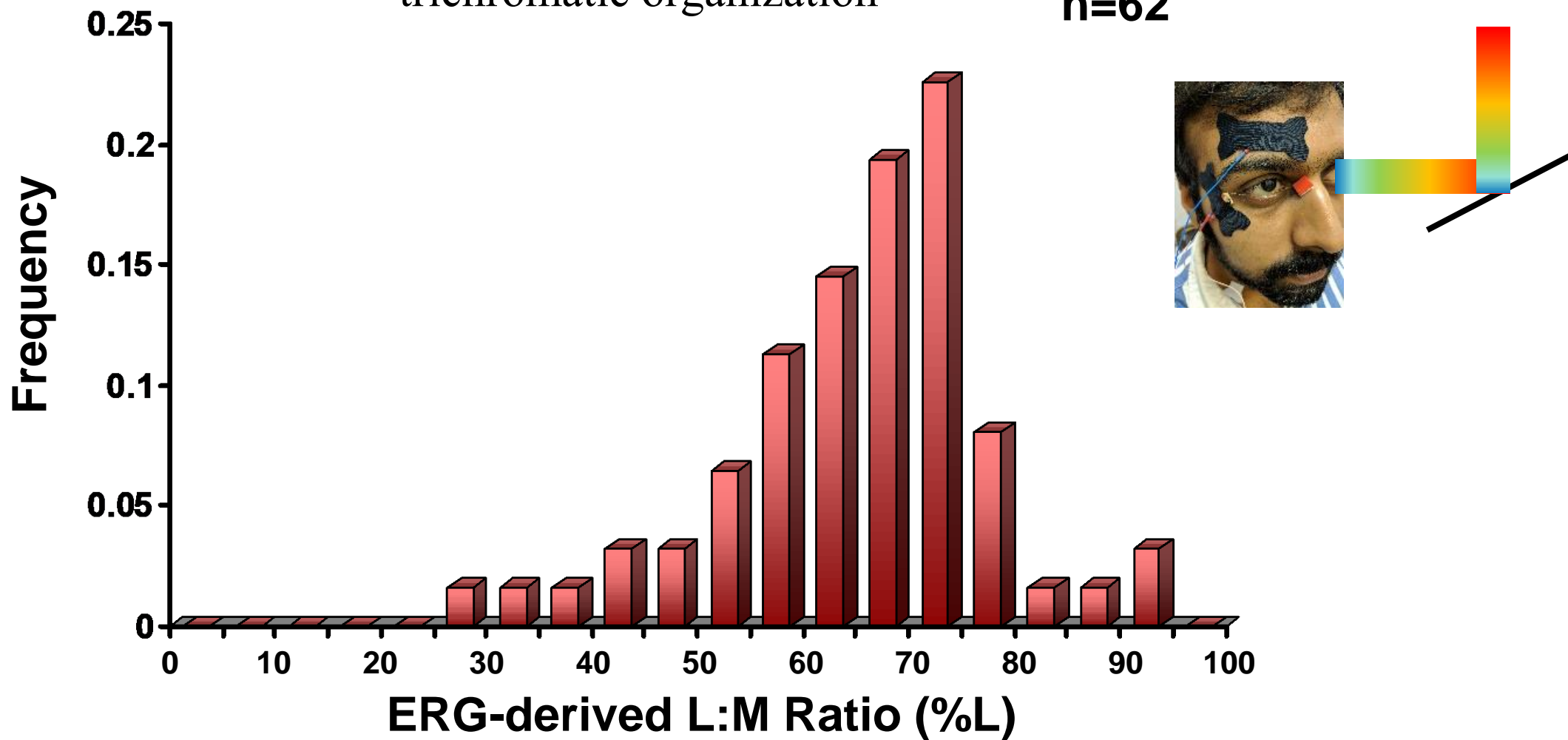
5 arcmin

* Roorda & Williams (*Nature* 1999)

Cones

- trichromatic organization-

n=62



From Carroll, Neitz, & Neitz (2002)

Variation with retinal eccentricity

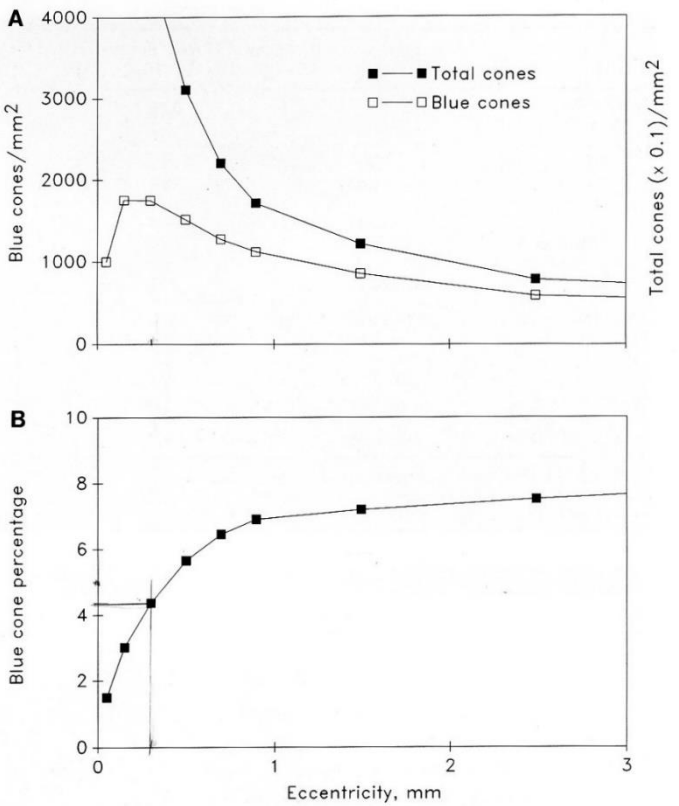
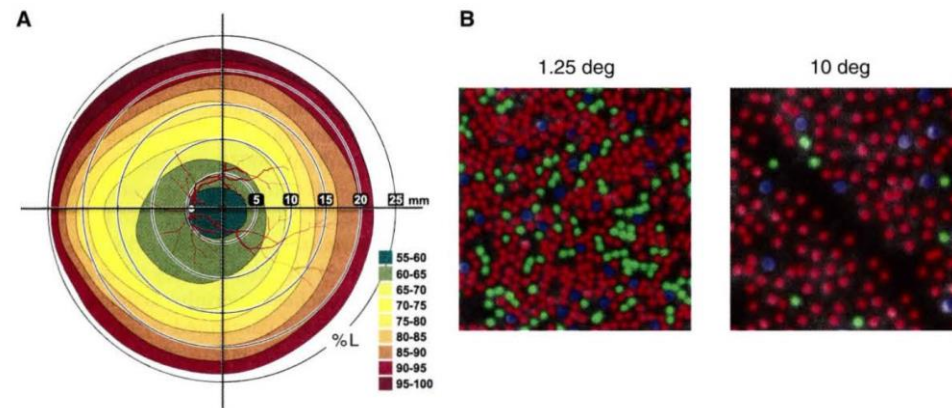
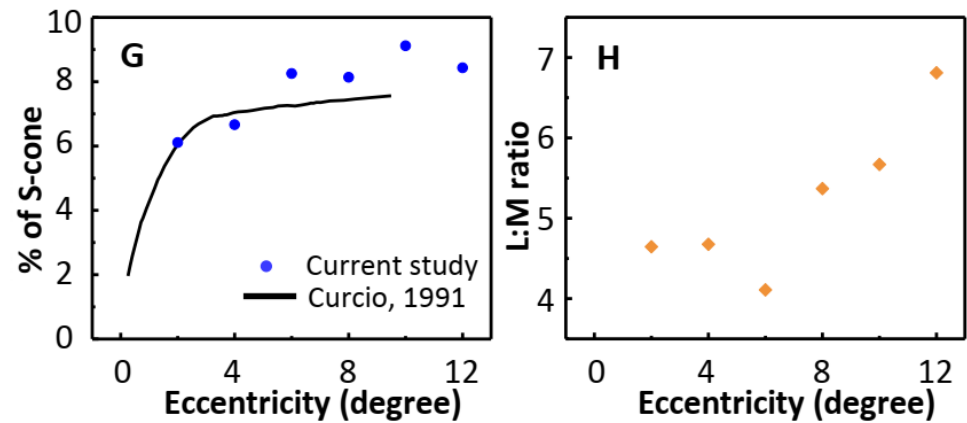


Fig. 8. **A.** Blue cone density (averaged across meridians) decreases less rapidly with eccentricity than the overall cone population. **B.** The proportion of cones that are blue increases with eccentricity. In order to generate these two graphs, the total number of cells and the total area in the entire model of the average retina were calculated for disks of ever-increasing diameter in a “bullseye” pattern centered on the fovea. A mean density was then calculated for each eccentricity ring in the bullseye.

Curcio CA, Allen KA, Sloan KR, Lerea CL, Hurley JB, Klock IB, Milam AH. (1991). Distribution and Morphology of Human Cone Photoreceptors Stained with Anti-Blue Opsin. *J. of Comparative Neurology* 312:610-624.

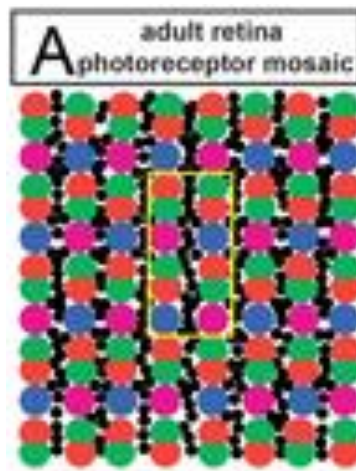


Hofer and Williams, Color vision and the Retinal Mosaic,
The New Visual Neurosciences, ed. Werner Chalupa

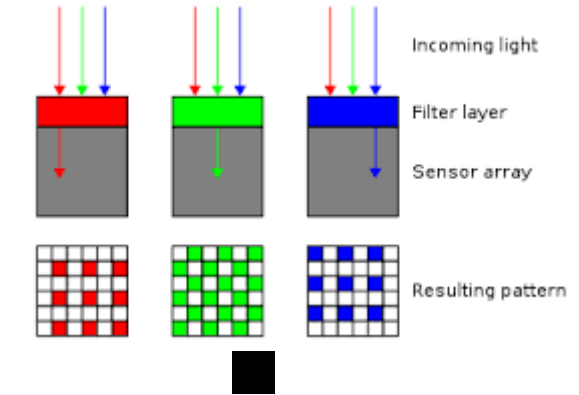
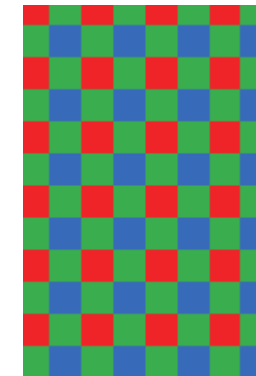


Zhang et al. PNAS 2019

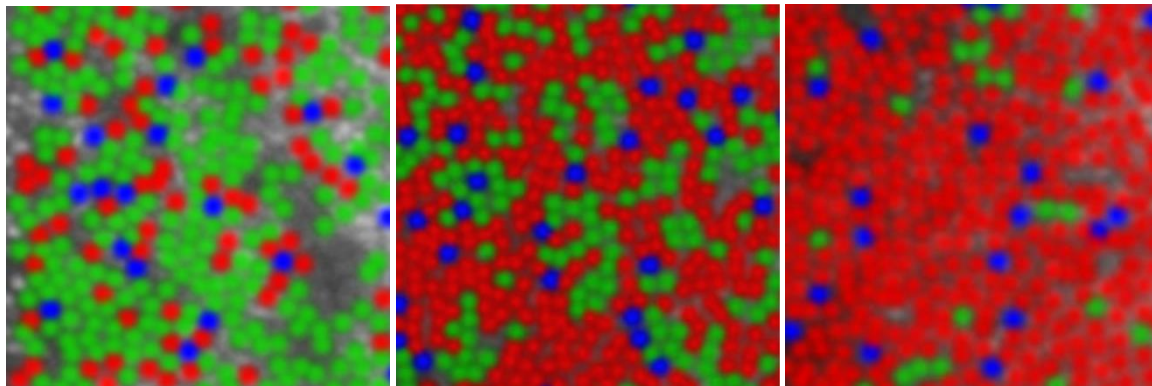
Zebra fish retina



Color CCD chip - Bayer filter -

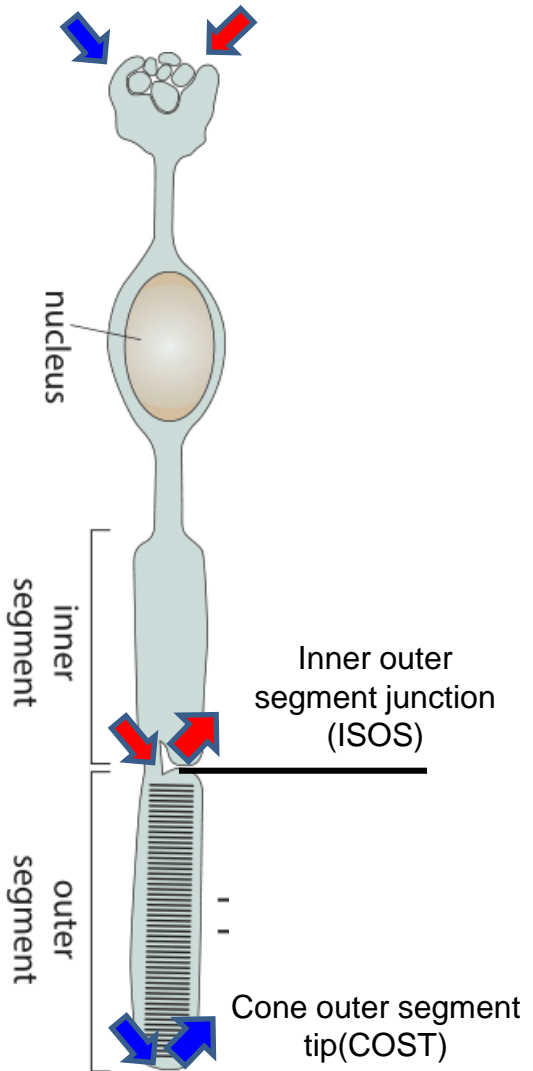
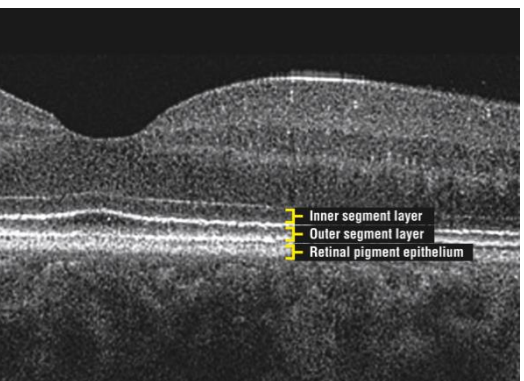


Human cone photoreceptor mosaic

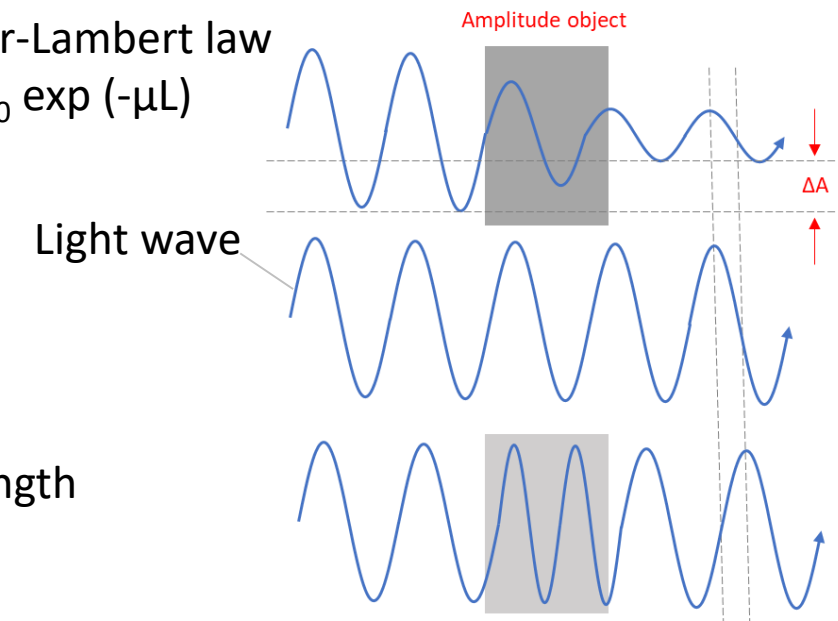


Light-evoked optical changes in cone photoreceptors

- Intensity
- Phase



Beer-Lambert law
 $I = I_0 \exp (-\mu L)$



$$\Delta\phi = \frac{2\pi}{\lambda} \times \text{OPL}$$

$$\text{OPL} = n \times T$$

OPL- Optical path length

n- refractive index

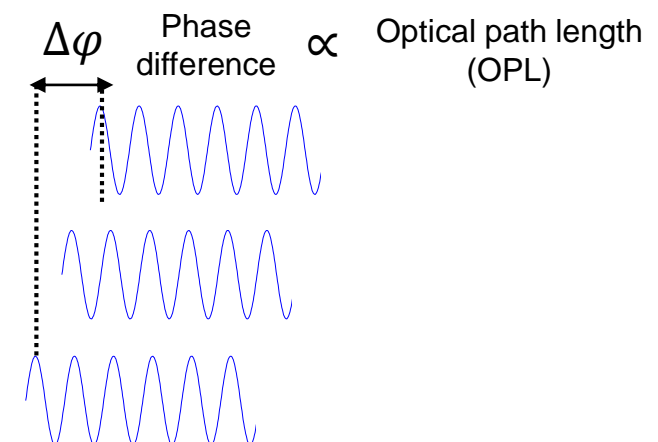
T- thickness

Light scattered from ISOS

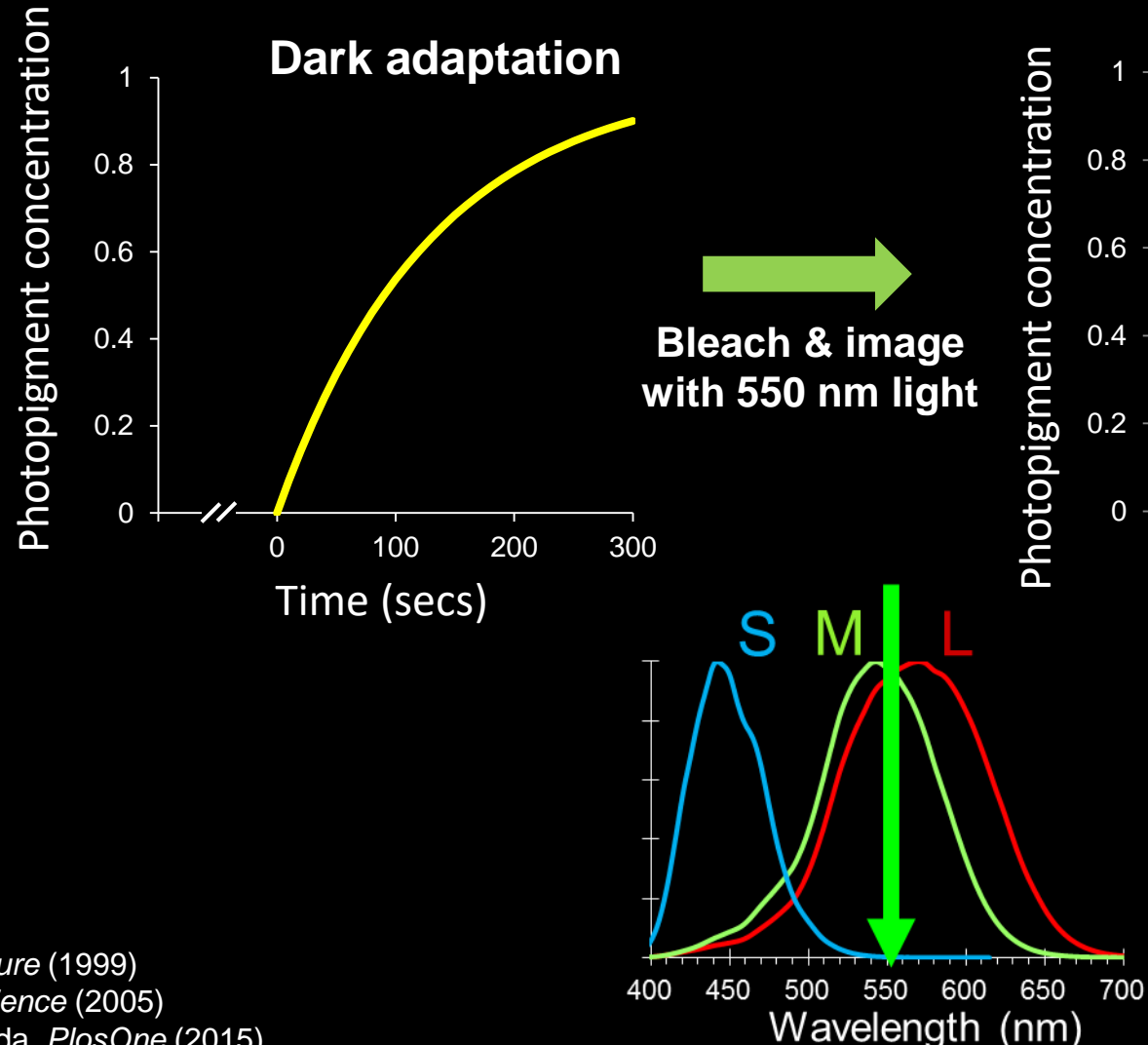
Light scattered from COST

Light scattered from COST
after Δt

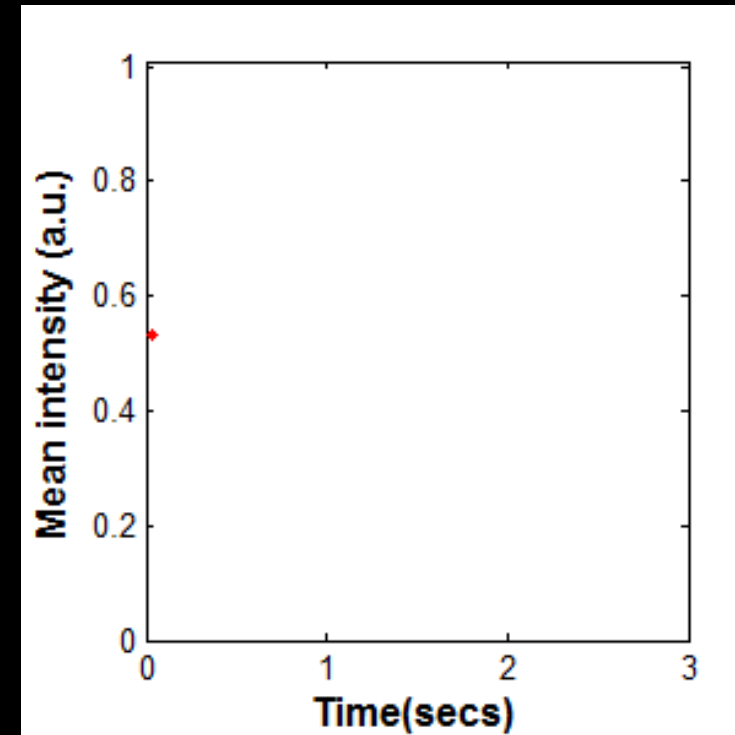
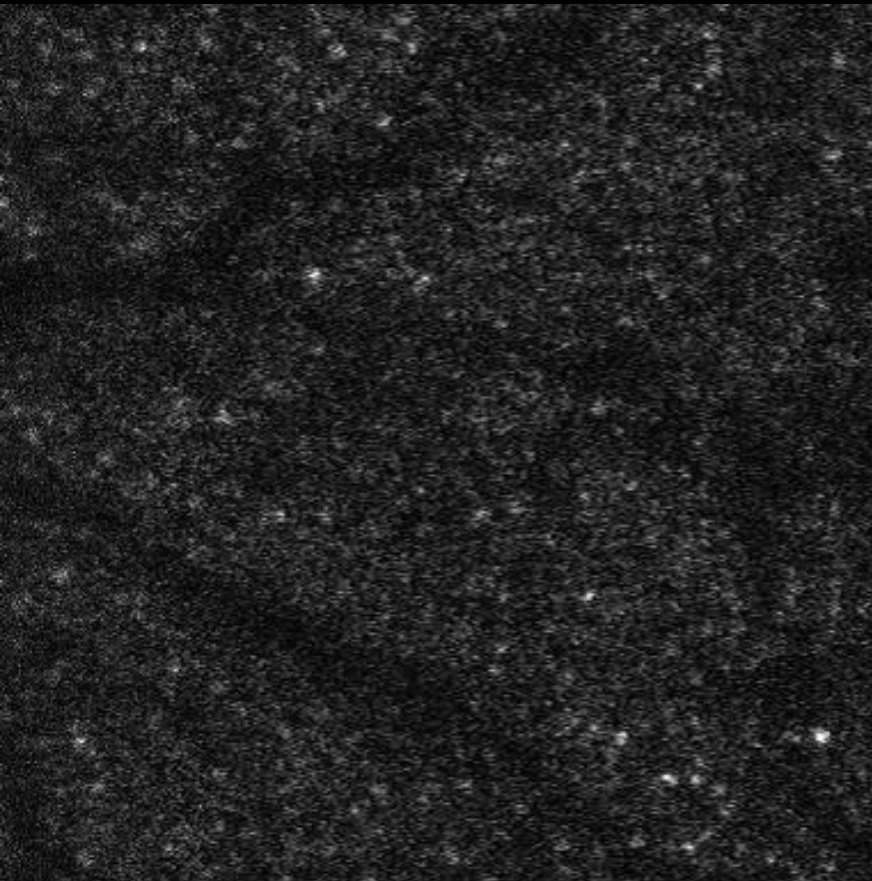
Light scattered from COST
after $2\Delta t$

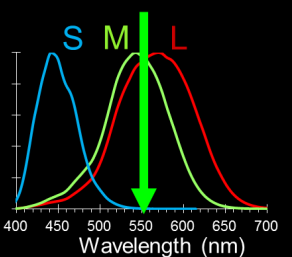


Identifying the spectral type of a cone via densitometry



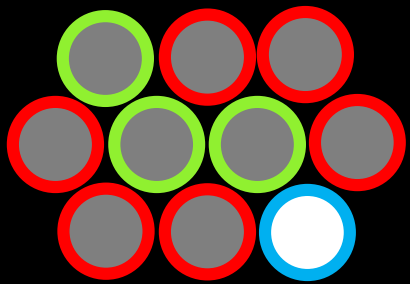
Dark adapted → Fully bleached retina
S-cones



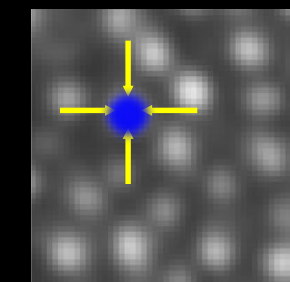
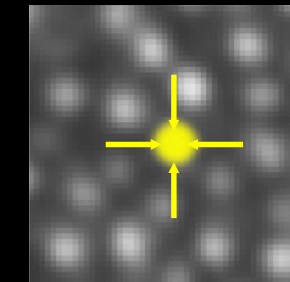
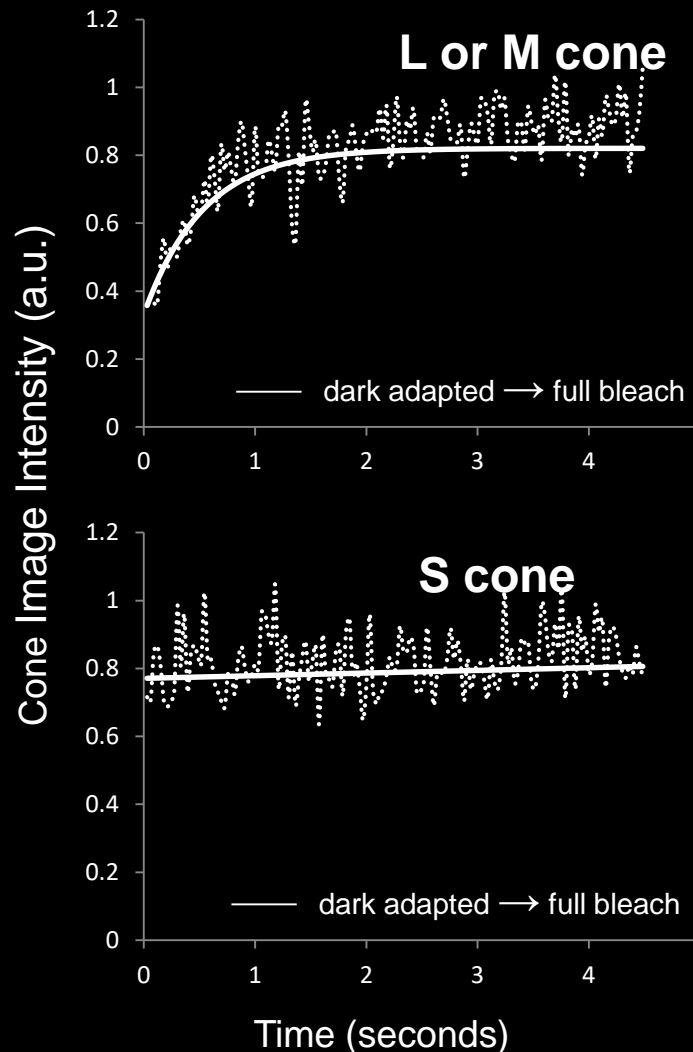
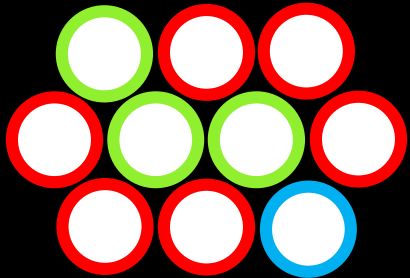


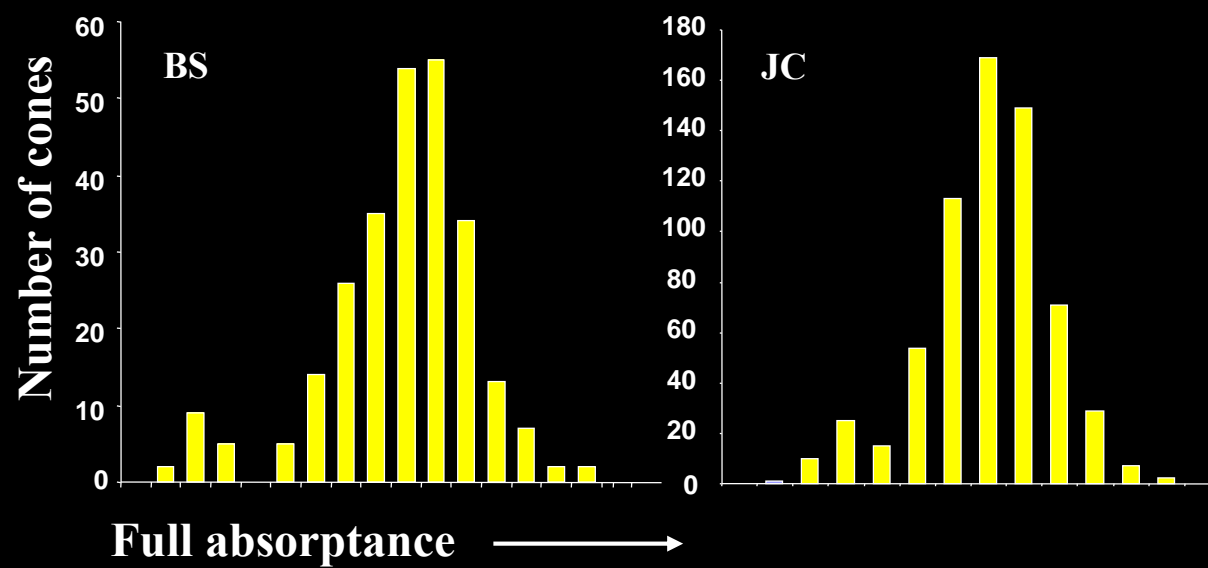
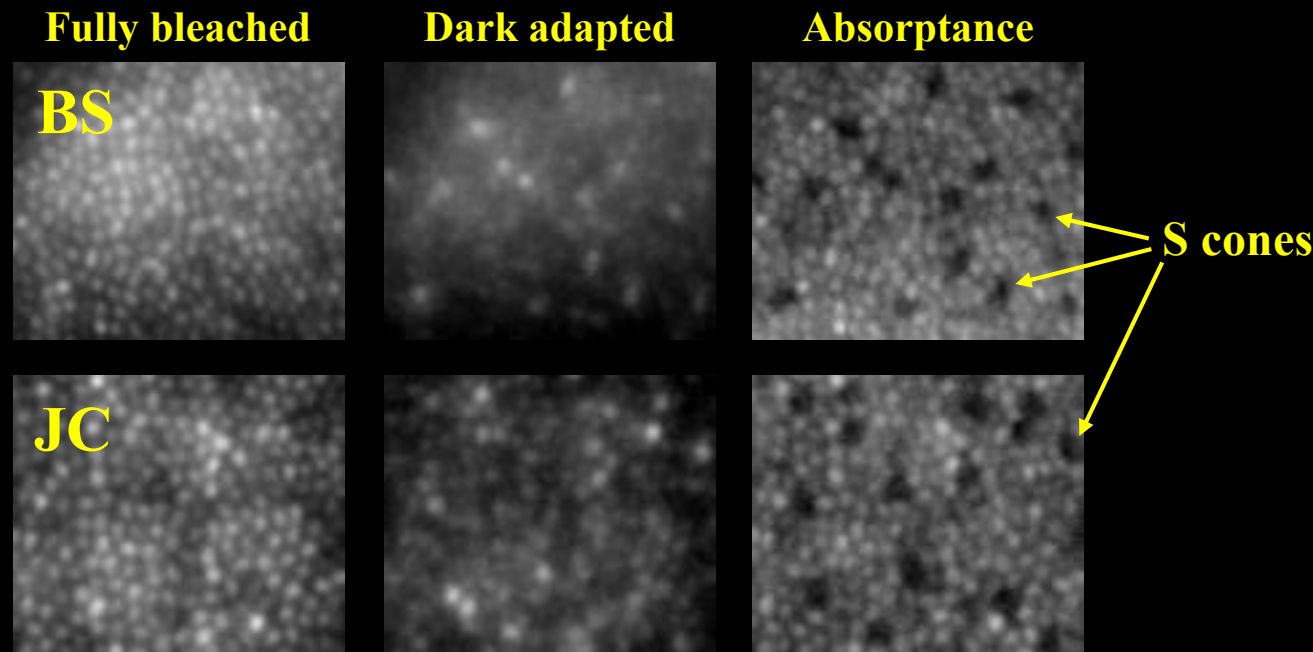
Isolating S-cones

550 nm image after 5 min
dark adaptation

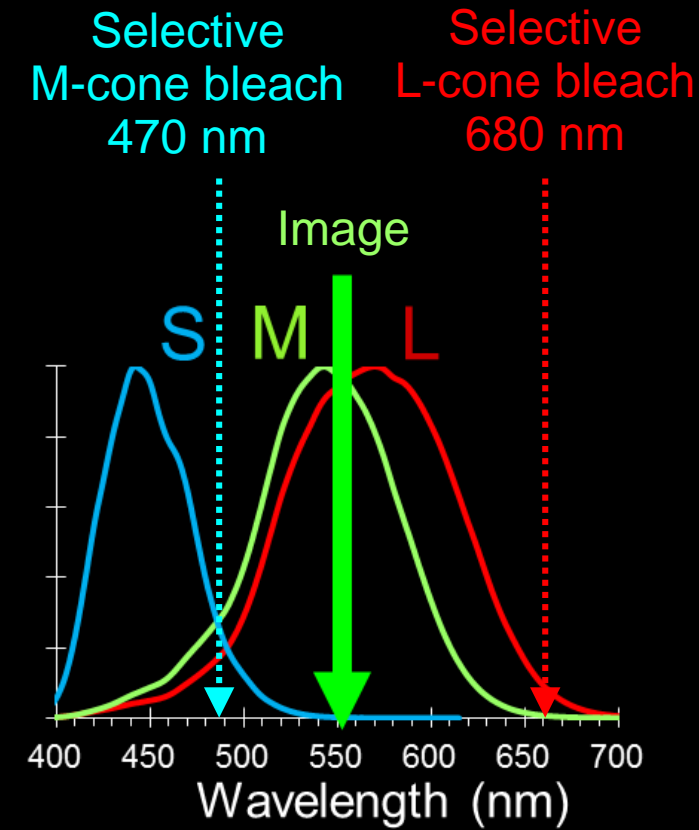
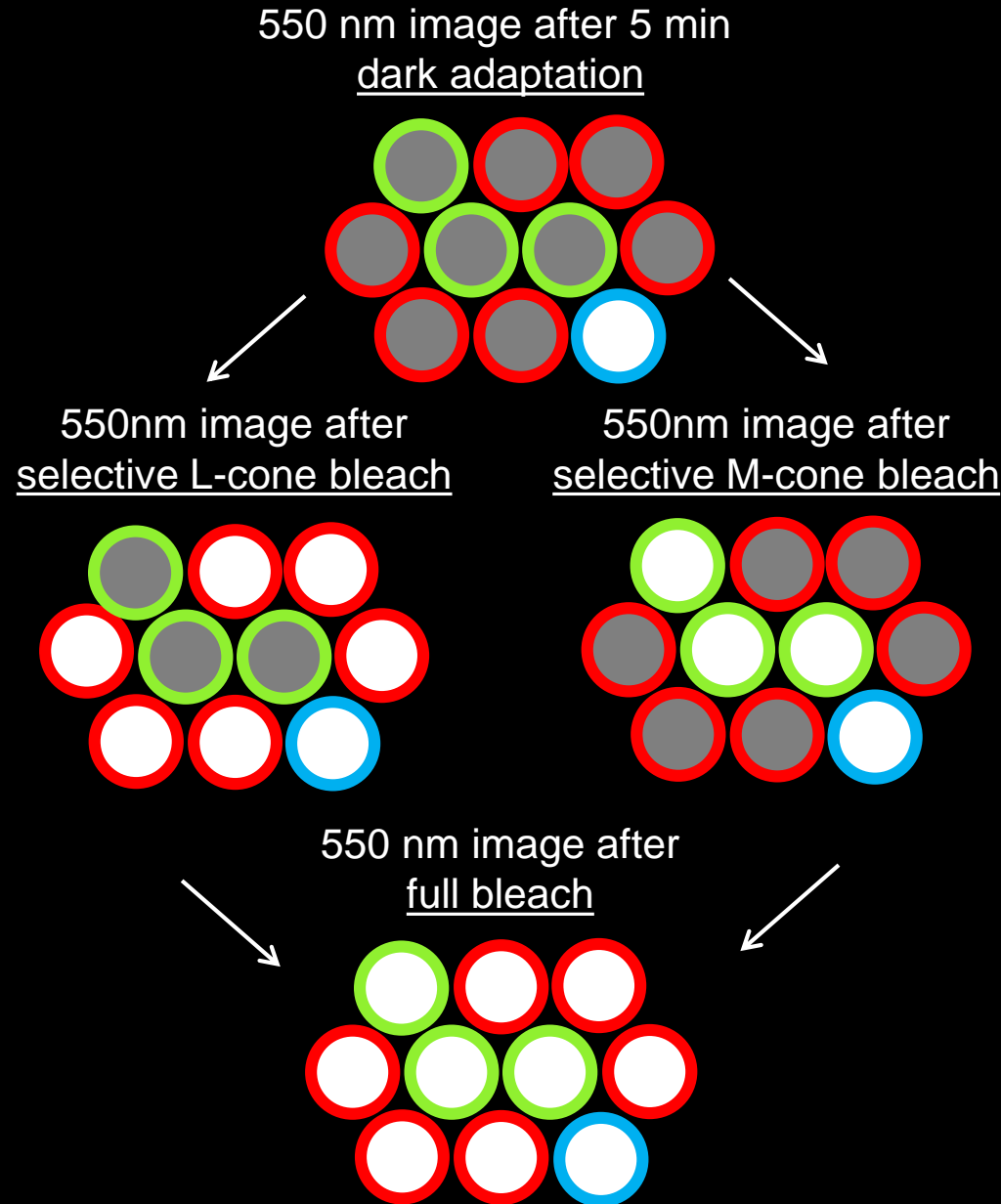


550 nm image after
full bleach

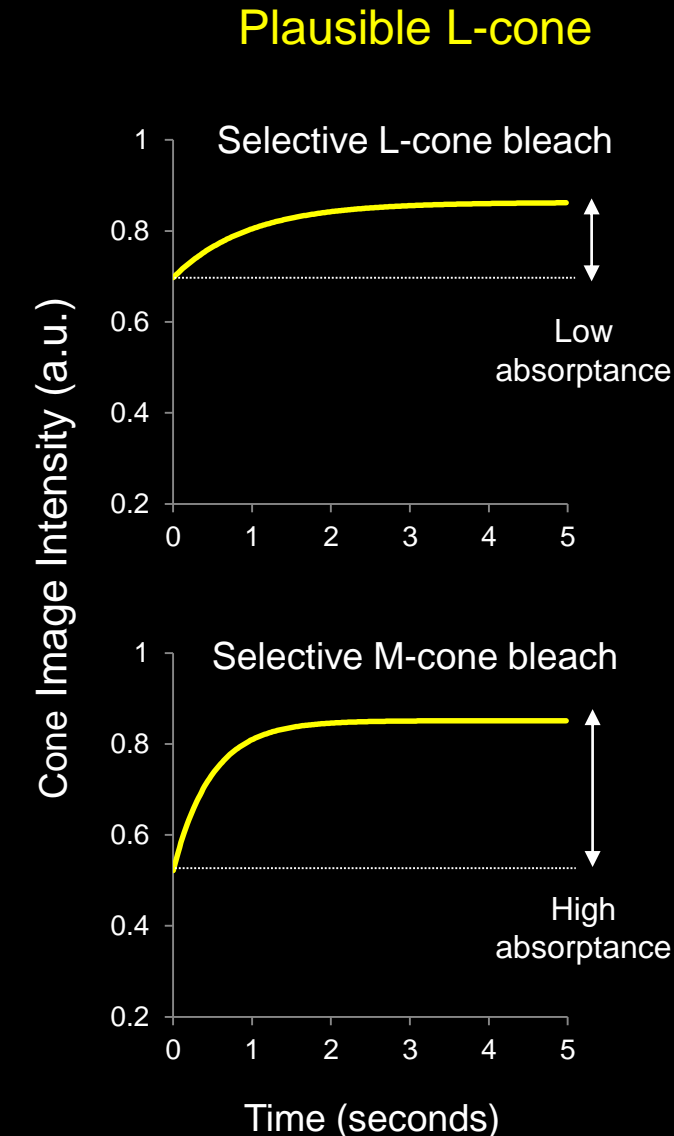
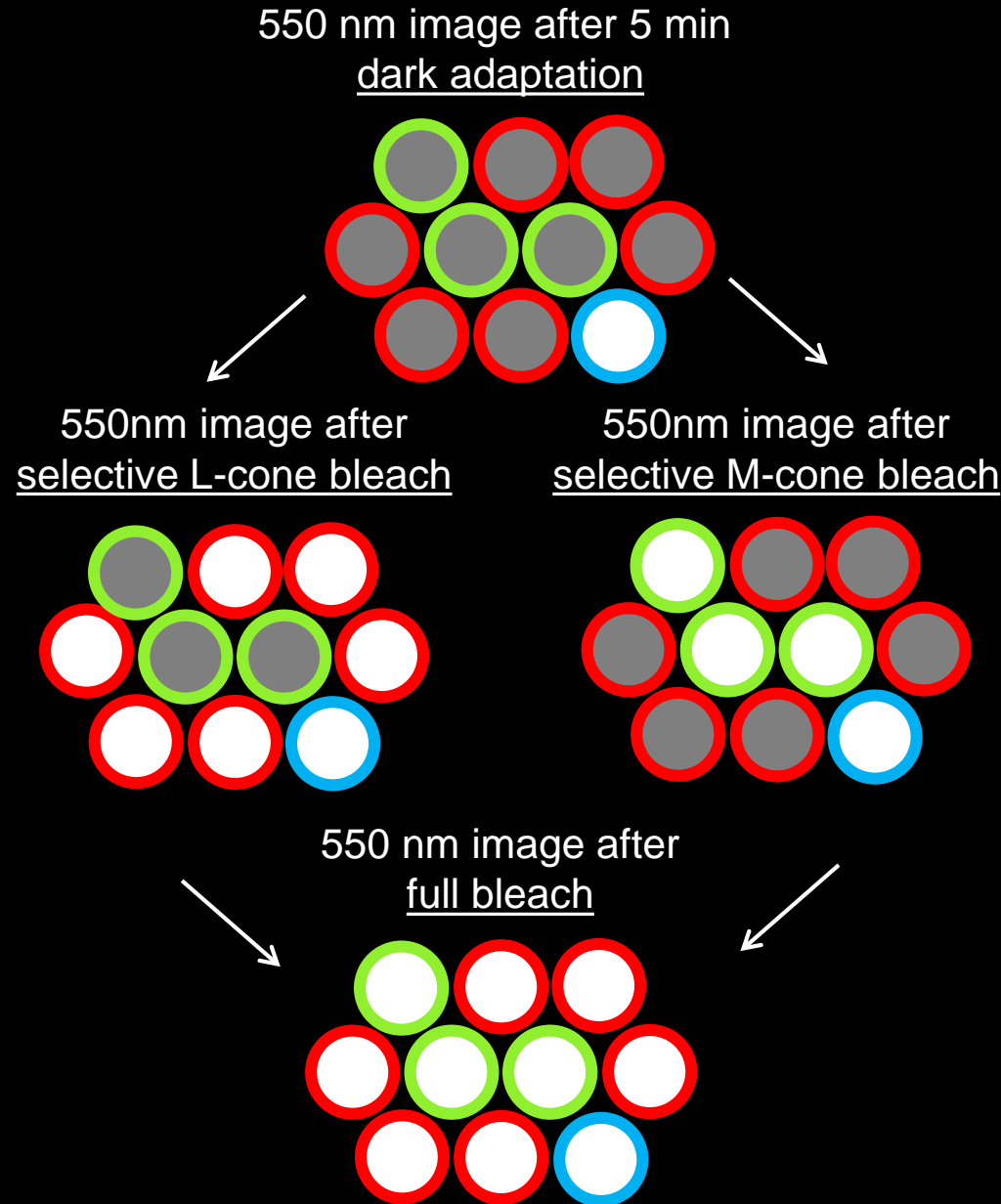




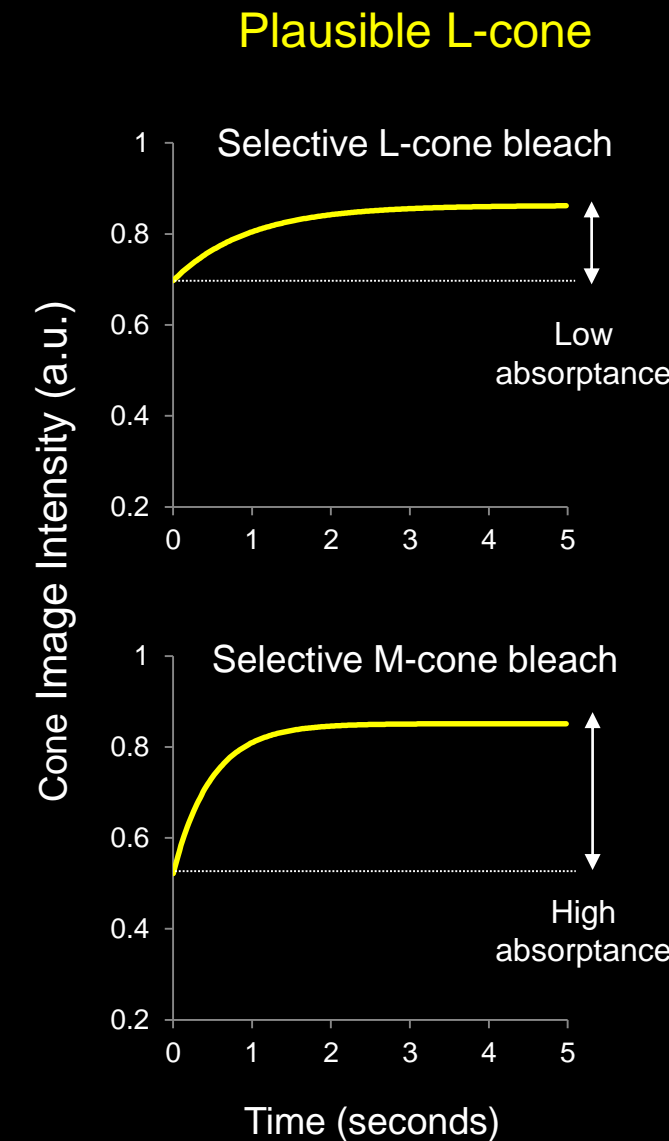
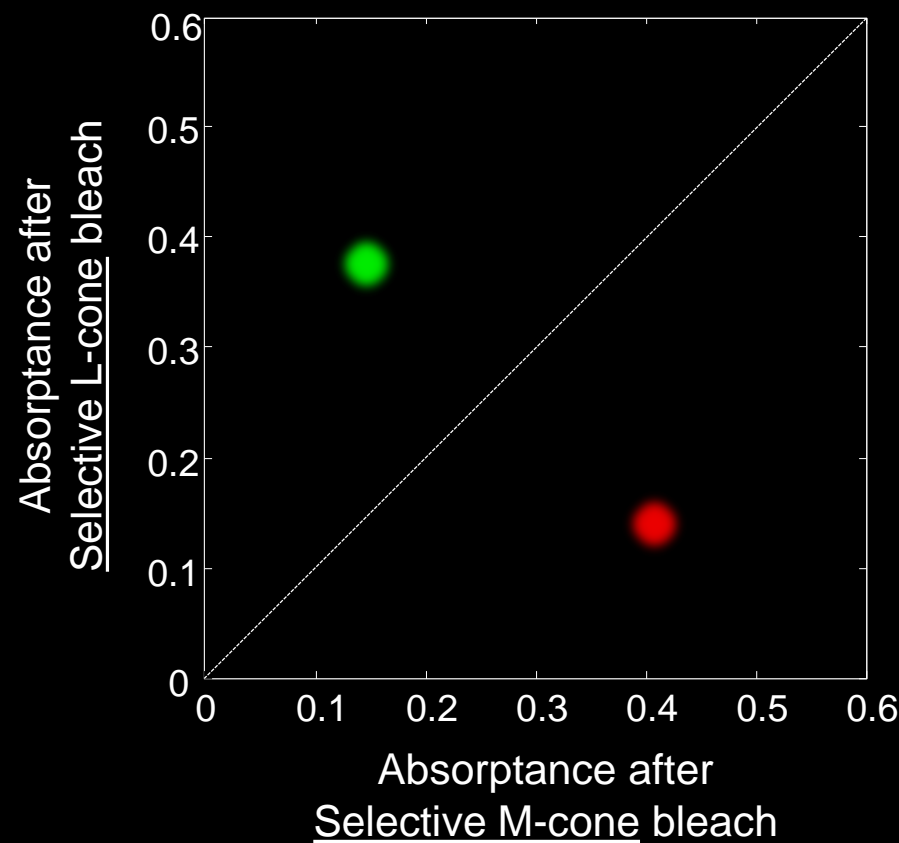
Distinguishing L & M cones



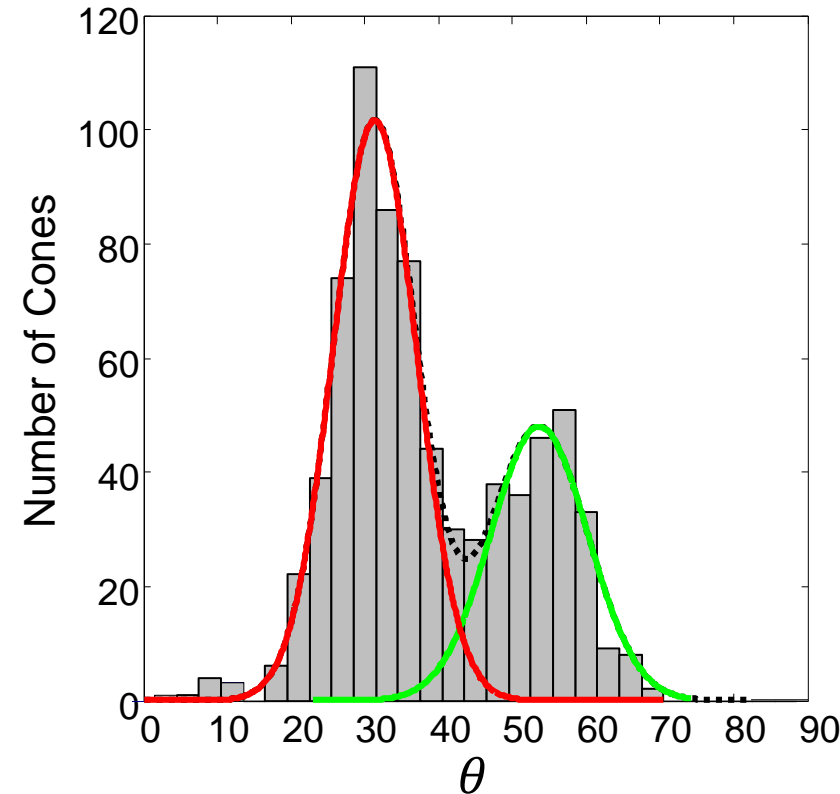
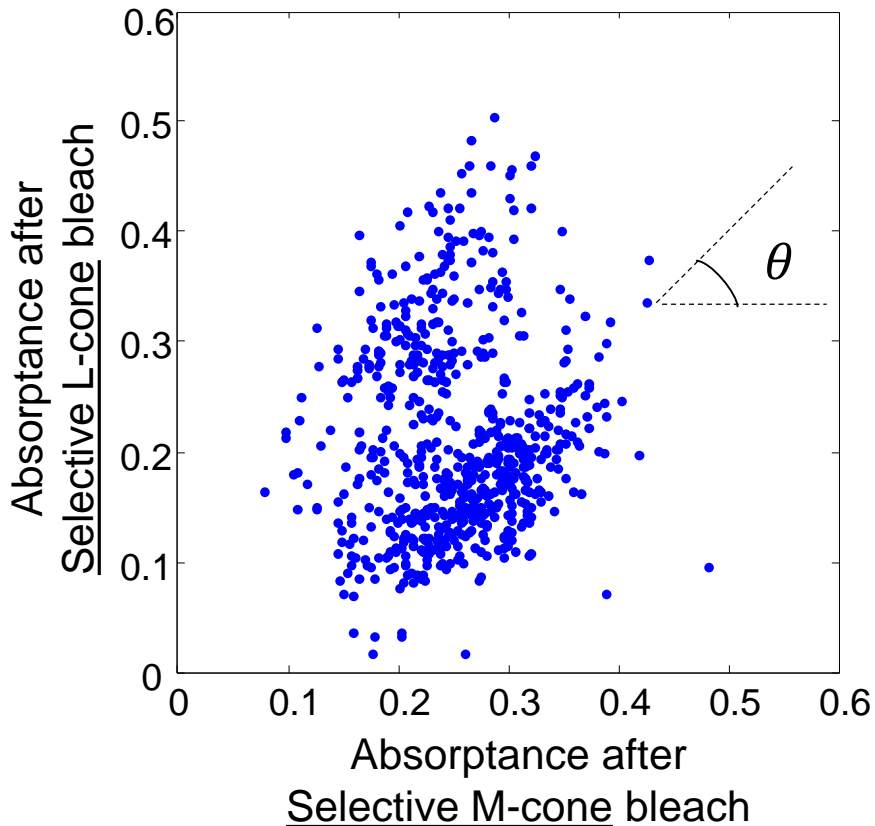
Distinguishing L & M cones



Distinguishing L & M cones

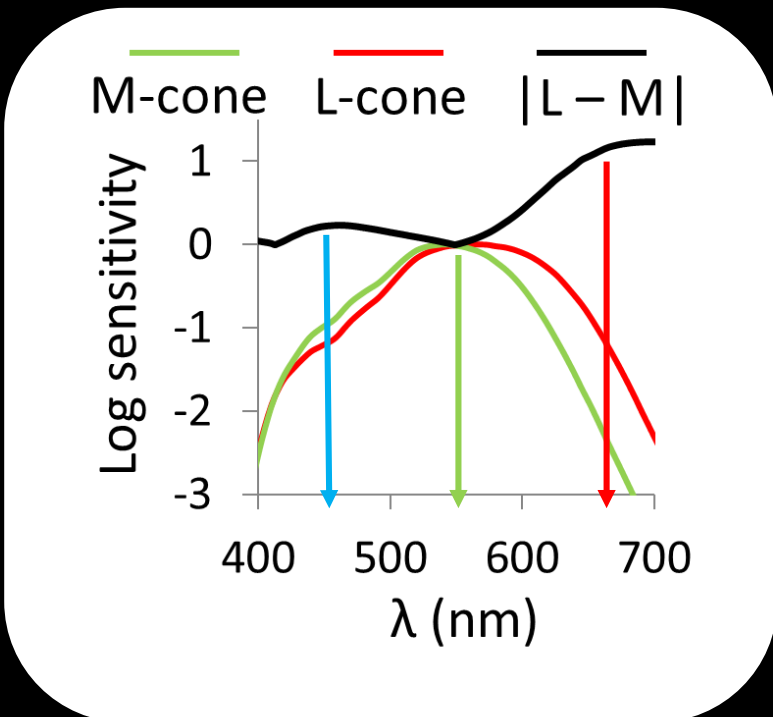


Distinguishing L and M cones

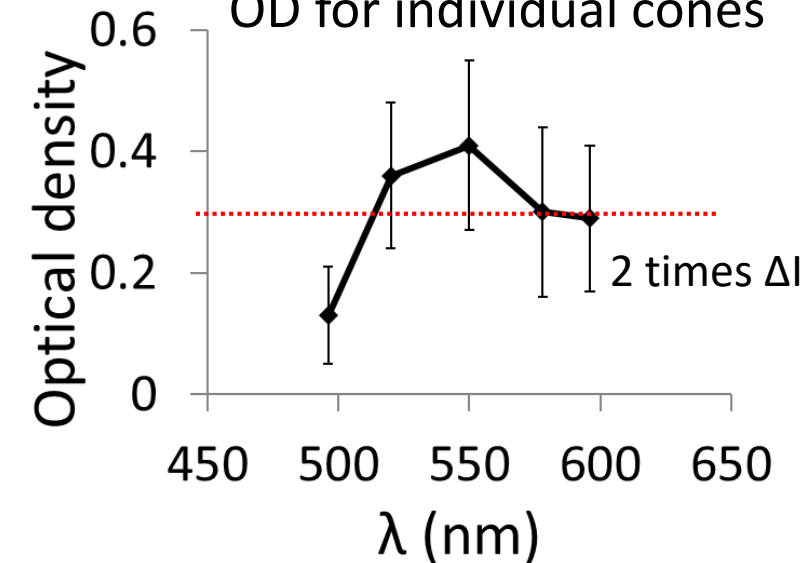


Selecting optimal wavelengths for separating L and M cones

Relative photopigment sensitivity



$$\text{Optical density}(\lambda) = \log_{10} (I_{\text{full bleach}}(\lambda) / I_{\text{dark adapt}}(\lambda))$$



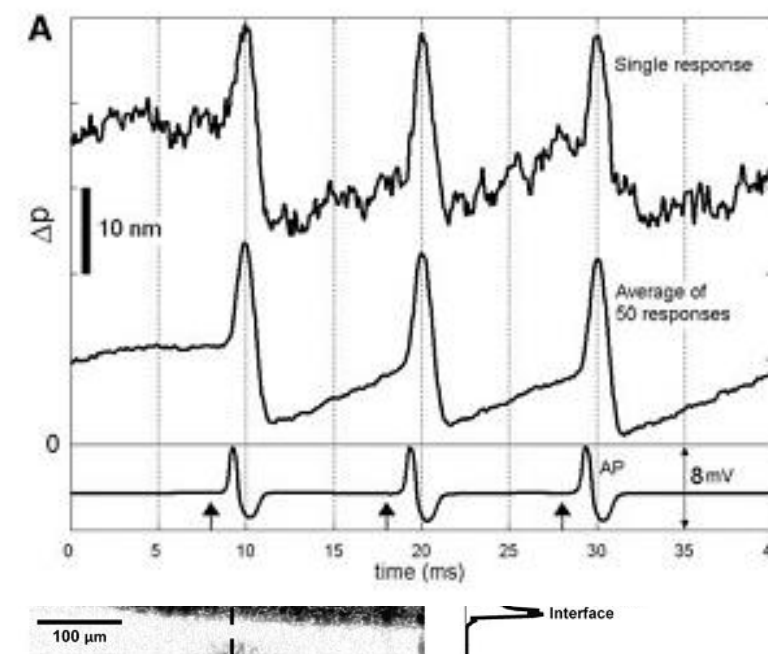
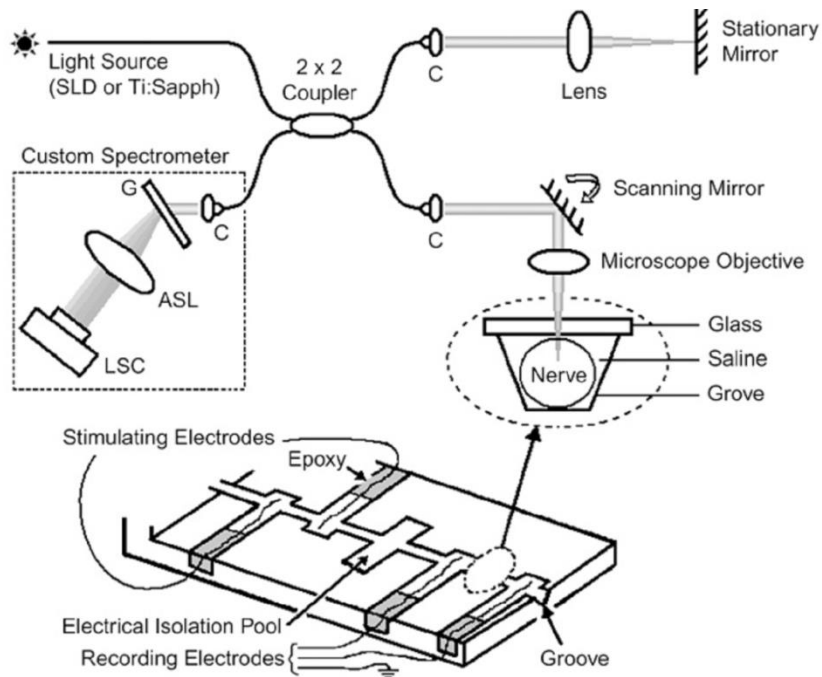
- $\lambda \approx 460 \text{ nm}$ & $\lambda \approx 660 \text{ nm}$, difference in sensitivity is high, but absorption is low.
- $\lambda \approx 550 \text{ nm}$, the difference in sensitivity is low, but absorption is high

- Macular pigment absorption leads to insufficient density at 496 nm
- At 578 nm and 596 nm, sufficient density may be available for probing differential L&M cone bleaching responses



Detection of neural action potentials using optical coherence tomography: intensity and phase measurements with and without dyes

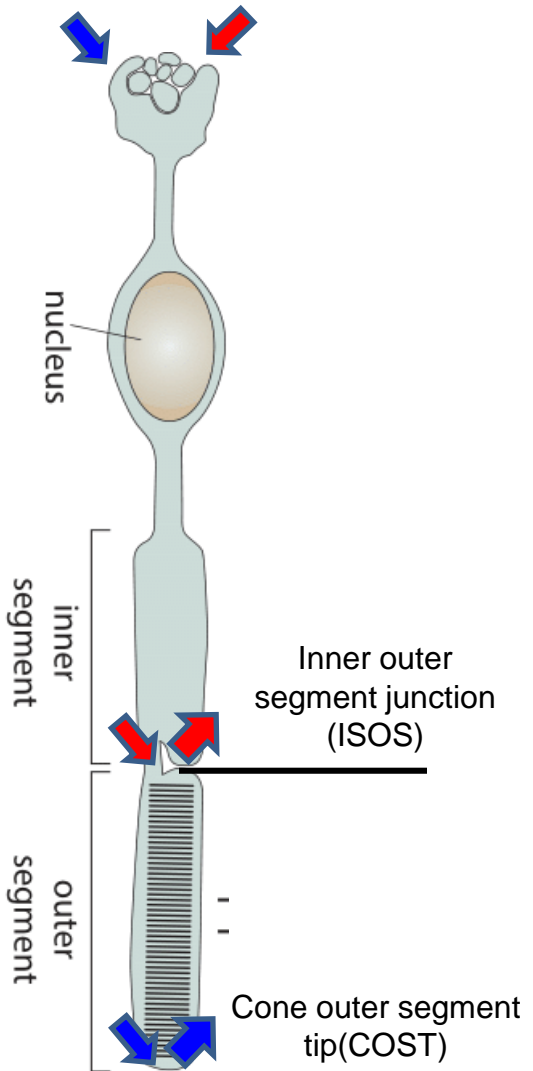
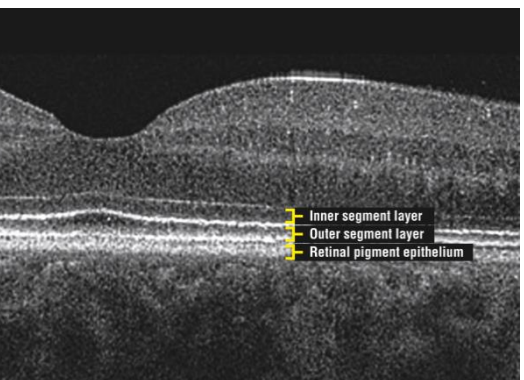
Taner Akkin^{1*}, David Landowne² and Aarthi Sivaprakasam¹



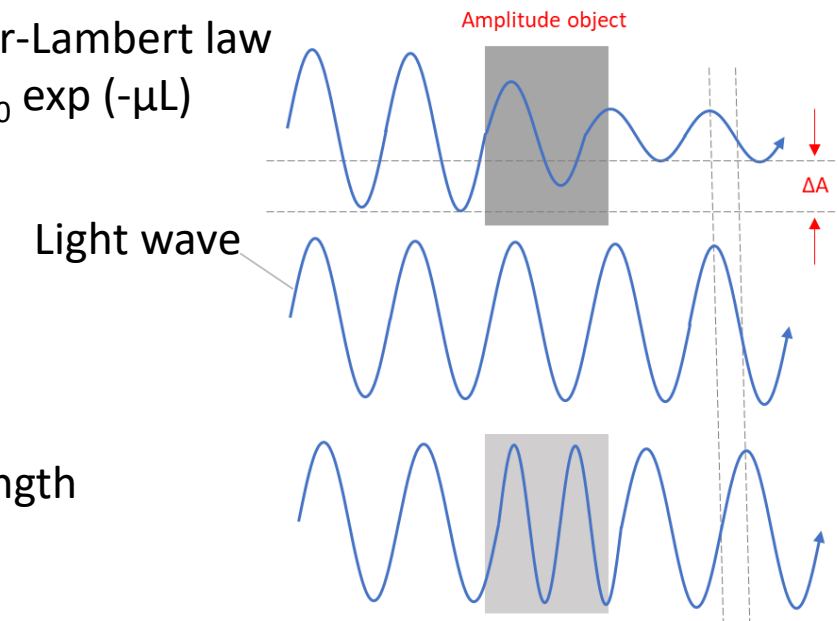
$$\begin{aligned} \text{Axial resolution} &\propto \Delta\phi \propto \Delta p \\ \text{Lateral resolution} &\propto \text{Numerical aperture} \approx 3 \times 3 \times 3 \mu\text{m}^3 \text{ in retina} \\ &\propto \text{Phase interference} \propto \text{Optical path length} \end{aligned}$$

Light-evoked optical changes in cone photoreceptors

- Intensity
- Phase



Beer-Lambert law
 $I = I_0 \exp (-\mu L)$



$$\Delta\phi = \frac{2\pi}{\lambda} \times \text{OPL}$$

$$\text{OPL} = n \times T$$

OPL- Optical path length

n- refractive index

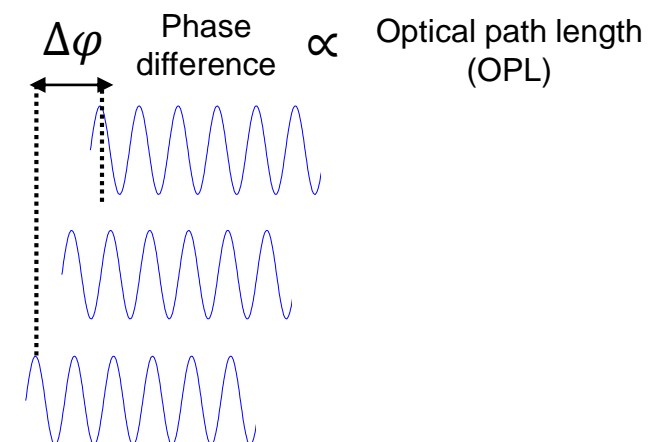
T- thickness

Light scattered from ISOS

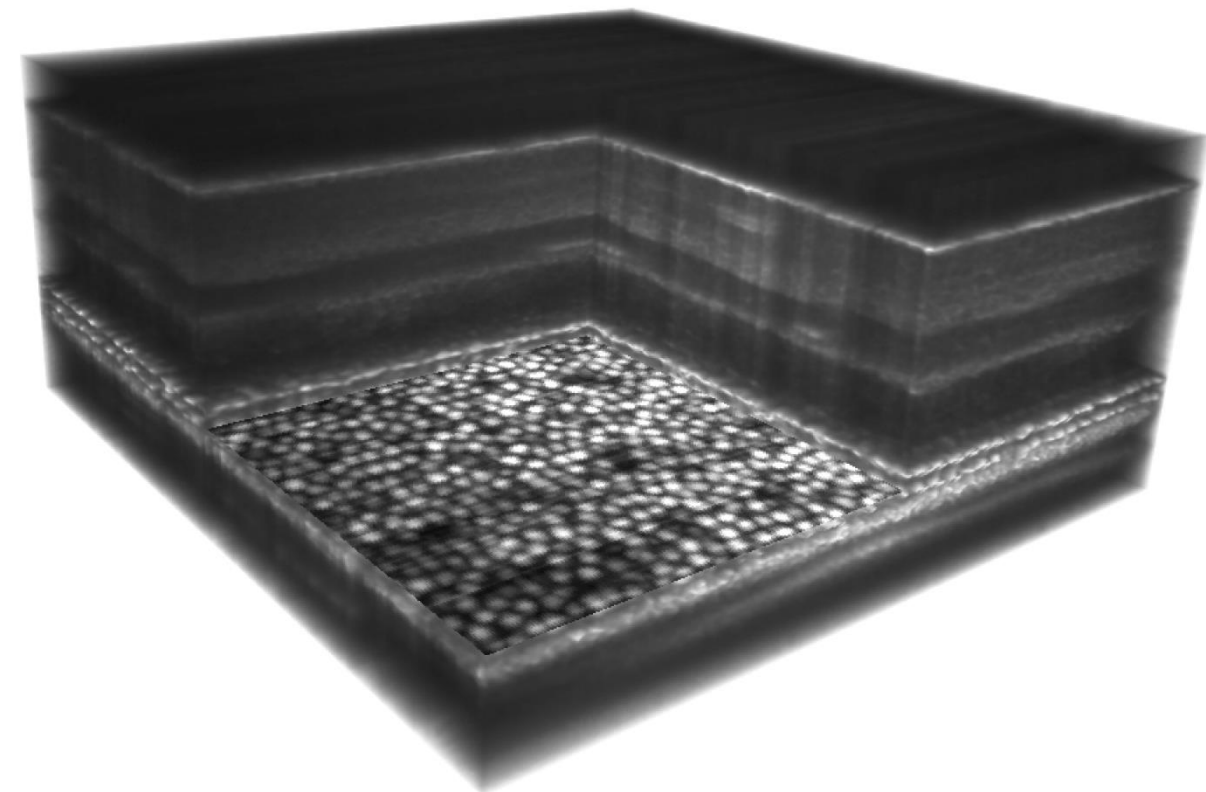
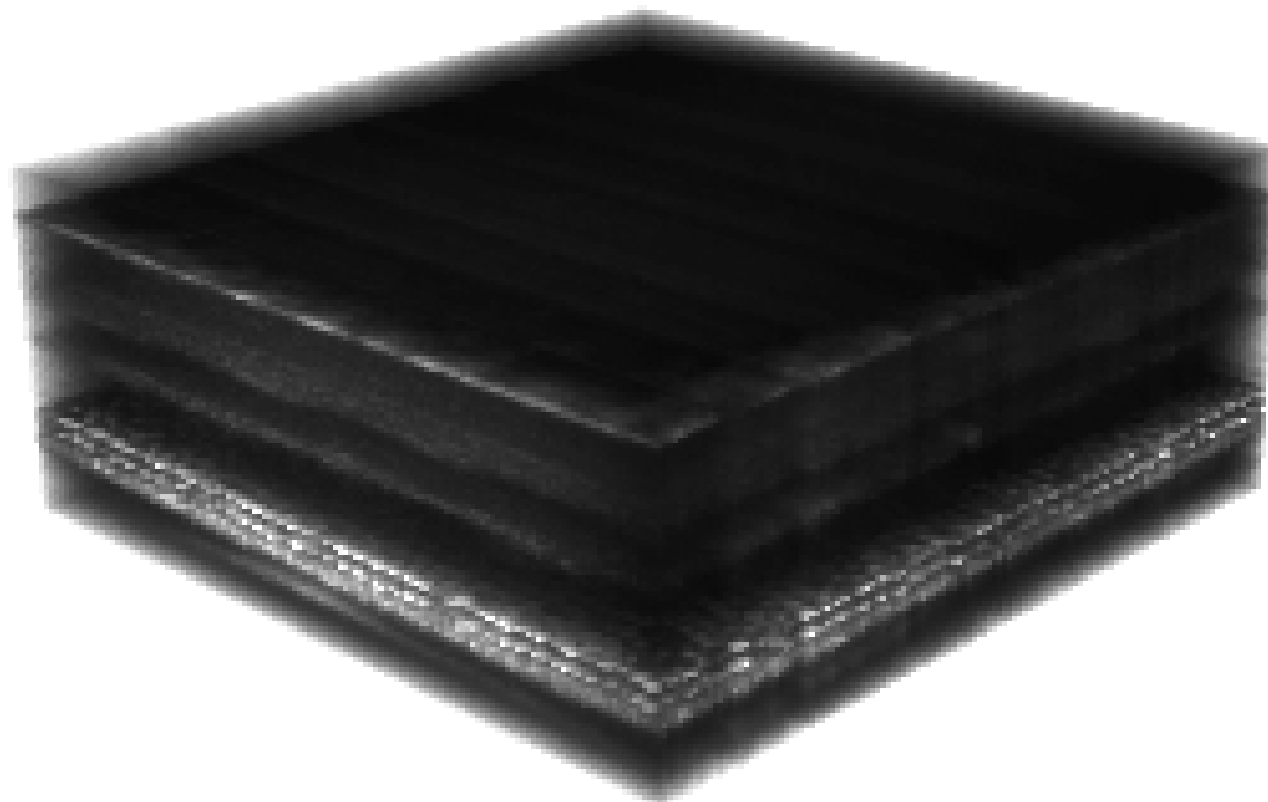
Light scattered from COST

Light scattered from COST
after Δt

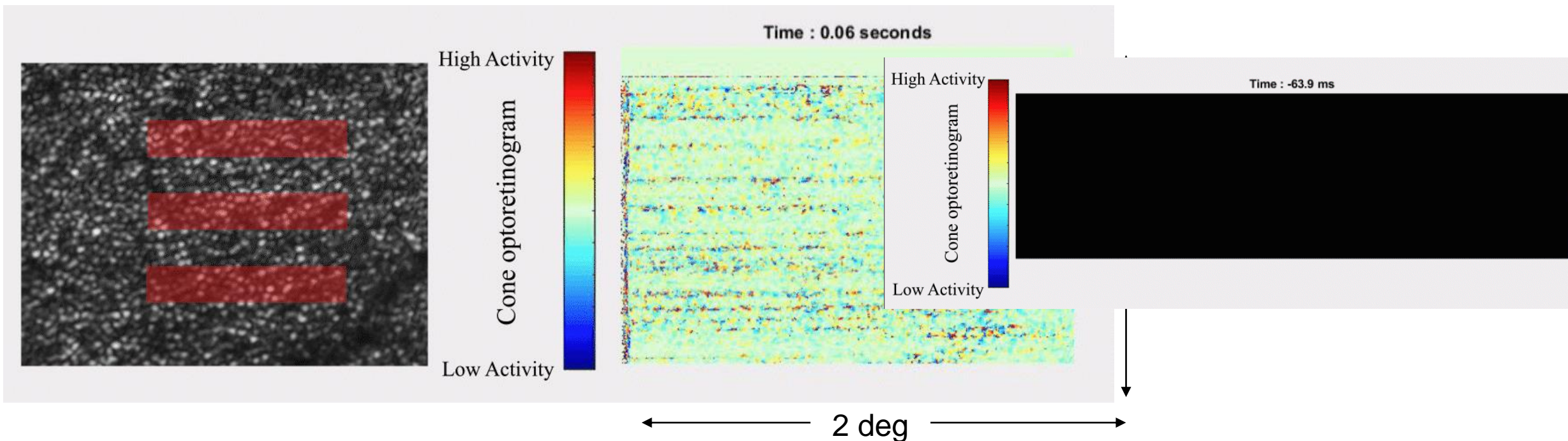
Light scattered from COST
after $2\Delta t$



Line-scan spectral domain OCT with Adaptive Optics



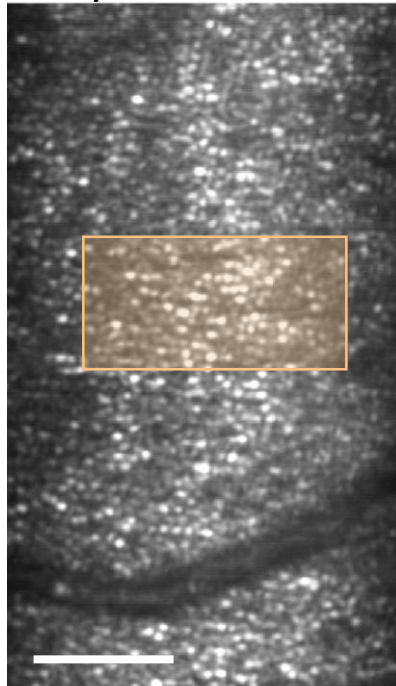
Optoretinography : Light induced optical changes in the retina – paradigm & examples –



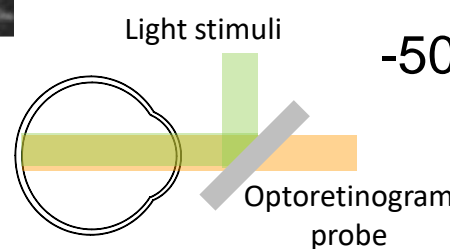
No AO, 4mm pupil, 7 deg temporal, 20 vol/sec

ORG – temporal response characteristics

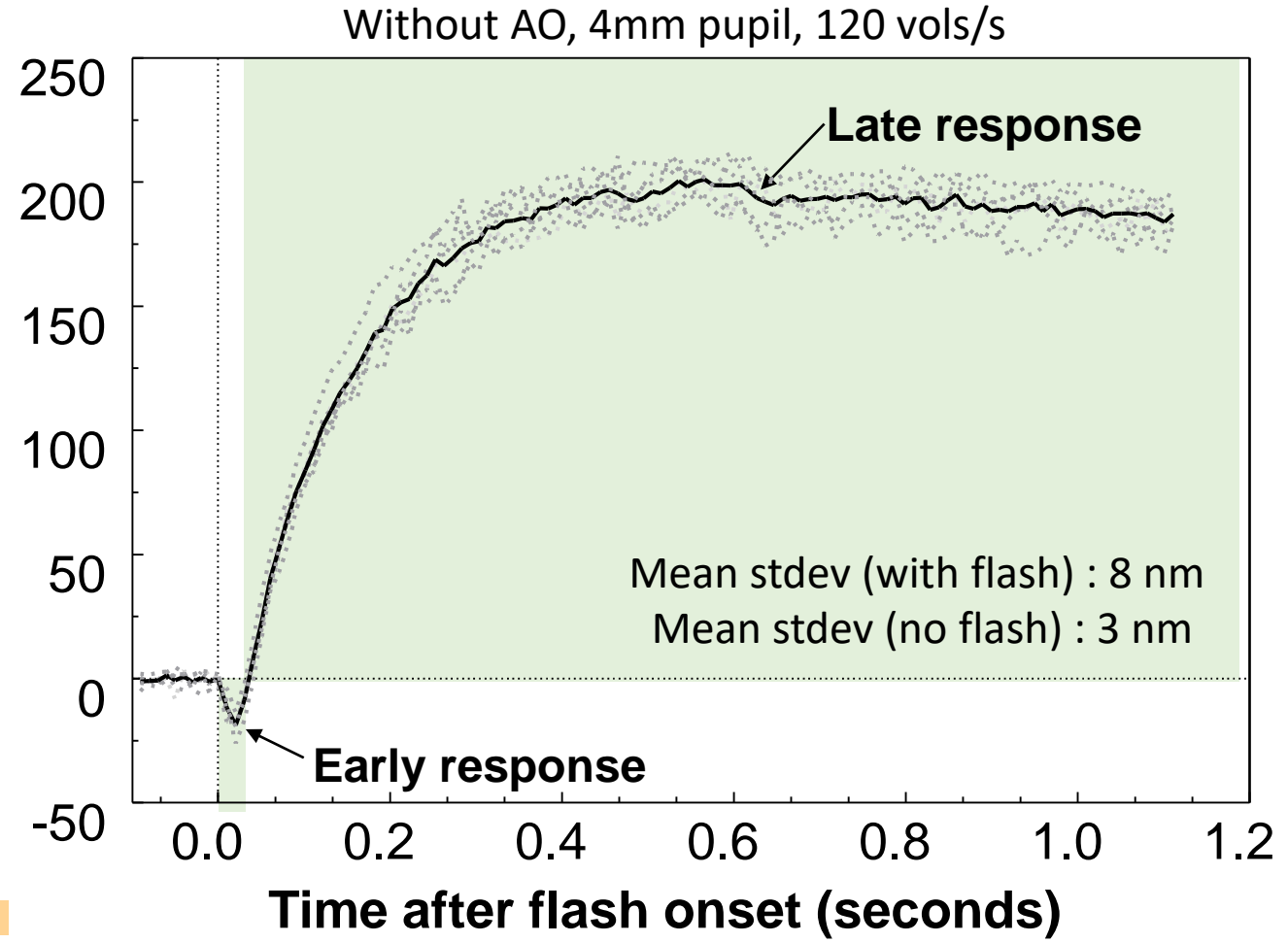
Non-AO LSO image
overlaid with stimulus



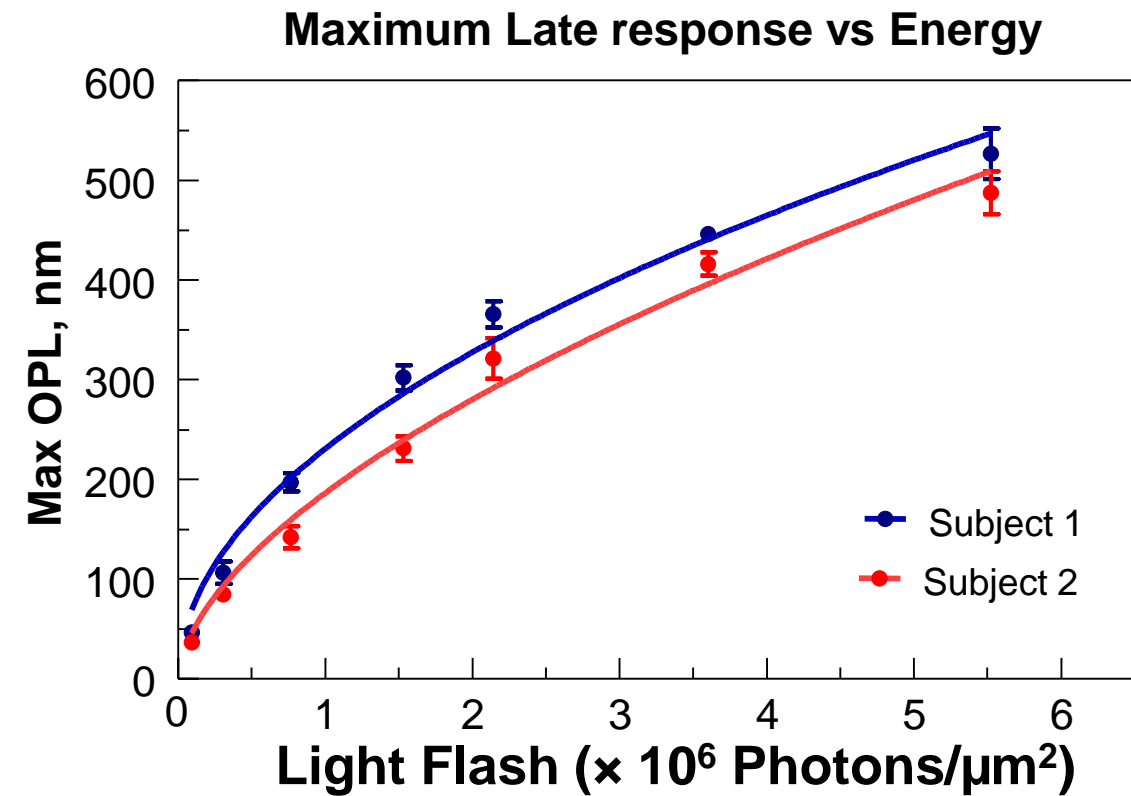
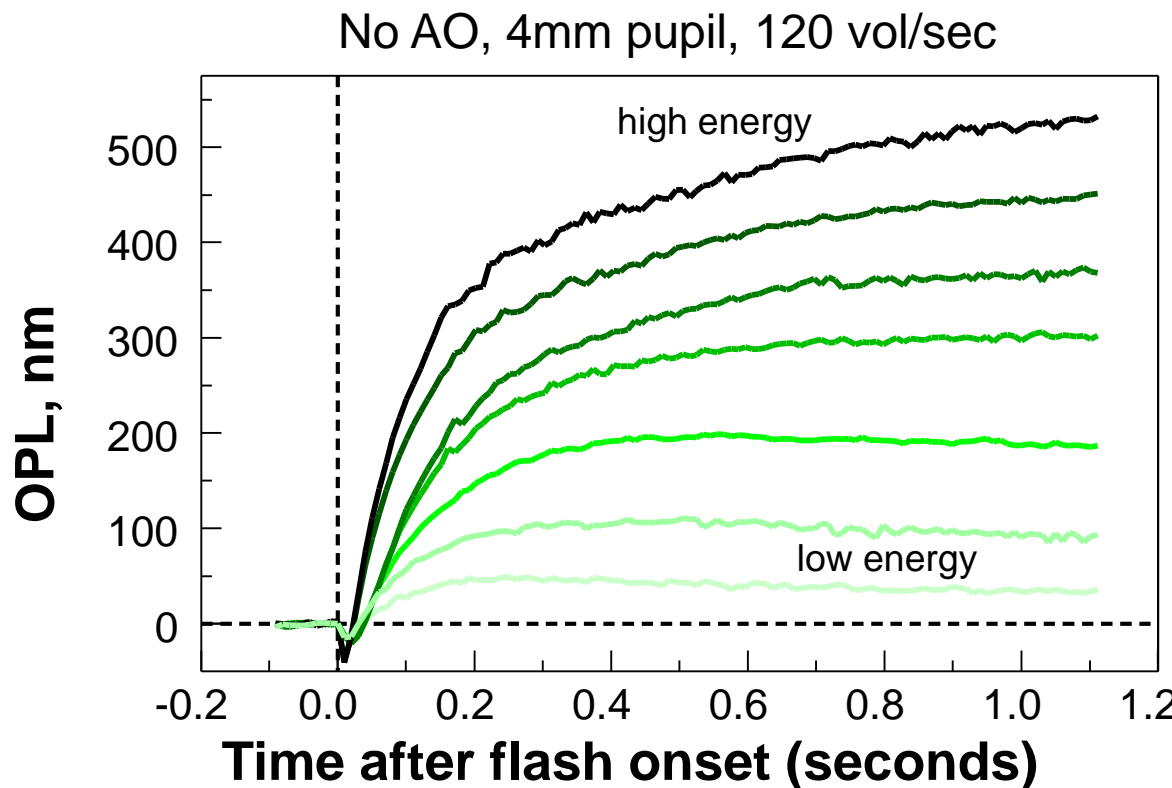
Scale bar: 100 μm



Optical path length (OPL)
(ISOS - COST) in nm

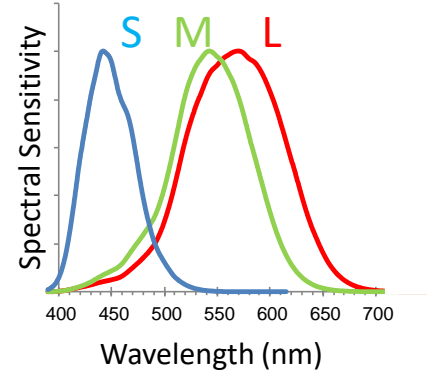


The late response component of the cone optoretinogram

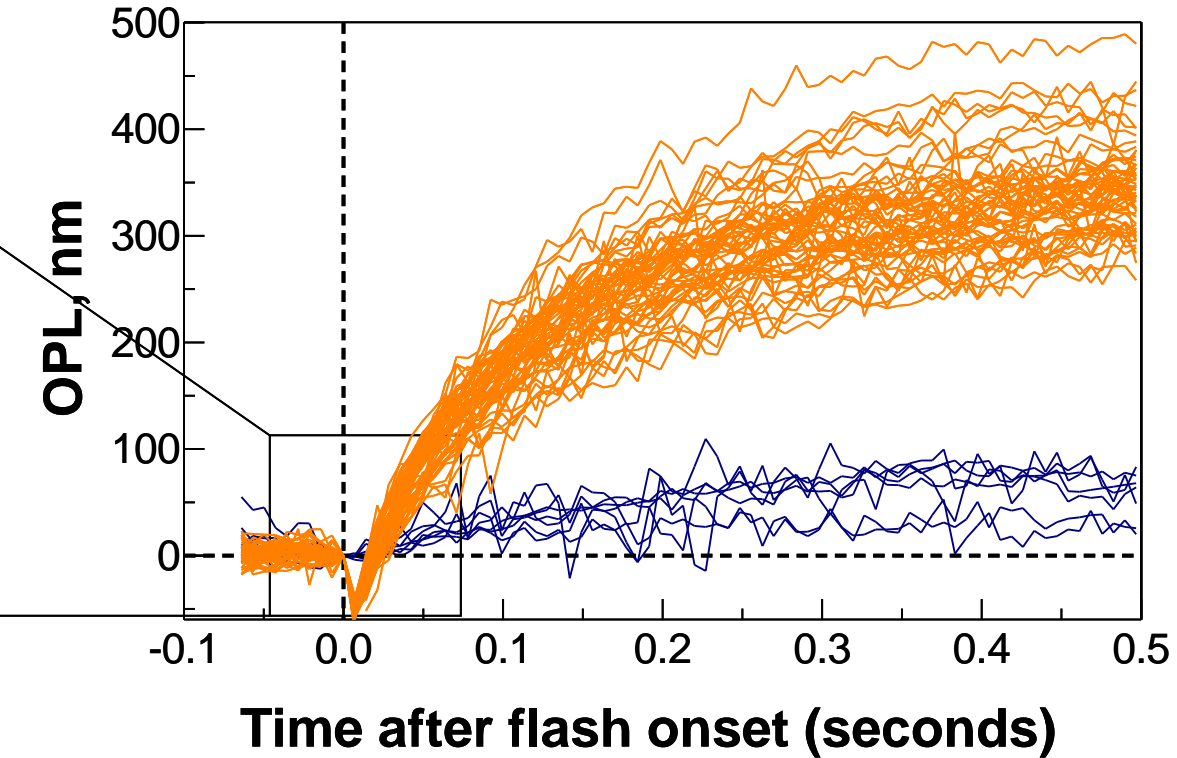
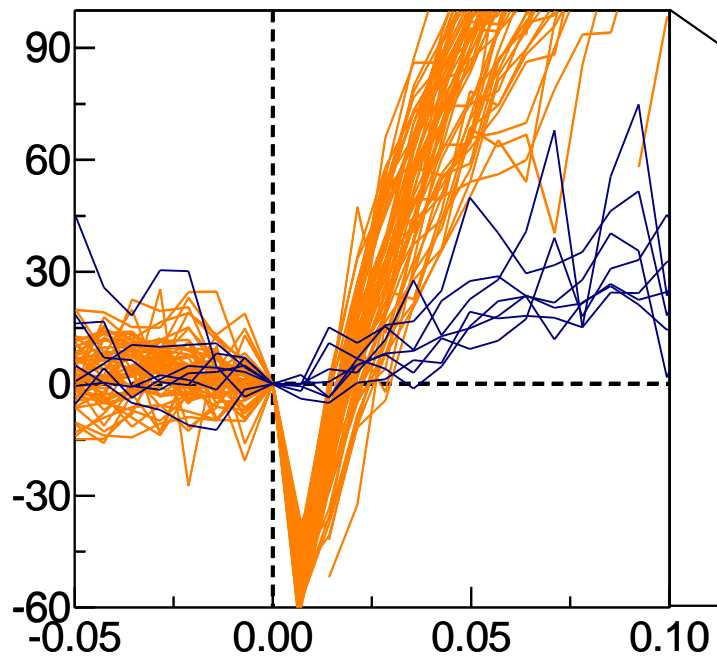
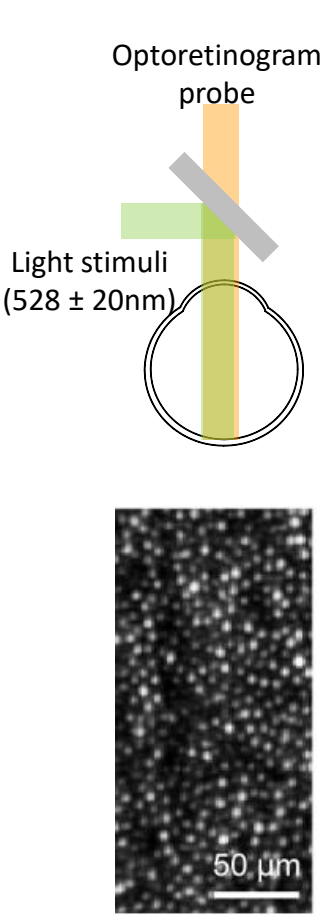


Light Flash ($\times 10^6$ Photons/ μm^2) (% bleach)

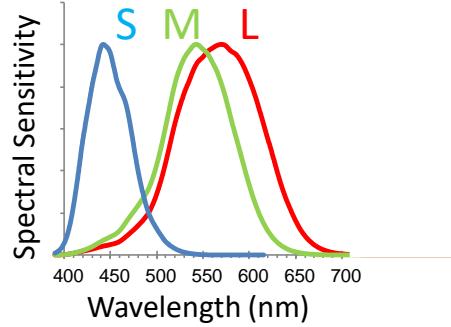
0.09 (1.2) 0.30 (3.9) 0.76 (9.5) 1.53 (17.9)
2.14 (23.9) 3.60 (36.1) 5.52 (48.4)



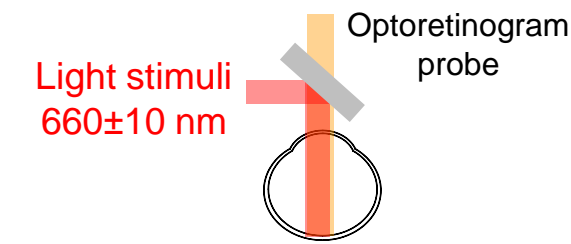
The early response in single cones



— L/M-cones — S-cones

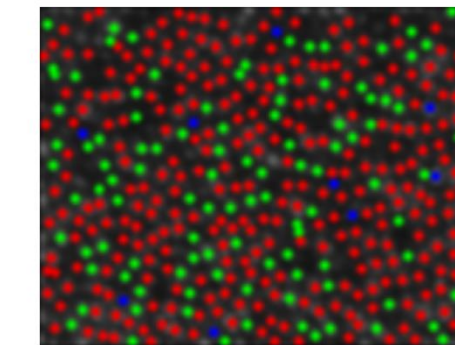
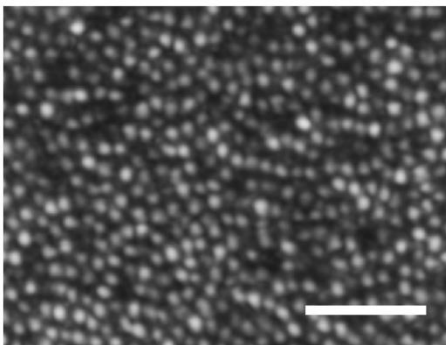
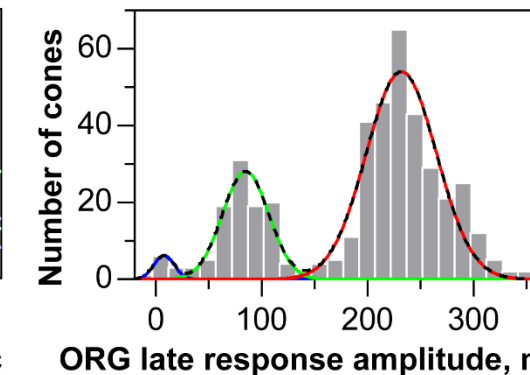
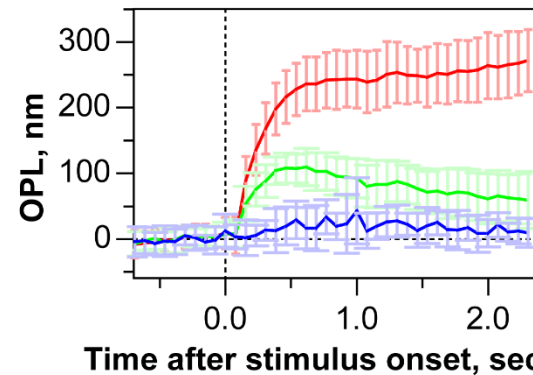


Cone spectral classification



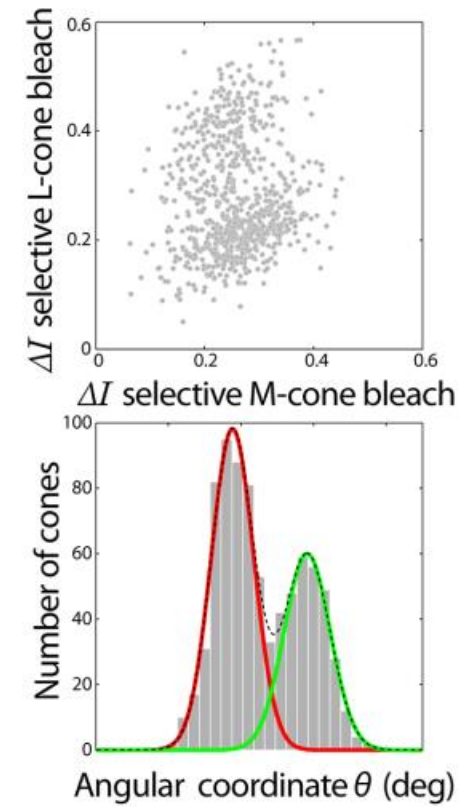
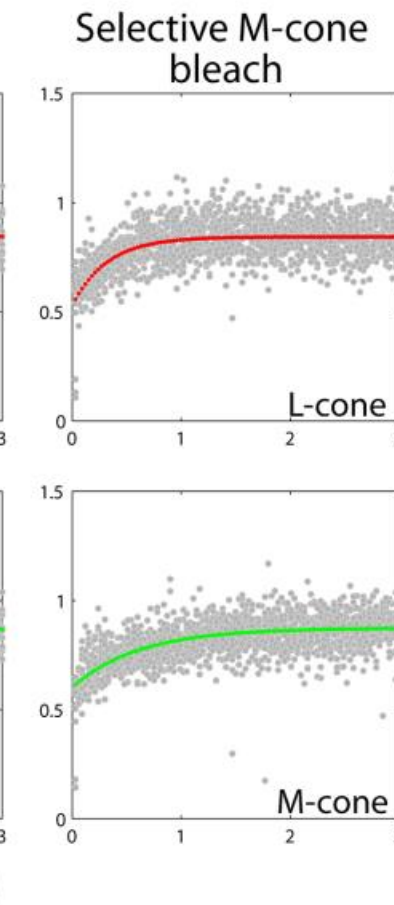
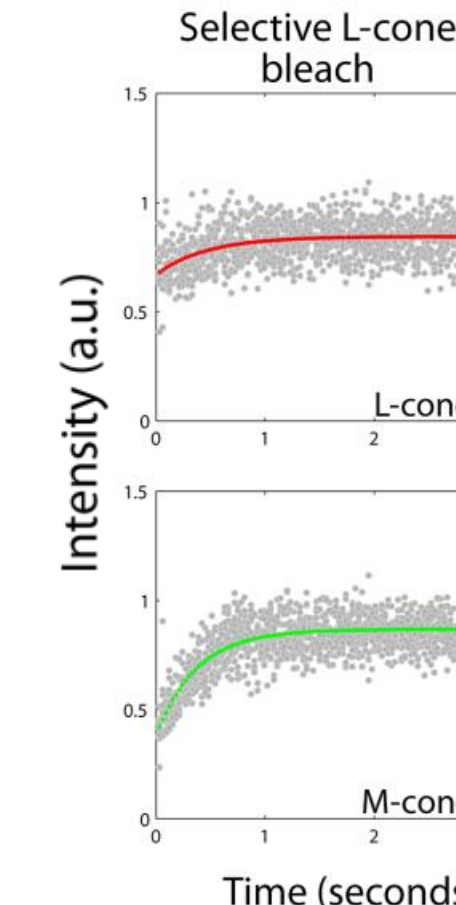
Optoretinography

- change in phase or OPL upon bleach -



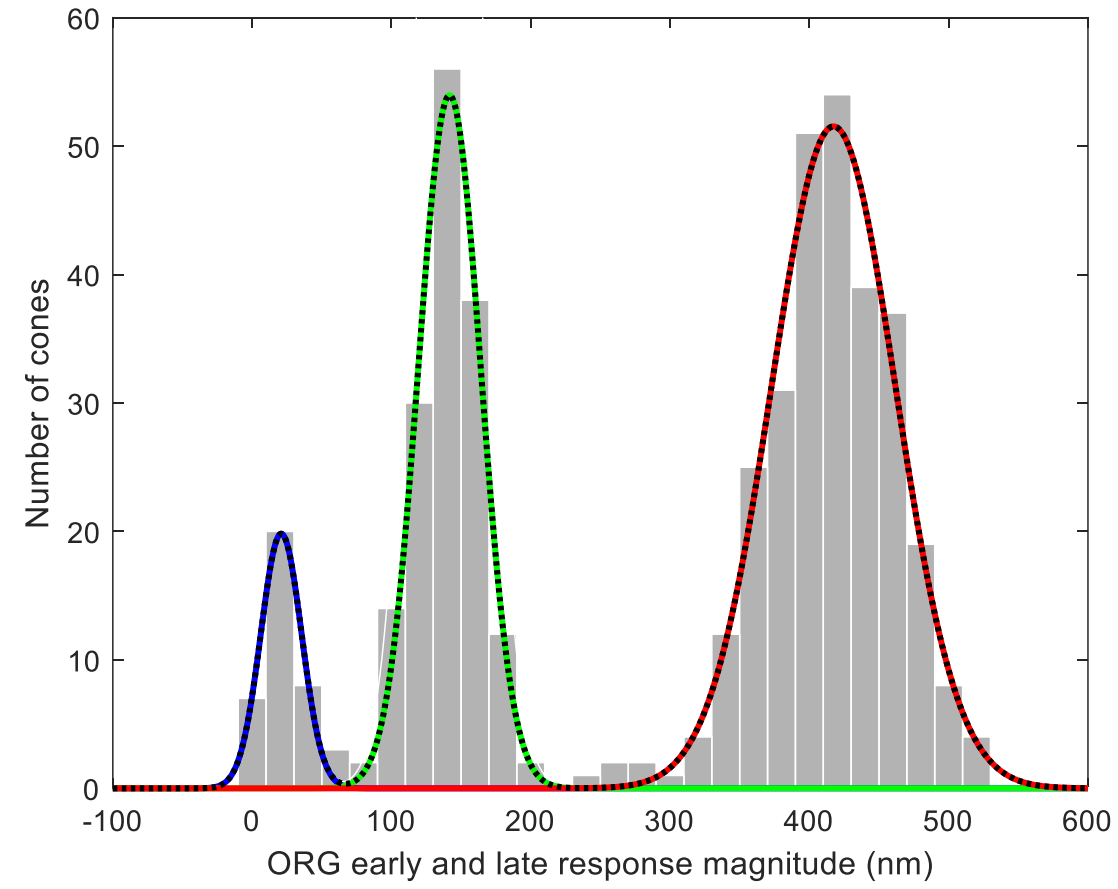
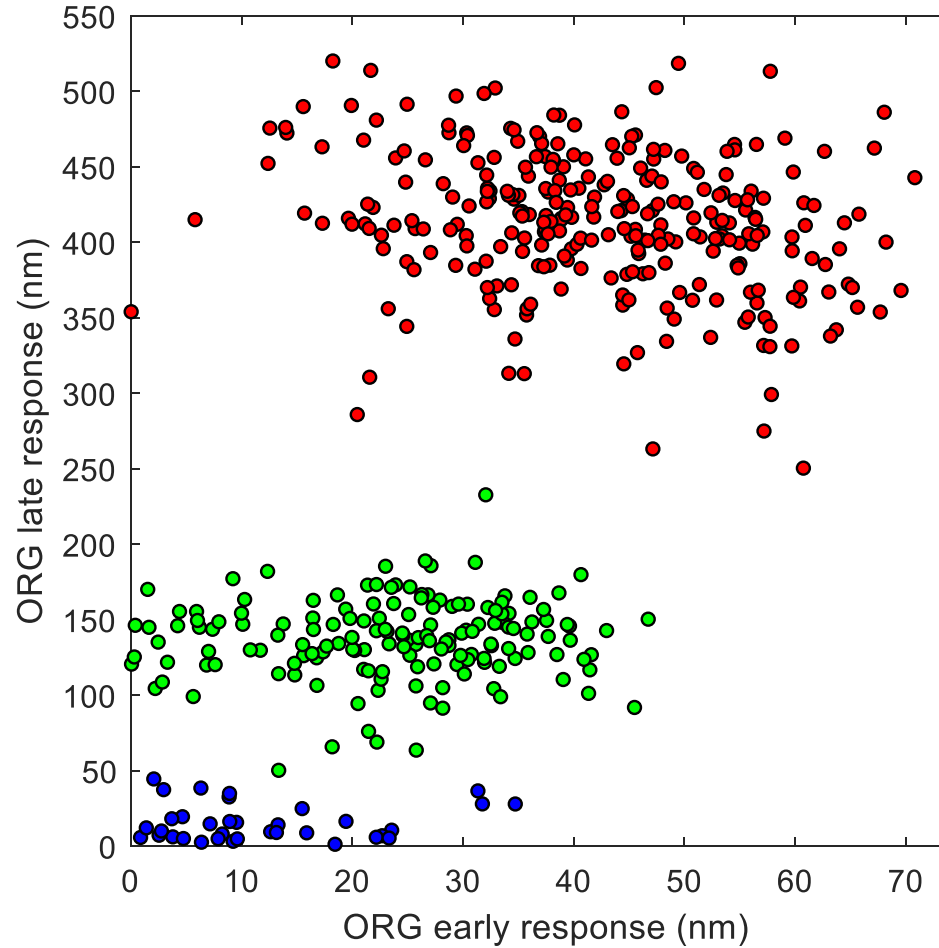
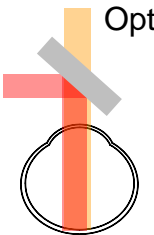
Densitometry

- change in image intensity upon bleach -



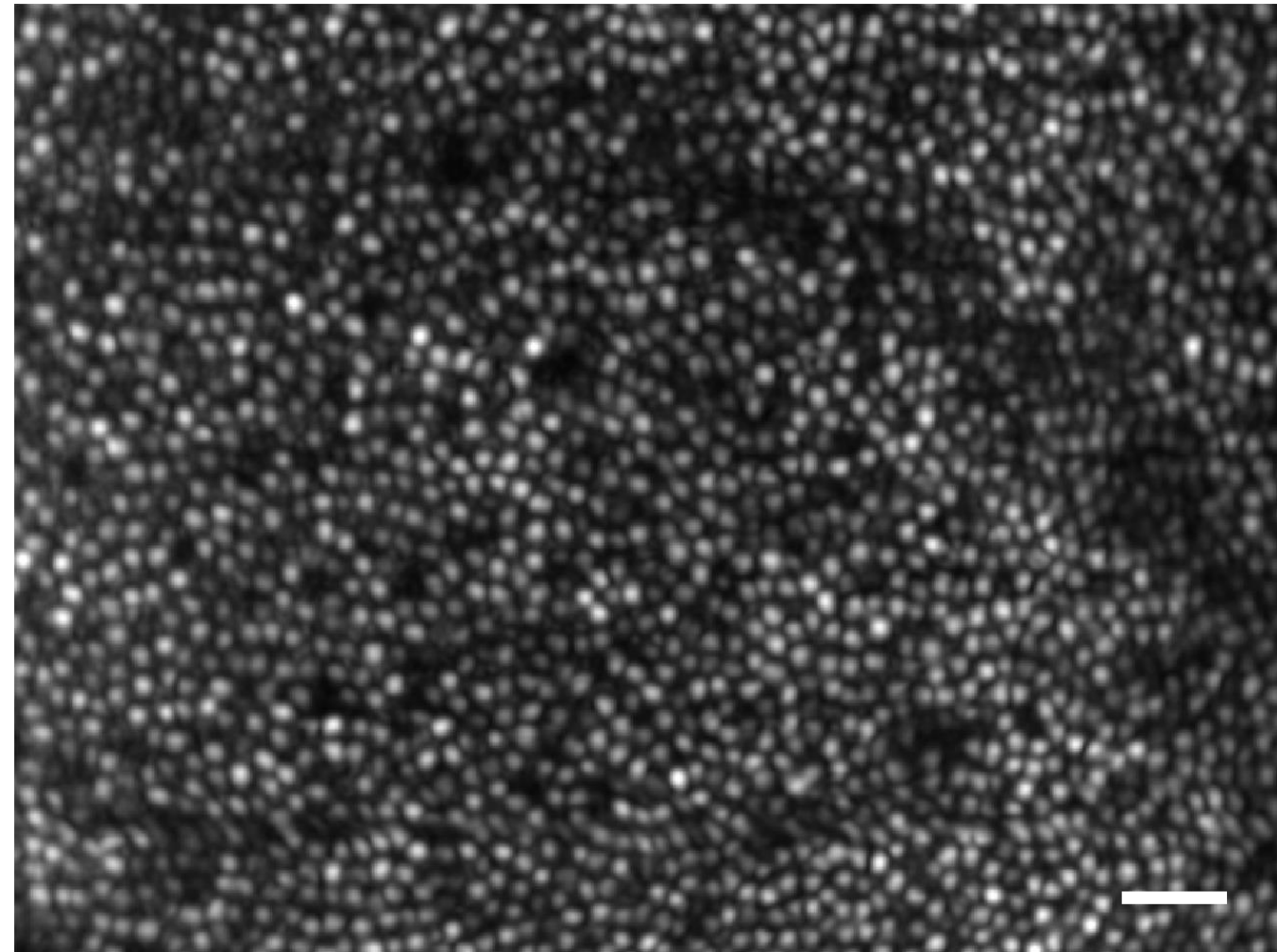
Single cone ORG early & late response

Light stimuli
 $660 \pm 10 \text{ nm}$



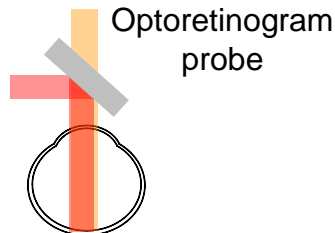
Classifying cone spectral types

With AO, 6.75 mm pupil, 3.5 deg temporal, 15 vol/sec



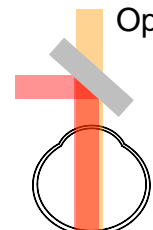
Scale bar: 25 μm

Light stimuli
 $660 \pm 10 \text{ nm}$

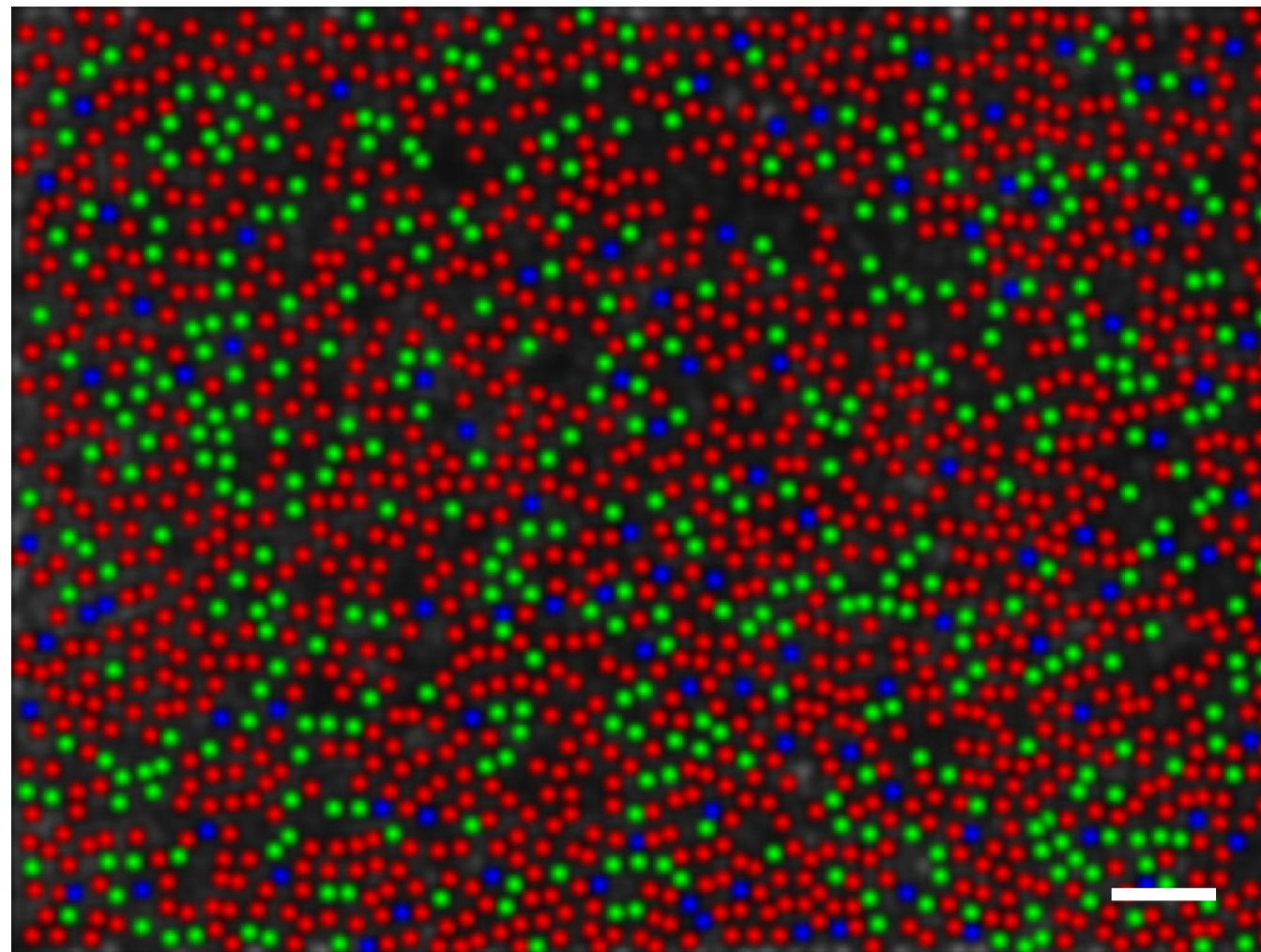
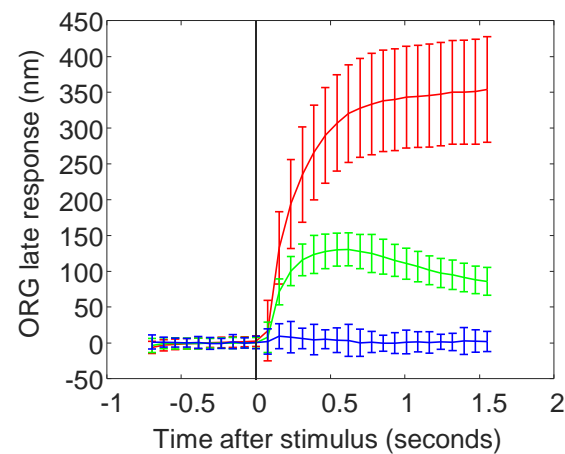


Classifying cone spectral types

Light stimuli
 $660 \pm 10 \text{ nm}$



With AO, 6.75 mm pupil, 3.5 deg temporal, 15 vol/sec

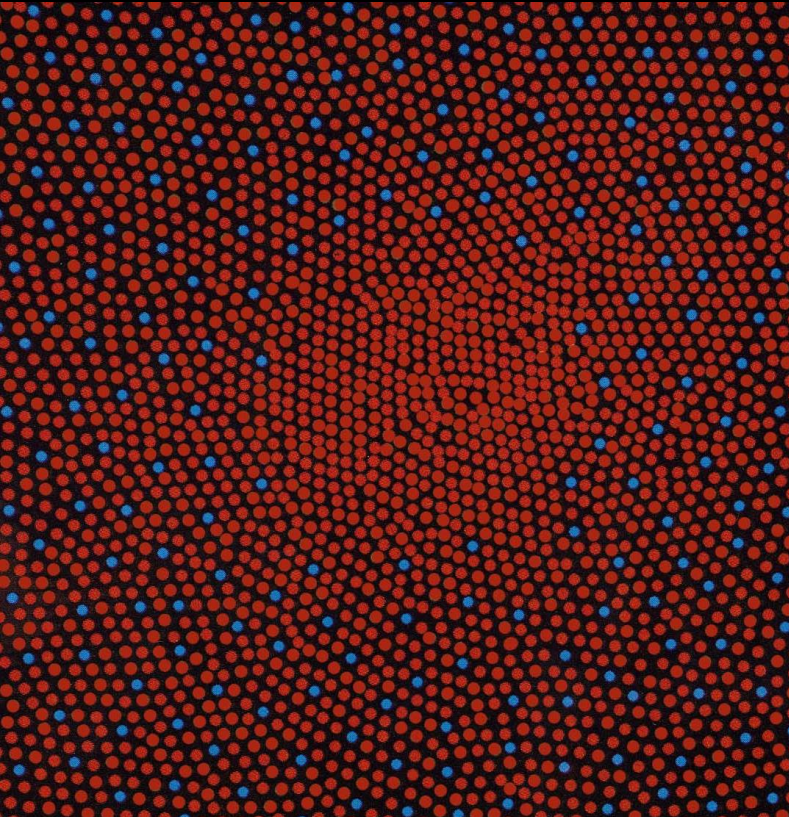


1659 cones

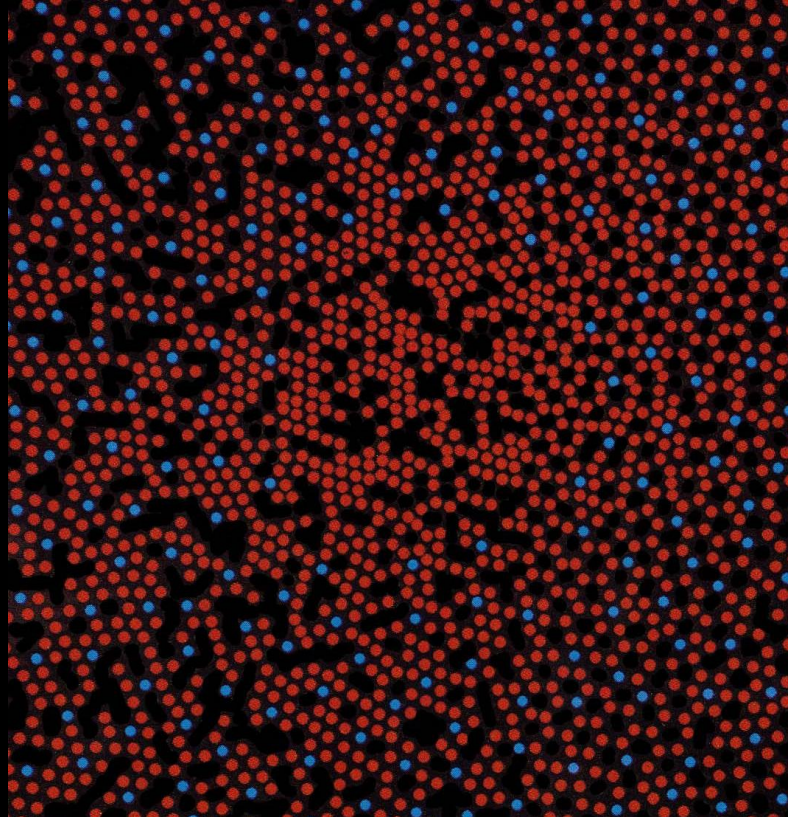
S-cones = 6.1 %

L:M = 3:1

What does a red-green dichromat's retina look like?

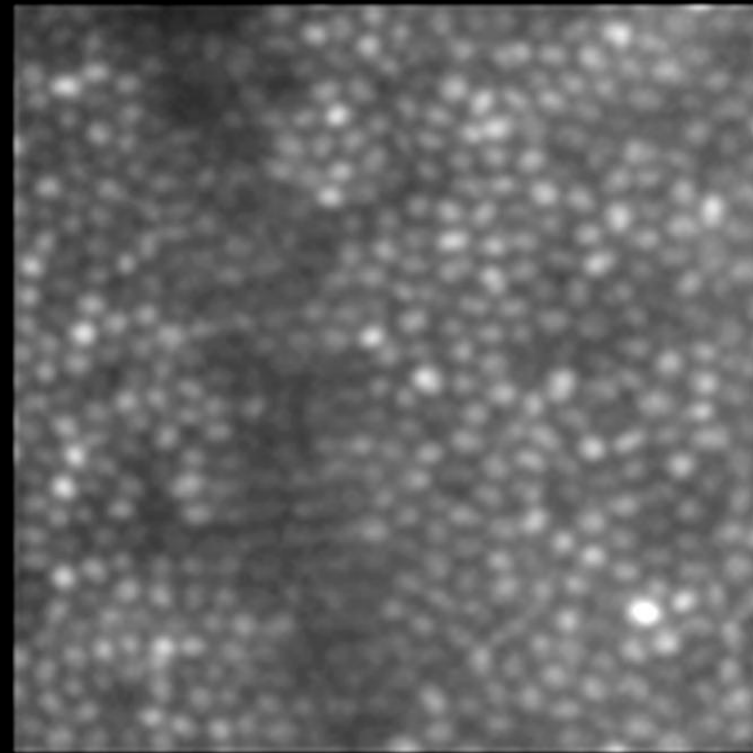


Replacement Model



Loss Model

Dichromats missing one gene have a complete mosaic of cones like a normal trichromat

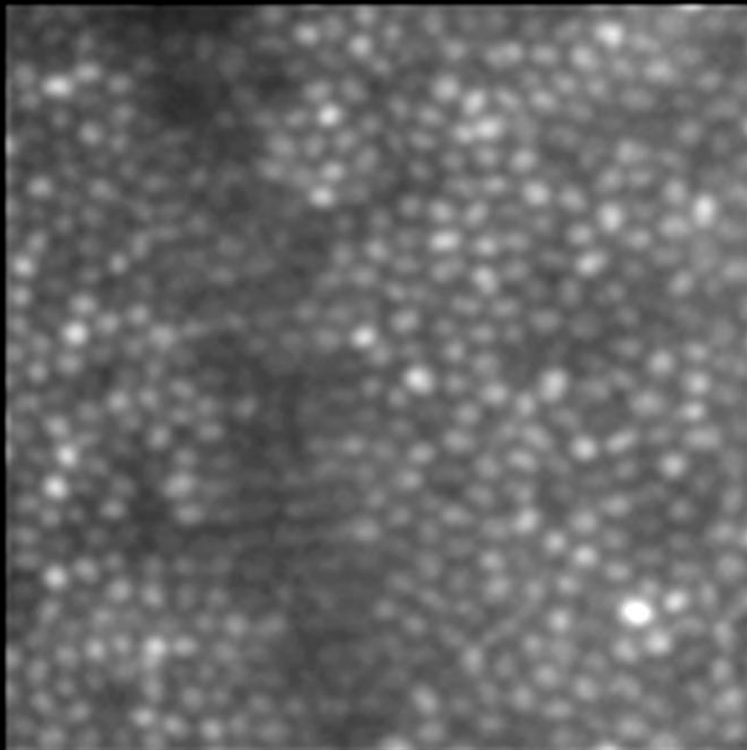


1 deg eccentricity

J. Carroll, M. Neitz, H. Hofer, J. Neitz, D. R. Williams (2004)

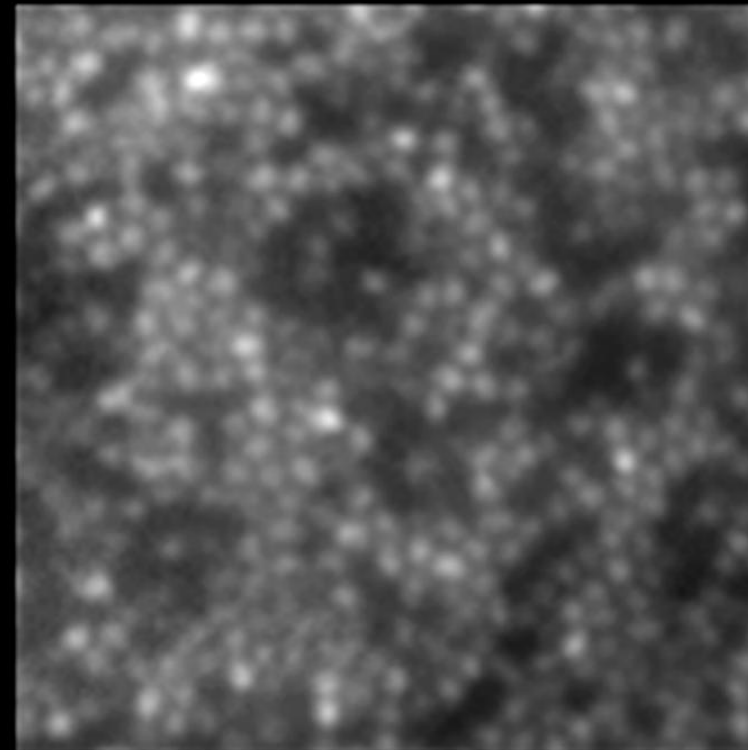
Patchy Loss of Cone Photoreceptors

Typical dichromat



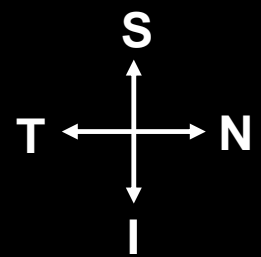
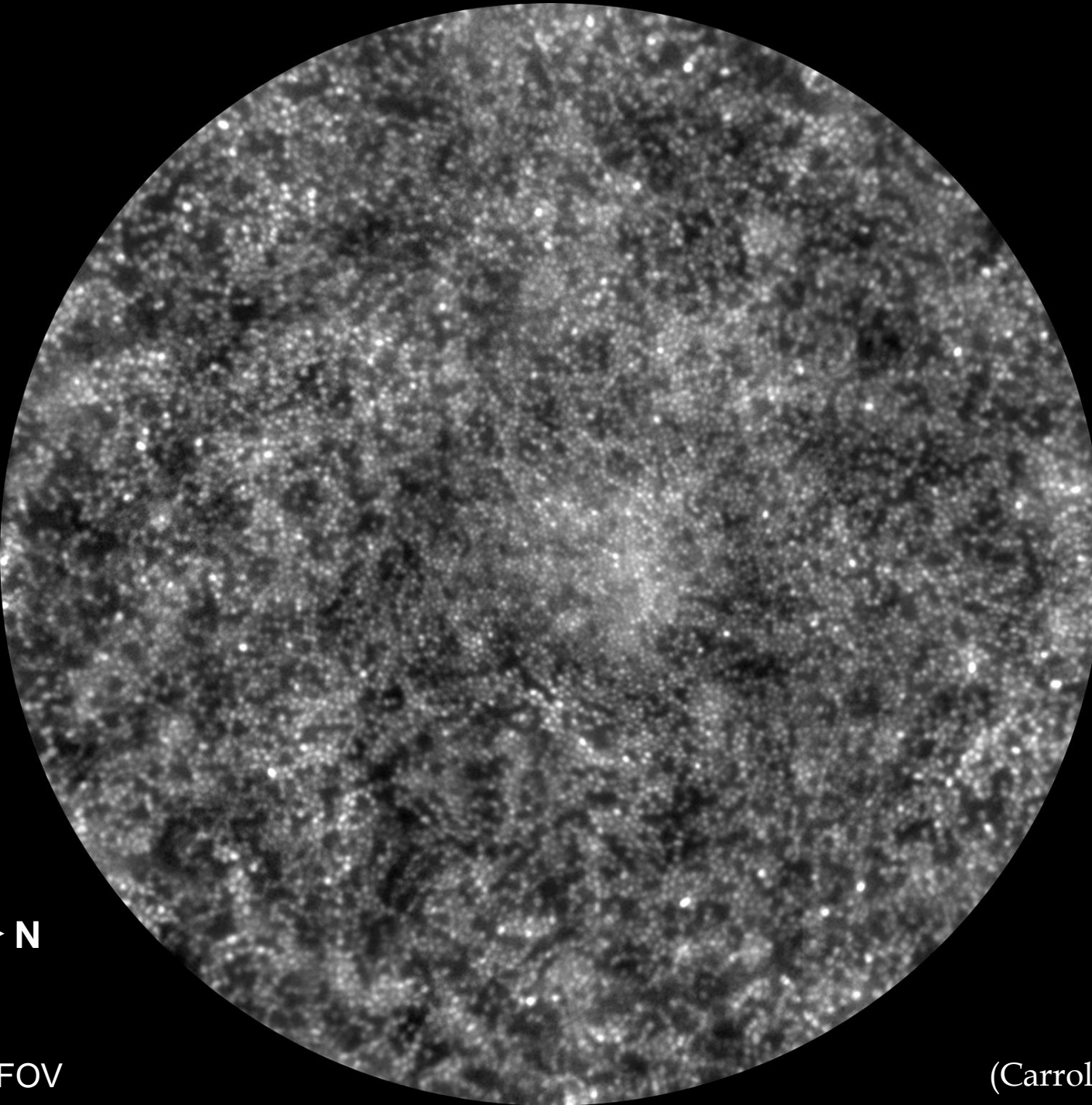
1 deg eccentricity

Deuteranope with LIAVA M pigment
(non-functional photopigment)



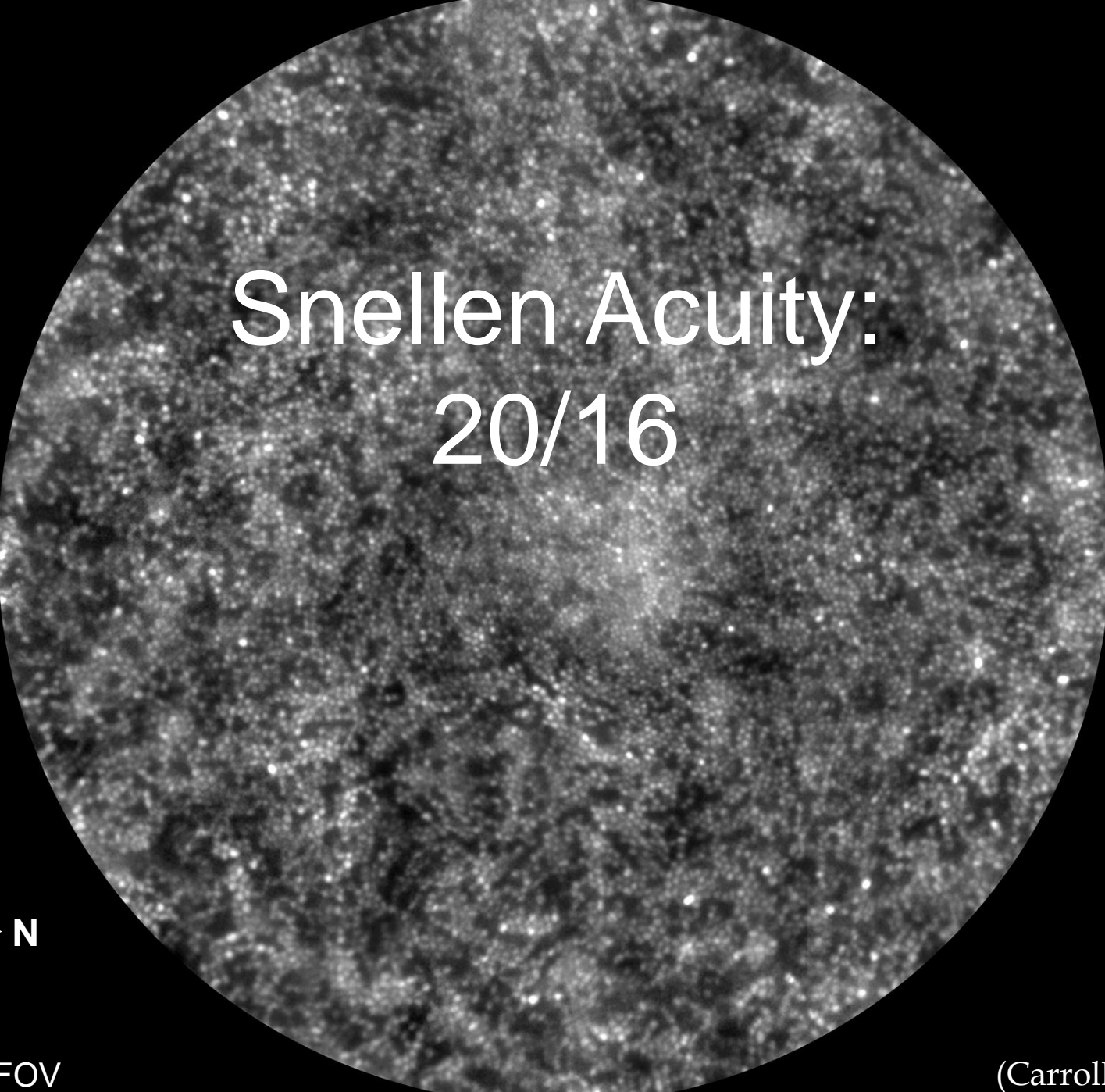
50 μm

J. Carroll, M. Neitz, H. Hofer, J. Neitz, D. R. Williams (2004)

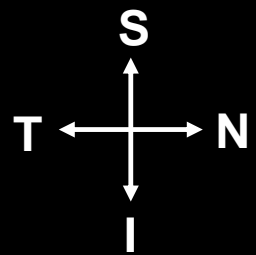


≈2.5 deg FOV

(Carroll et al., 2004)



Snellen Acuity:
20/16



≈2.5 deg FOV

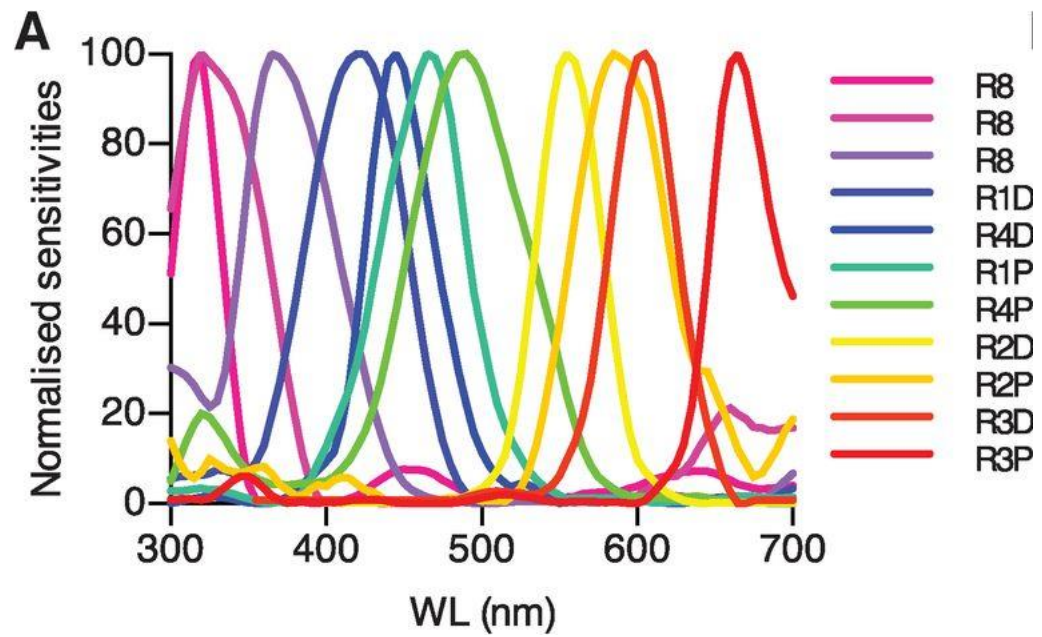
(Carroll et al., 2004)



Monterey Bay
Aquarium



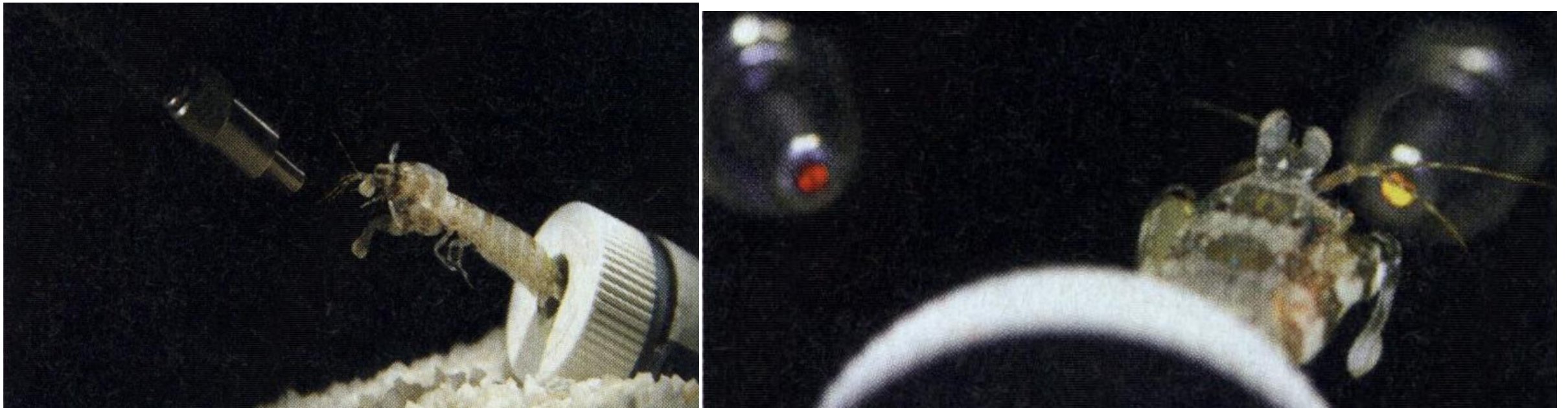
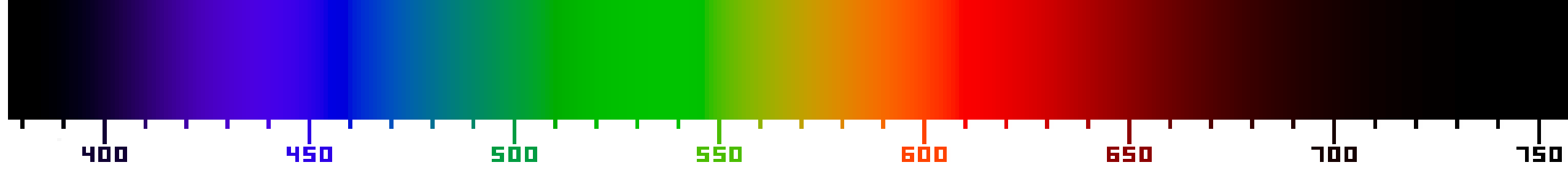
the mantis shrimp



(Thoen et al 2014 *A Different Form of Color Vision in Mantis Shrimp*)

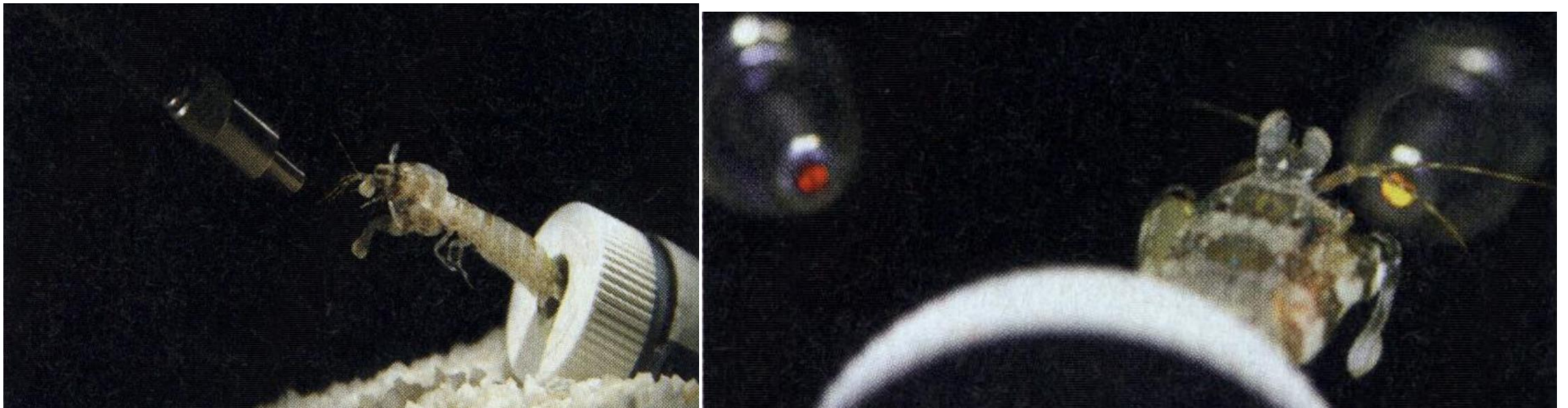
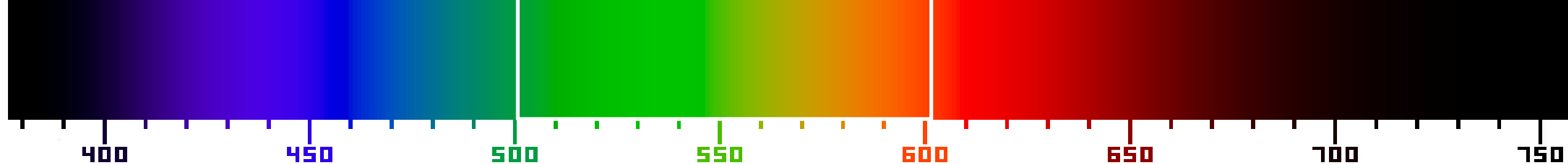


the mantis shrimp retina's 12 spectral sensitivities



(Thoen et al 2014 *A Different Form of Color Vision in Mantis Shrimp*)

mantis shrimp can perform color discrimination tasks



(Thoen et al 2014 *A Different Form of Color Vision in Mantis Shrimp*)

mantis shrimp color vision is coarser than humans'!
(~20nm vs ~2nm resolution)

Cones are just one part of the puzzle

Color vision requires intricate neural processing at various stages in the visual system

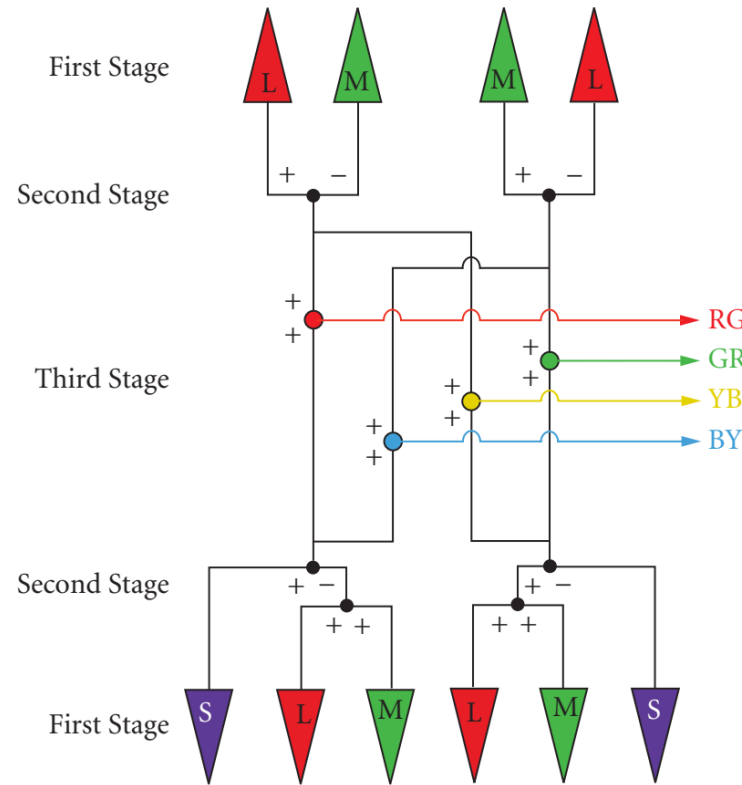


FIGURE 39 Three-stage Müller zone model. *First stage:* L-, M-, and S-cone photoreceptors (top and bottom). *Second stage:* L-M and M-L cone opponency (top) and S-(L+M) and (L+M)-S cone opponency (bottom). *Third stage:* Color opponency (center) is achieved by summing the various cone-opponent second-stage outputs.

